Acta Universitatis Szegediensis

Acta Biologica Szegediensis

Volume 57, Number 2, 2013

University of Szeged, Szeged, Hungary

Acta Biologica Szegediensis

Acta Biologica Szegediensis is an international peer-reviewed journal edited by the University of Szeged. It is published yearly in two issues per volume (ISSN 1588-385X print form; ISSN 1588-4082 online form) as a member of the Acta Universitatis Szegediensis family of scientific journals (ISSN 0563-0592).

Acta Biologica Szegediensis publishes novel findings in various fields of biology with special focus on innovative research in modern experimental life sciences. The journal publishes experimental and theoretical papers, reviews, short communications, and descriptions of new methods. Letters to the editor, and conference proceedings may also be published, subject to the approval of the Editor-in-Chief.

ACTA BIOLOGICA SZEGEDIENSIS VOLUME 57(2), 2013

Table of Contents

Review Article

Nikolett Baranyi, Sándor Kocsubé, Csaba Vágvölgyi, János Varga
Current trends in aflatoxin research 95

Articles

Tamás Marik, Csaba Várszegi, László Kredics, Csaba Vágvölgyi, András Szekeres
Mass spectrometric investigation of alamethicin 109

Csilla Gömöri, Elvira Nacsa-Farkas, Erika Beáta Kerekes, Sándor Kocsubé, Csaba Vágvölgyi, Judit Krisch
Evaluation of five essential oils for the control of food-spoilage and mycotoxin producing fungi 113

Lóránt Hatvani, László Manczinger, Tamás Marik, Szilvia Bajkán, Lívia Vidács, Ottó Bencsik, András Szekeres, Isidora Radulov, Lucian Nita, Csaba Vágvölgyi
The complete degradation of acetanilide by a consortium of microbes isolated from river Maros 117

Panchanand Mishra, Surendra C. Sabat
A modified method of total RNA isolation and quantitative analysis of superoxide dismutase gene expression from different organs of *Ipomoea carnea* 121

Hossein Mozafari, Zahra Asrar, Farkhondeh Rezanejad Shahram Pourseyedi, Mohammad Mehdi Yaghoobi
Calcium and L-histidine interaction on growth improvement of three tomato cultivars under nickel stress 131

Alina G. Profir, Camelia Vizireanu
Sensorial analysis of a functional beverage based on vegetables juice 145

Ulrike Zanzen, Gudrun Lisa Bovenkamp, Katla Sai Krishna, Josef Hormes, Alexander Prange
Antibacterial action of copper ions on food-contaminating bacteria 149

Katalin Mikite, Nóra Merész, András Papp
Changes and relationship of somatosensory cortical electrical activity and hind paw defensive reflex in rats under various anesthetics 153

Eszter Antalfi, Sándor Fehér
Xylotomic similarities and natural habitat of the fossil remains of Bükkábrány 161

On the cover: *Aspergillus flavus* infection on corn-cob (see Baranyi et al. in this issue).

Volume 57(2):95-107, 2013
Acta Biologica Szegediensis
http://www.sci.u-szeged.hu/ABS

REVIEW ARTICLE

Current trends in aflatoxin research

Nikolett Baranyi, Sándor Kocsubé, Csaba Vágvölgyi, János Varga*

Department of Microbiology, Faculty of Science and Informatics, University of Szeged, Szeged, Hungary

ABSTRACT Aflatoxins are decaketide-derived secondary metabolites which are produced by a complex biosynthetic pathway. Aflatoxins are among the economically most important mycotoxins. Aflatoxin B_1 exhibits hepatocarcinogenic and hepatotoxic properties, and is frequently referred to as the most potent naturally occurring carcinogen. Acute aflatoxicosis epidemics occurred in several parts of Asia and Africa leading to deaths of several hundred people. Recent data indicate that aflatoxins are produced by 20 species assigned to three sections of the genus *Aspergillus*: sections *Flavi*, *Nidulantes* and *Ochraceorosei*. The economically most important producer is *A. flavus* and its relatives. Compounds with related structures include sterigmatocystin, an intermediate of aflatoxin biosynthesis produced by several Aspergilli and species assigned to other genera, and dothistromin produced by a range of non-*Aspergillus* species. Aflatoxin producers and consequently aflatoxin contamination occur frequently in various food products mainly in tropical and subtropical areas of the world. However, climate change led to the occurrence of aflatoxin producing species, especially *A. flavus* in areas where they were not prevalent previously. Molecular genetic and genomic studies led to the clarification of aflatoxin and sterigmatocystin biosynthetic pathways in a range of producing organisms, and provided insight into the metabolism and effect of aflatoxins. In this review, we wish to give an overview on recent progress of aflatoxin research including producing organisms, occurrence, biosynthesis and molecular detection of aflatoxins.
Acta Biol Szeged 57(2):95-107 (2013)

KEY WORDS

aflatoxin
Aspergillus
climate change
biosynthesis
sequence-based identification

Secondary metabolism is mainly a characteristic of filamentous fungi. The diversity and complexity of secondary metabolites is astounding, and species of *Aspergillus* are rich in genes for secondary metabolism (Nierman et al. 2005; Kobayashi et al. 2007; Rokas et al. 2007). Secondary metabolites are usually not required for growth of the organism in culture, but do contribute to the fitness of the organism in its natural environment. Secondary metabolites have an impact on our daily life either as toxins or as beneficial compounds. Beneficial secondary metabolites made by species of *Aspergillus* include food additives such as kojic acid or citric acid, antibiotics such as penicillin, and cholesterol reducing drugs such as lovastatin (Endo et al. 1976; Adrio and Demain 2003). In contrast, the repertoire of fungal secondary metabolites also includes harmful products known as mycotoxins.

Aflatoxins are the most thoroughly studied mycotoxins, which are produced by species assigned to the *Aspergillus* genus. They were discovered when the toxicity of animal feeds containing contaminated peanut meal led to the death of more than 100,000 turkeys from acute liver necrosis in the early sixties (Turkey-X disease; Blout 1961; Sargeant et al. 1961; van der Zijden et al. 1962). *Aspergillus flavus* was identified as the producing fungus, and aflatoxins were named after the toxic agent. Aflatoxins have both toxic and carcinogenic properties, posing serious threats to both animal and human health (Bennett and Klich 2003). Comprehensive studies have shown that aflatoxin is a risk factor for human hepatocellular carcinoma, especially in Asia and sub-Saharan Africa (Groopman et al. 2005). Several deaths were also attributed to acute aflatoxicosis (Nyikal et al. 2004). Because of its toxicity, over 100 countries restrict the content of aflatoxins in the food and feed supplies (van Egmond et al. 2007).

Aflatoxins are a group of structurally related difuranocoumarins that were named as aflatoxins B_1, B_2, G_1, and G_2 based on their fluorescence under UV light (blue or green) and relative chromatographic mobility during thin-layer chromatography. Aflatoxin B_1 (Fig. 1) is the most potent natural carcinogen known (Squire 1981, IARC 2012), and is usually the major aflatoxin produced by toxigenic strains. Apart from those mentioned above, over a dozen of other structural analogs including aflatoxins P_1, Q_1, B_{2a} and G_{2a} have been described as mammalian biotransformation products of the major metabolites, while aflatoxin D_1 was detected in ammoniated maize, and aflatoxin B_3 as a metabolite of *A. flavus* (Cole and Schweikert 2003, Varga et al. 2009). Aflatoxin M_1, a hydroxylated metabolite is found primarily in animal tissues and fluids (milk and urine) as a metabolic product of aflatoxin B_1 (Varga et al. 2009; Fig. 1).

In this review, an overview of recent data on aflatoxins will be presented including the range of aflatoxin producing fungi,

Accepted April 11, 2014
*Corresponding author. E-mail: jvarga@bio.u-szeged.hu

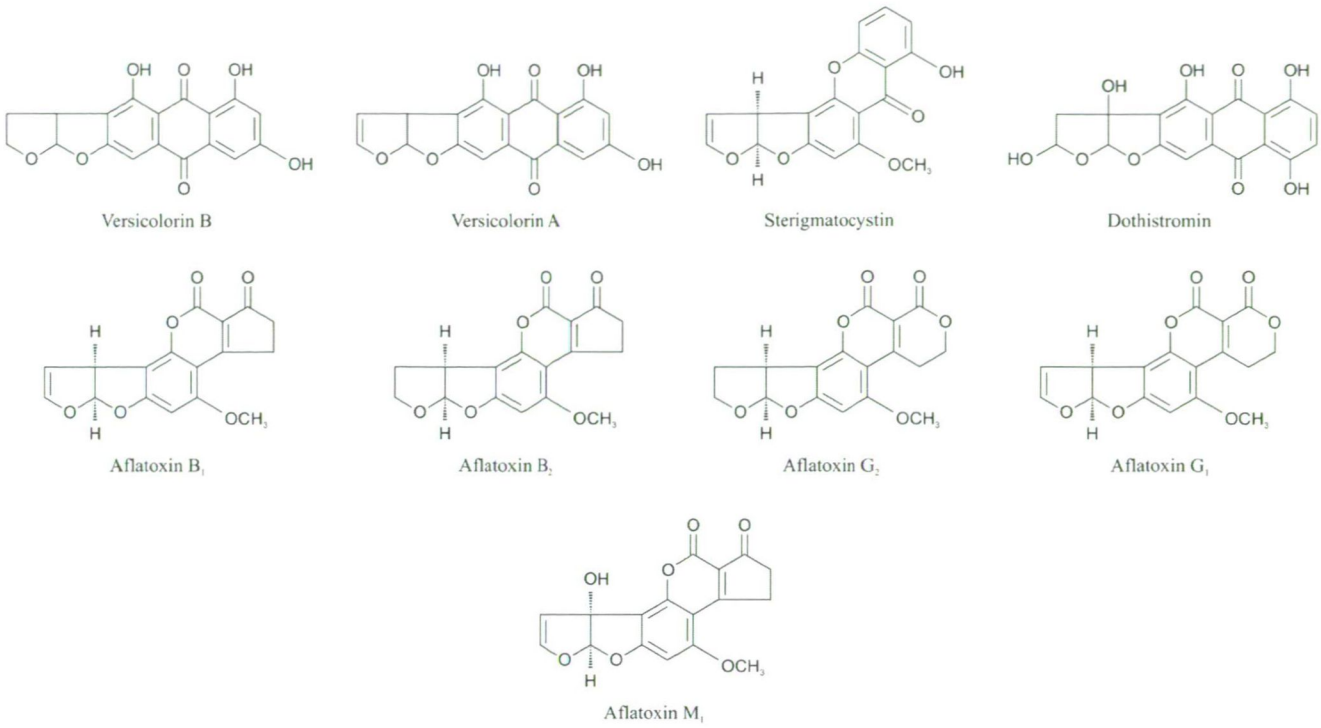

Figure 1. Structures of the most important aflatoxins and their structural relatives.

occurrence of aflatoxins and producers in various matrices, and biosynthesis and molecular detection of aflatoxins.

Aflatoxin producers

A thorough review has been published recently on the re-evaluation of aflatoxin production in fungi (Varga et al. 2009). At that time, 13 species have been found to be able to produce aflatoxins, all belonging to the *Aspergillus* genus. Since then, 7 more species have been found to be able to produce these compounds including *A. pseudonomius, A. pseudocaelatus* (Varga et al. 2011), *A. togoensis* (Rank et al. 2011), *A. mottae, A. sergii, A. transmontanensis* (Soares et al. 2012) and *A. novoparasiticus* (Gonçalves et al. 2012). These data indicate that aflatoxins are produced by at least 20 species assigned to three sections of the genus *Aspergillus*: sections *Flavi, Nidulantes* and *Ochraceorosei* (Varga et al. 2009; Fig. 2, Table 1). Some aflatoxin producing species have been described as *Emericella* species (one of the sexual stages of the *Aspergillus* genus). However, according to the Amsterdam declaration on fungal nomenclature, only one name can be applied for a fungus (Hawksworth et al. 2011). Under the current rules of the International Code of Nomenclature for algae, fungi, and plants (Hawksworth 2011b; Melbourne Code, McNeill et al. 2012) and the discussions held by the International Commission on *Penillium* and *Aspergillus* (ICPA; http://www.aspergilluspenicillium.org/index.php/single-name-nomenclature/88-single-names/105-aspergillus-options), the *Aspergillus* name was chosen as the valid one for these species (Hawksworth 2011a; Samson et al. unpublished data).

Only B-type aflatoxins are produced by most species, although species related to *A. parasiticus* and *A. nomius* are usually able to produce G-type aflatoxins too (Table 1). Ex-type isolates of *A. oryzae*, *A. fasciculatus*, *A. kambarensis*, *A. effusus* and *A. flavus* var. *columnaris* were treated as synonyms of *A. flavus*, ex-type isolates of *A. toxicarius* and of *A. chungii* (NRRL 4868) were considered not distinct from *A. parasiticus* (Soares et al. 2012), and *A. zhaoqingensis* has been synonymised with *A. nomius* (Varga et al. 2011). Although, aflatoxin production was claimed for several other species and fungal genera (and actually even for bacteria), none of these observations could have been confirmed (Varga et al. 2009). Recently, a *Fusarium kyushuense* isolate was also claimed to produce aflatoxins, but this report also could not be confirmed (Schmidt-Heydt et al. 2009; Varga et al. 2009).

A structurally related compound, the carcinogenic sterigmatocystin is an intermediate of the aflatoxin biosynthesis, and may be important as it can be produced in rather large amounts on cheese and occasionally in cereals (Pitt and Hocking 2010; Samson et al. 2010). Sterigmatocystin has been reported in several phylogenetically and phenotypically different genera (Rank et al. 2011). The major source of sterigmatocystin in foods and indoor environments is *Aspergillus versicolor* and its relatives (Samson et al. 2010).

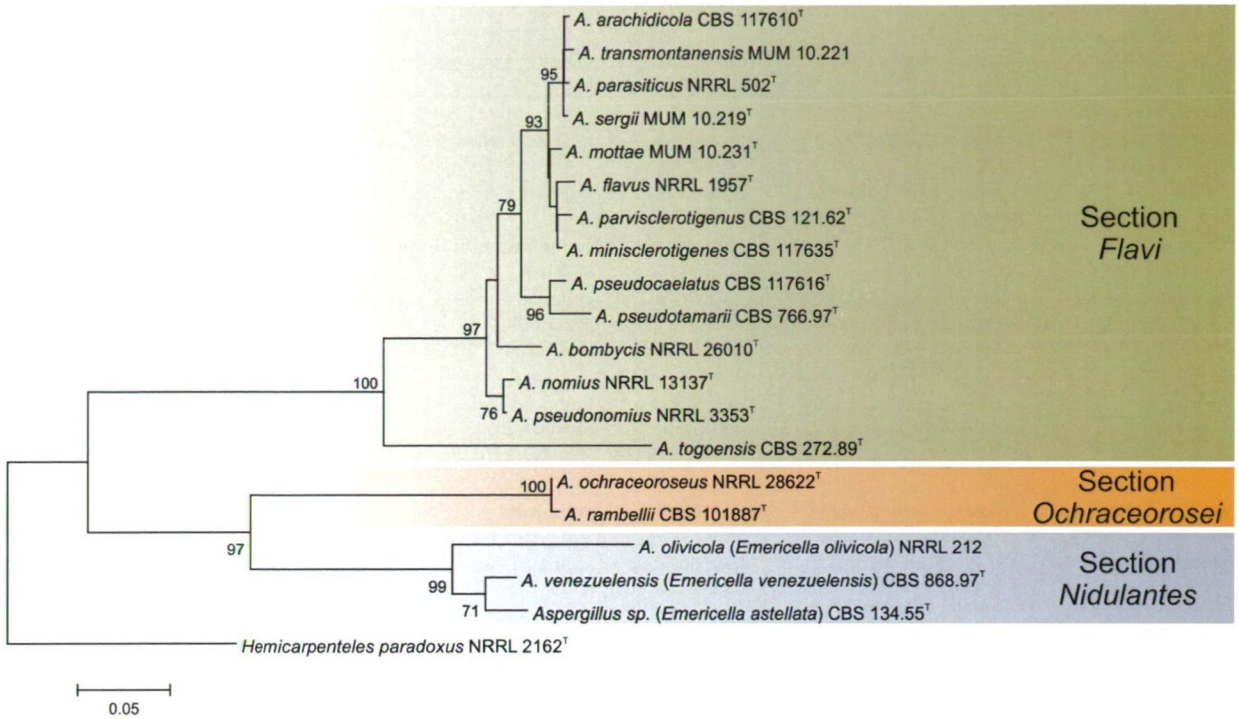

Figure 2. Phylogenetic tree of aflatoxin producing fungi based on partial calmodulin sequence data.

Production of this mycotoxin was confirmed in 31 *Aspergillus*, five *Chaetomium* species and in *Botryotrichum pillulifera, Bipolaris sorokiana* and *Humicola nordinii* under the growth conditions tested using multiple detection methods (Rank et al. 2011). Sterigmatocystin production was also confirmed in *Aspergillus inflatus* (=*Penicillium inflatum;* Rank et al. 2011), which species belongs to *Aspergillus* section *Cremei* according to multilocus phylogenetic studies (Varga et al. unpublished results). More recently, Jurjević et al. (2012, 2013) described 9 new species assigned to section *Versicolores* which are also able to produce this compound. Sterigmatocystin production was also confirmed in *Podospora anserina* (Matasyoh et al. 2011), and the gene cluster responsible for the biosynthesis of sterigmatocystin was also identified (Slot and Rokas 2011). Apart from sterigmatocystin, the immediate precursor of aflatoxin, O-methylsterigmatocystin was also found in *Chaetomium cellulolyticum, Chaetomium longicolleum, Chaetomium malaysiense* and *Chaetomium virescens* (Rank et al. 2011). Besides, the ex-type strain of the newly described species *A. bertholletius* was also found to produce O-methylsterigmatocystin, indicating that the genome of this species also carries the aflatoxin biosynthetic gene cluster (Taniwaki et al. 2012). Although sterigmatocystin is a precursor of aflatoxins, only *Aspergillus ochraceoroseus, A. rambellii* (Frisvad et al. 1999; Klich et al. 2000), and some species belonging to section *Nidulantes* accumulate both sterigmatocystin and aflatoxins (Frisvad et al. 2004; Frisvad and Samson 2004). Members of *Aspergillus* section *Flavi*, which includes the major aflatoxin producers, efficiently convert sterigmatocystin through 3-methoxysterigmatocystin to aflatoxins (Frisvad et al. 1999). An exception in this section is *A. togoensis*, which is able to produce both aflatoxins and sterigmatocystin (Wicklow et al. 1989; Rank et al. 2011).

Another metabolite structurally related to aflatoxins is dothistromin produced by *Dothistroma septosporum*, an important forest pathogen causing red band needle blight disease of pine trees (Bradshaw 2004). Dothistromin is similar in structure to versicolorin B, a precursor of aflatoxin biosynthesis. Full genome sequencing of *D. septosporum* made it possible to identify the genes taking part in the biosynthesis of this compound (Bradshaw et al. 2013). Interestingly, in contrast with other secondary metabolite biosynthesis genes which form gene clusters, most of the genes taking part in dothistromin biosynthesis were found to be spread over six separate regions on chromosome 12 of the pathogen (Bradshaw et al. 2013). The coordinated control of this dispersed set of secondary metabolite genes is achieved by the transcription factor *AflR* (Chettri et al. 2013).

Occurrence of aflatoxin producing fungi and aflatoxins in various habitats

Aflatoxins are primarily produced by *Aspergillus flavus* and *A. parasiticus* on agricultural commodities including cereals

Table 1. *Aspergillus* species able to produce aflatoxins and other mycotoxins.

Species	Occurrence	Type of aflatoxin produced	Other mycotoxins	References
Aspergillus section *Flavi*				
A. arachidicola	Argentina, Brazil	Aflatoxins B_1, B_2 & G_1, G_2	kojic acid, aspergillic acid	Pildain et al. 2008, Calderari et al. 2013
A. bombycis	Japan, Indonesia, Brazil	Aflatoxins B_1, B_2 & G_1, G_2	kojic acid, aspergillic acid	Peterson et al. 2001, Calderari et al. 2013, Okano et al. 2012
A. flavus	Worldwide	Aflatoxins B_1 & B_2	cyclopiazonic acid, kojic acid, aspergillic acid	Varga et al. 2009
A. minisclerotigenes	Argentina, USA, Australia, Nigeria, Portugal, Benin, Argentina, Morocco, Algeria, (Kenya?)	Aflatoxins B_1, B_2 & G_1, G_2	cyclopiazonic acid, kojic acid, aspergillic acid	Pildain et al. 2008, Soares et al. 2012, Moore et al. 2013, Guezlane-Tebibel et al. 2012, El Mahgubi et al. 2013, (Probst et al. 2012)
A. nomius	USA, Japan, Thailand, India, Brazil, Hungary, Serbia	Aflatoxins B_1, B_2 & G_1, G_2	kojic acid, aspergillic acid, tenuazonic acid	Kurtzman et al. 1987, Olsen et al. 2008, Manikandan et al. 2009, Calderari et al. 2013, Okano et al. 2012, unpublished observations
A. novoparasiticus	Colombia, Brazil	Aflatoxins B_1, B_2 & G_1, G_2	kojic acid	Gonçalves et al. 2012
A. parasiticus	USA, Japan, Australia, Brazil, India, South America, Uganda, Portugal, Italy, Serbia	Aflatoxins B_1, B_2 & G_1, G_2	kojic acid, aspergillic acid	Varga et al. 2009, Soares et al. 2012, Baquião et al. 2013, unpublished observations
A. parvisclerotigenus	Nigeria	Aflatoxins B_1, B_2 & G_1, G_2	cyclopiazonic acid, kojic acid	Geiser et al. 2000, Frisvad et al. 2005
A. pseudocaelatus	Argentina	Aflatoxins B_1, B_2 & G_1, G_2	cyclopiazonic acid, kojic acid	Varga et al. 2011
A. pseudonomius	USA	Aflatoxin B_1	kojic acid	Varga et al. 2011
A. pseudotamarii	Japan, Argentina, Brazil, India	Aflatoxin B_1, B2 & G1, G2	cyclopiazonic acid, kojic acid	Ito et al. 2001, Baranyi et al. 2013, Calderari et al. 2013, Massi et al. submitted
A. togoensis	Central Africa	Aflatoxin B_1	sterigmatocystin	Wicklow et al. 1989, Rank et al. 2011
A. transmontanensis	Portugal	Aflatoxins B_1, B_2 & G_1, G_2	aspergillic acid	Soares et al. 2012
A. mottae	Portugal	Aflatoxins B_1, B_2 & G_1, G_2	cyclopiazonic acid, aspergillic acid	Soares et al. 2012
A. sergii	Portugal	Aflatoxins B_1, B_2 & G_1, G_2	cyclopiazonic acid, aspergillic acid	Soares et al. 2012
Aspergillus section *Ochraceorosei*				
A. ochraceoroseus	Ivory Coast	Aflatoxins B_1 & B_2	sterigmatocystin	Frisvad et al. 1999
A. rambellii	Ivory Coast	Aflatoxins B_1 & B_2	sterigmatocystin	Frisvad et al. 2005
Aspergillus section *Nidulantes*				
A. astellatus (=Emericella astellata)	Ecuador	Aflatoxin B_1	sterigmatocystin, terrein	Frisvad et al. 2004
A. olivicola (=Emericella olivicola)	Italy	Aflatoxin B_1	sterigmatocystin, terrein	Zalar et al. 2008
A. venezuelensis (=Emericella venezuelensis)	Venezuela	Aflatoxin B_1	sterigmatocystin, terrein	Frisvad and Samson 2004

(wheat, maize, rice), cotton, peanut, tree nuts, pepper, spices and others (Varga et al. 2009). Aflatoxins were also detected and *Aspergillus flavus* was identified from water from a cold water storage tank by Paterson et al. (1997). More recently, the fungal flora of tap water from an Iranian university hospital was investigated and the results of this study showed that hospital water should be considered as a potential reservoir of fungi particularly *Aspergillus* including *A. flavus* (Hedayati et al. 2011). *A. flavus* is also frequently isolated from indoor air, particularly in subtropical and tropical areas (Hedayati et al. 2007, 2010; Sepahvand et al. 2013). Recently, this species was also identified in large quantities in indoor air in Croatia and Hungary (Varga et al., unpublished results).

The most important aflatoxin producer, *A. flavus* can cause both pre- and postharvest contamination of various agricultural products. Although, the native habitat of this species is

Table 2. Genes taking part in aflatoxin biosynthesis.

Gene	(synonym)	Enzyme or product	Step in aflatoxin biosynthesis pathway
aflA	*(fas-2)*	Fatty acid synthase α	malonyl-CoA → condensed polyketide noranthrone
aflB	*(fas-1)*	Fatty acid synthase β	malonyl-CoA → condensed polyketide noranthrone
aflC	*(pksA)*	Polyketide synthase	malonyl-CoA → condensed polyketide noranthrone
hypC		Anthrone oxidase	noranthrone → norsolonic acid
aflD	*(nor-1)*	Reductase	norsolonic acid (NOR)→ averantin (AVN)
aflE	*(norA)*	NOR-reductase	norsolonic acid (NOR)→ averantin (AVN)
aflF	*(norB)*	Dehydrogenase	norsolonic acid (NOR)→ averantin (AVN)
aflG	*(avnA)*	Cytochrome P450 monooxigenase	averantin (AVN)→ hydroxyaverantin (HAVN)
aflH	*(adhA)*	Alcohol dehydrogenase	hydroxyaverantin (HAVN)→averufin (AVR)
aflI	*(avfA)*	Averufin monooxygenase	averufin (AVR)→ versiconal hemiacetal aceteate (VHA)
aflJ	*(estA)*	Cytosole esterase enzyme	versiconal hemiacetal aceteate (VHA)→ versiconal (VAL)
aflK	*vbs*	Versicolorine B synthase	versiconal (VAL)→ versicolorin B
aflL	*verB*	Cytochrome P450 monooxigenase/ desaturase	versicolorin B → versicolorin A, versicolorin B →demethyldihydrosterigmatocystin (DMDHST)
aflM	*ver-1*	Ketoreductase enzyme	versicolorin A → demethylsterigmatocystin (DMST)
aflN	*verA*	Cytochrome P450 monooxigenase	versicolorin A → demethylsterigmatocystin (DMST)
aflO	*dmtA (mt-1) / omtB*	O-methyltransferase I/ O-methyltransferase B	demethylsterigmatocystin (DMST) → sterigmatocystin (ST) dihydrodemethylsterigmatocystin (DHDMST) → dihydrosterigmatocystin (DHST)
aflP	*omtA*	O-methyltransferase II/ O-methyltransferase A	sterigmatocystin (ST) → O-methylsterigmatocystin (OMST) dihydrosterigmatocystin (DHST) → dihydro-O-methylsterigmatocystin (DHOMST)
aflQ	*ordA*	Monooxygenase	O-methylsterigmatocystin (OMST) → aflatoxin B_1 and G_1 dihydro-O-methylsterigmatocystin (DHOMST) → aflatoxin B_2 and G_2
aflR	*aflR*	Transcription activator	Pathway regulator
aflS	*aflJ*	Transcription enhancer	Pathway regulator
aflT	*aflT*	ABC transporter protein	Unassigned
aflU	*cypA*	Cytochrome P450 monooxigenase	Unassigned
aflV	*cypX*	Cytochrome P450 monooxigenase	Unassigned
aflW	*moxY*	Monooxygenase	Unassigned
aflX	*ordB*	Monooxygenase	Unassigned
aflY	*hypA*	Hypothetical protein	Unassigned

soil and decaying vegetation, it is able to invade many types of organic substrates whenever conditions are favorable for its growth. *A. flavus* is also an important pathogen of various cultivated plants including maize, cotton and peanut, and cause serious yield losses throughout the world. Since aflatoxin production is favored by moisture and high temperature, *A. flavus* is able to produce aflatoxins in warmer, tropical and subtropical climates (Varga et al. 2009). Consequently, aflatoxin contamination of agricultural products in countries with temperate climate, including Central European countries was not treated as a serious health hazard. However, recently several papers have dealt with the effects of climate change on the appearance of aflatoxin producing fungi and aflatoxins in foods (Cotty and Jaime-Garcia 2007; Miraglia et al. 2009; Paterson and Lima 2010; Tirado et al. 2010). Based on these studies, aflatoxin producing fungi and consequently aflatoxins are expected to become more prevalent with climate change in countries with temperate climate. Indeed, several recent reports have indicated the occurrence of aflatoxin producing fungi and consequently aflatoxin contamination in agricultural commodities in several European countries that did not face with this problem before. In western Romania, Curtui et al. (1998) reported that all the examined maize samples were free from aflatoxins in 1997. However, more recently, Tabuc et al. (2009) have found that about 30% of maize samples collected between 2002 and 2004 in southeastern Romania were contaminated with aflatoxin B_1 (AFB_1), and in 20% of these samples the level of toxin exceeded the European Union limit of 5 μg/kg. In Serbia, Jakić-Dimić et al. (2009) isolated *A. flavus* from 18.7% of the maize samples analyzed, and aflatoxins were also detected in 18.3% of the samples, while Jaksić et al. (2011) detected aflatoxins in 41.2% of the analyzed maize samples in the range of 2-7 μg/kg. Polovinski-Horvatović et al. (2009) observed aflatoxin M_1 in 30.4% of milk samples collected from small farms in Serbia in amounts exceeding the allowable legislation of the European Union. Similarly, Torkar and Vengust (2007) detected aflatoxin M_1 above the EU limit in 10% of the examined milk samples in Slovenia. Halt (1994) detected aflatoxins in 9.4% of Croatian flour samples, and isolated *A. flavus* from 38% of the flour samples in 2004 (Halt et al. 2004). Although Haberle (1988) could not detect aflatoxins in Croatian milk samples, Bilandzić et al. (2010)

could detect aflatoxin M_1 above the EU limit in some milk samples collected in Croatia. Regarding Hungary, Richard et al. (1992) examined the mycotoxin producing abilities of 22 isolates collected from various sources in Hungary, and none of the isolates were found to produce aflatoxins. However, more recently, Borbély et al. (2010) have examined mycotoxin levels in cereal samples and mixed feed samples collected in eastern Hungary, and detected AFB_1 levels above the EU limit in 4.8% of the samples. Dobolyi et al. (2011, 2013) identified aflatoxin producing *A. flavus* isolates in several maize fields in Hungary. Aflatoxin contamination of maize (2003) and milk (2007, 2011, 2012) originating from Hungary, Serbia, Romania and Slovenia have also been detected recently in the frame of the Rapid Alert System for Food and Feed of the European Union (https://webgate.ec.europa.eu/rasff-window/portal/). In recent surveys, *A. flavus* was also identified in various agricultural products including maize, wheat and barley in Hungary (Tóth et al. 2012).

Due to the extreme weather conditions in 2012 in Central Europe, aflatoxin contamination of maize and milk caused serious problems in several countries including Serbia, Romania and Croatia (http://en.wikipedia.org/wiki/2013_aflatoxin_contamination). Aflatoxins were also detected in maize kernels in Hungary after harvest in 2012 (Tóth et al. 2013).

Apart from *A. flavus*, other aflatoxin producers have also been observed in Central Europe. *A. nomius* was detected for the first time in the region in cheese samples in Hungary, and in maize in Serbia (Varga et al., unpublished observations). Since *A. nomius* is also able to produce G-type aflatoxins, these data explain their detection in some Serbian maize samples (Kos et al. 2013).

Aflatoxin producers have also been found to be able to cause human infections. *Aspergillus flavus* is considered as the second most important cause of invasive aspergillosis, and also frequently identified in other human infections (Hedayati et al. 2007). Other aflatoxin producing species identified as causes of human diseases include *A. nomius* which was identified from human onychomycosis and keratitis cases (Manikandan et al. 2009), and *A. pseudotamarii* identified from a keratitis case in India (Baranyi et al. 2013). Aflatoxin producing abilities of *A. nomius* have also been proven under *ex vivo* conditions (Klich et al. 2009; Baranyi et al. 2013, unpublished results).

Aflatoxin biosynthesis

Molecular analysis of aflatoxin production in *A. flavus* and *A. parasiticus* led to the identification of an about a 75 kb DNA cluster consisting of two specific transcriptional regulators (*aflR* and *aflS*), and at least 30 co-regulated downstream metabolic genes in the aflatoxin biosynthetic pathway (Liu and Chu 1998; Bhatnagar et al. 2003; Yu et al. 2004; Georgianna and Payne 2009; Ehrlich et al. 2012). Sterigmatocystin is a penultimate precursor of aflatoxin biosynthesis and also a toxic and carcinogenic substance produced by many species belonging mainly to sections *Versicolores* and *Nidulantes* of the *Aspergillus* genus. Sterigmatocystin production also occurs in the phylogenetically unrelated genera *Monocillium*, *Chaetomium*, *Humicola* and *Bipolaris* (Varga et al. 2009; Rank et al. 2011). Two genes, *aflR* and *aflS*, located divergently adjacent to each other within the aflatoxin cluster are involved in the regulation of aflatoxin or sterigmatocystin gene expression. The gene *aflR* encodes a sequence-specific zinc-finger DNA-binding protein (Zn(II)2Cys6), which is required for transcriptional activation of most, if not all, of the structural genes (Chang et al. 1993, 1995, 1999; Payne et al. 1993; Woloshuk et al. 1994; Yu et al. 1996; Flaherty and Payne 1997; Ehrlich et al. 1998; Price et al. 2006).

Aflatoxin biosynthesis is also regulated by *aflS* (formerly *aflJ*), a gene that resides next to *aflR*. The genes *aflS* and *aflR* are divergently transcribed, and they have independent promoters (Georgianna and Payne 2009). The intergenic region between them, however, is short and it is possible that they share binding sites for transcription factors or other regulatory elements (Ehrlich and Cotty, 2002). The precise role of *AflS* in aflatoxin biosynthesis remains unclear (Georgianna and Payne 2009).

The biosynthesis of aflatoxins occurs through a series of highly organized oxidation-reduction reactions (Dutton 1988; Bhatnagar et al. 1992; Minto and Townsend 1997). Aflatoxin biosynthesis starts with conversion of hexanoyl-CoA and 7 malonyl-CoAs to a condensed polyketide noranthrone by the products of two fatty acid synthase genes, *aflA* and *aflB* (whose original names were: *fas-1* and *fas-2*) and a polyketide synthase gene, *aflC* (*pksA*) (Cary et al. 2000). *HypC*, an open reading frame in the region between the *aflC* (*pksA*) and *aflD* (*nor-1*) genes in the aflatoxin biosynthesis gene cluster, encodes a 17-kDa anthrone oxidase which is involved in the catalytic conversion of noranthrone to norsolonic acid (NOR) (Ehrlich 2009). NOR is the first stable metabolite which can be isolated. *AflD* (*nor-1*), *aflE* (*norA*) and *aflF* (*norB*) have an important role in the reduction from NOR to averantin (AVN). NOR is converted to AVN by reductase-, and dehydrogenase enzymes, and this reaction is reversible depending on NADP(H) or NAD(H) (Bennett and Christensen 1983; Dutton 1988; Yabe et al. 1991a; Bhatnagar et al. 1992). The next catalytic step is the conversion of AVN to hydroxyaverantin (HAVN) by a cytochrome P450 monooxigenase enzyme that is encoded by the gene *aflG* (*avnA*) (Yu et al. 1997). Yu and his colleagues (1997) have demonstrated in their gene disruption and substance feeding studies, that HAVN and possibly an additional compound are the intermediers during conversion of AVN to averufin (AVR). The alcohol dehydrogenase encoded by *aflH* (*adhA*) (Chang et al. 2000) can catalyse the conversion from HAVN to AVR.

Some of the catalytic steps in the conversion of AVR to versicolorin B (VERB) have not yet been assigned to a spe-

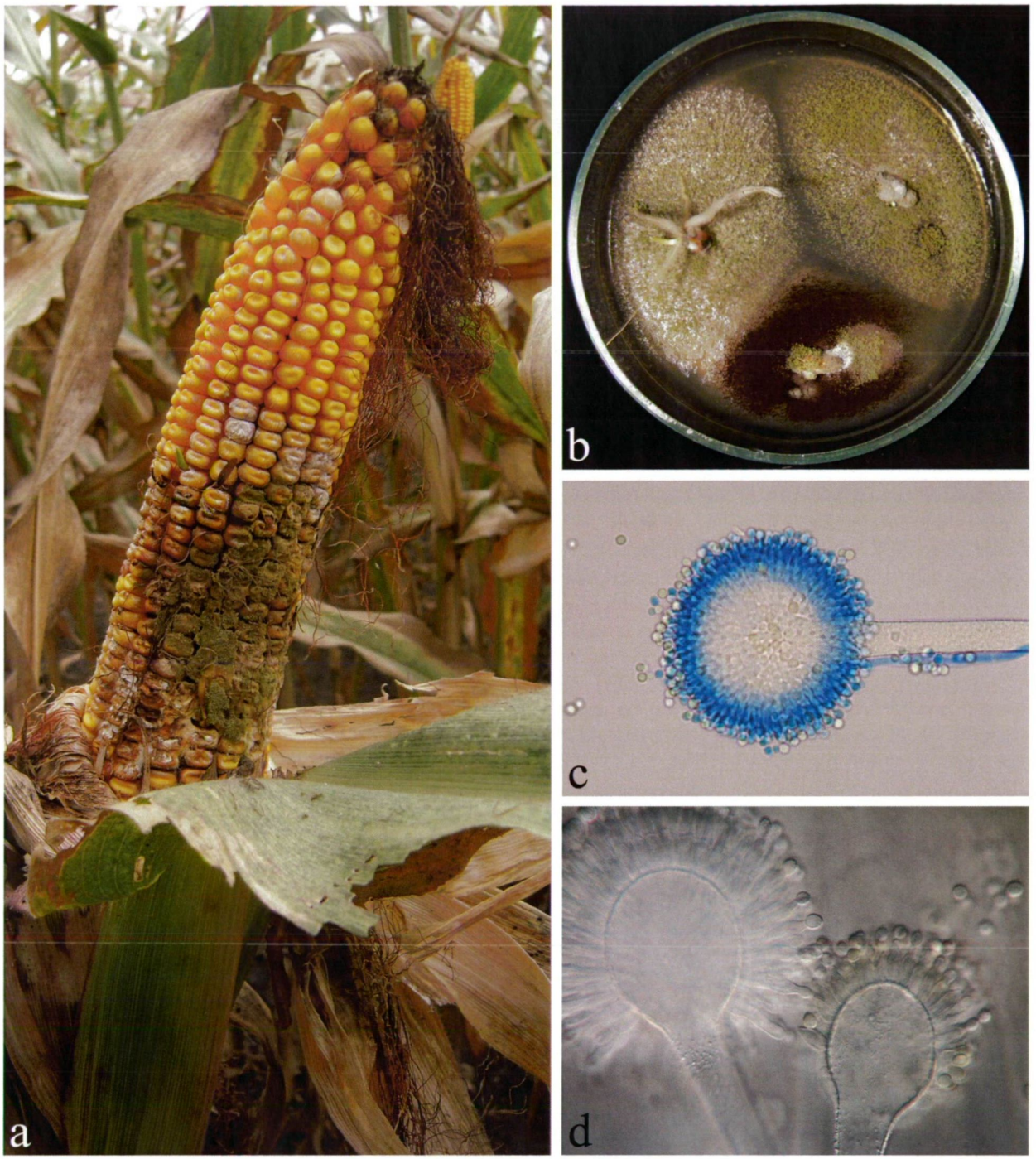

Figure 3. *Aspergillus flavus*. a. Occurrence of *A. flavus* on a maize cob. b. Colonies of *A. flavus* growing on malt extract agar from wheat grain. c-d. *A. flavus* conidial heads.

cific gene in the cluster. Three genes are possible candidates for individual steps: *aflV* (*cypX*), *aflW* (*moxY*), and *aflI* (*avfA*) (Bhatnagar et al. 2003). AVR is converted to hydroxyversicolorone (HVN) by a microsome enzyme in the presence of NADPH (averufin monooxygenase; Yabe et al. 2003). The gene which encodes this enzyme is *aflI* (*avfA*) (Yu et al. 2000a). The *aflV* (*cypX*) and *aflW* (*moxY*) genes (Yu et al. 2000b), also have an important role in the conversion of AVR to versiconal hemiacetal acetate (VHA). The gene *aflV* (*cypX*) encodes a P450 monooxygenase enzyme and *aflW* (*moxY*) encodes a

monooxygenase enzyme (Keller et al. 2000).

Hydroxyversicolorone (HVN) is converted to VHA by a VHA synthase enzyme that requires NADPH as a cofactor. The gene which encodes this enzyme has not been identified yet (Yabe et al. 2003). A cytosolic esterase enzyme encoded by the gene *aflJ* (*estA*) is involved in the conversion of VHA to versiconal (VAL).

The conversion of VHA to VERB is the key step in aflatoxin formation since it closes the bisfuran ring of aflatoxin. Silva et al. (1996), Silva and Townsend (1996), and McGuire (1996) cloned and demonstrated the function of the VERB syntase gene (*vbs*) in the conversion of VHA to VERB in *A. parasiticus*. The new name of *vbs* gene is *aflK* (Yu et al. 2004).

The formation of versicolorin A (VERA) from VERB is a branch point in aflatoxin biosynthetic pathway (Bathnagar et al. 1991; Bathnagar et al. 1993; Yabe and Hamasaki 1993). Similarly to AFB_2 and AFG2, VERB contains a tetrahydrobisfuran ring in its structure; and, like AFB1 and AFG1, VERA contains a dihydrobisfuran ring. The branching step between B- and G-type aflatoxins is the desaturation reaction from VERB to VERA (Yabe et al. 1991b). The *aflL* (*verB*) gene encodes a cytochrome P450 monooxygenase/ desaturase which is presumed to be involved in the conversion of VERB to VERA in aflatoxin biosynthesis. The gene responsible for the conversion directly from VERB to demethyldihydrosterigmatocystin (DMDHST) and then to AFB_2 and AFG_2 has not yet been defined. It is possible that *aflL* (*verB*) participates in conversion of both VERB to VERA and VERB to DMDHST (Yu et al. 2004).

The dihydrobisfuran ring in VERA and the tetrahydrobisfuran ring in VERB are maintained through the next steps. The intermediates after these versicolorins are demethylsterigmatocystin (DMST) for VERA and dihydrodemethylsterigmatocystin (DHDMST) for VERB (Yabe et al. 1989). *AflM* (*ver-1*) and *aflN* (*verA*) are required for the conversion of versicolorin A (VERA) to demethylsterigmatocystin (DMST), because the *aflM* (*ver-1*) gene encodes a ketoreductase enzyme (Skory et al. 1992) and *aflN* (*verA*) gene encodes a cytochrome P-450 monooxygenase enzyme (Matsushima et al. 1994). The exact function of *aflN* (*verA*) has not yet been identified (Yu et al. 2004). The conversion of VERA to DMST requires more then one enzymatic activity (Yabe and Nakajima 2004).

DMST and DHDMST contain two free hydroxyl groups, 7-OH and 6-OH. Two distinct O-methyltransferase activities were demonstrated by Yabe et al. (1989) in *A. parasiticus*. O-methyltransferase I catalyzes the transfer of the methyl groups from S-adenosylmethionine (SAM) to the hydroxyl groups of DMST and DHDMST in order to produce sterigmatocystin (ST) and dihydrosterigmatocystine (DHST) (Yabe and Nakajima 2004). The gene for this O-methyltransferase in *A. parasiticus* was cloned by Motomura et al. (1999) and was named *dmtA* or *mt-1* for O-methyltransferase I. The same gene was concurrently cloned by Yu et al. (2000a) in *A. parasiticus*, *A. flavus*, and *A. sojae*. This gene was named *omtB*. The new name of *dmtA* or *omtB* gene is *aflO*.

O-methyltransferase II enzyme is also involved in aflatoxin biosynthesis (Yabe et al. 1989). The rule of O-methyltransferase II is the conversation of ST to O-methylsterigmatocystine (OMST) and DMST to dihydro-O-methylsterigmatocystine (DHOMST) by transferring a methyl group of SAM to 7-OH of ST and DMST (Yabe and Nakajima 2004). O-methyltransferase II was purified by Keller et al. (1993) and its gene, *aflP* (*omtA*), was isolated based on the amino acid sequence of the purified enzyme (Yu et al. 1993). The absence of an *aflP* (*omtA*) homolog in *A. nidulans* is responsible for ST as the final product in this fungus.

The final step in the formation of aflatoxins is the conversion of OMST or DHOMST to aflatoxins B_1, B_2, G_1 and G_2, requiring the presence of a NADPH-dependent monooxygenase encoded by *aflQ* (*ordA*) (Prieto and Woloshuk 1997; Yu et al. 1998). The formation of the G toxins involves an additional step, possibly involving the enzyme encoded by *aflX* (*ordB*) (Yu et al. 1998; Yabe et al. 1999). Another gene, *aflT*, encodes an ABC transporter protein that may be necessary for aflatoxin efflux from the cells. Former studies (Yu et al. 1998) are suggested that additional enzymes are required for the synthesis of G-group aflatoxins. It is clear that *aflU* (*cypA*) encodes a cytochrome P450 monooxygenase for the formation of G-group aflatoxins (Ehrlich et al. 2004). Most recently, the *nadA* gene was also found to play a role in AFG_1/AFG_2 formation (Yu 2012). Cai et al. (2008) disrupted the *nadA* gene and reported that NadA is a cytosolic enzyme for the conversion from a new aflatoxin intermediate named NADA, which is between OMST and AFG_1. *A. flavus* produces only AFB_1 and AFB_2, whereas *A. parasiticus* produces all four major aflatoxins, AFB_1, AFB_2, AFG_1, and AFG_2. Only the G-group aflatoxin producer, *A. parasiticus*, has intact *nadA* and *aflF* (*norB*) genes (Yu 2012). Preliminary data suggests that *aflF* (*norB*) encodes another enzyme predominantly involved in AFG_1/AFG_2 formation (Ehrlich 2008).

Molecular detection of aflatoxin producing fungi

Early attempts tried to confirm aflatoxin production in fungi using 1-3 genes (Shapira et al. 1996), however, these studies could not get reliable results. A multiplex reverse transcription-polymerase chain reaction (RT-PCR) protocol was elaborated by Degola et al. (2007). It was developed to discriminate aflatoxin-producing from aflatoxin-nonproducing strains of *A. flavus*. Five genes of the aflatoxin gene cluster of *A. flavus*, two regulatory (*aflR and aflS*) and three structural (*aflD, aflO, aflQ*, which synonyms are: *nor-1, omtB, ordA*), were targeted with specific primers to highlight their expression in mycelia cultivated under including conditions for aflatoxins production (Levin 2012).

Three different systems have been used for detection of aflatoxin producing isolates of these fungi targeting genes involved in the biosynthesis of aflatoxins: 1. a multiplex PCR assay targeting the *aflD* (*nor-1*), *aflR*, *aflP* (*omt-1*) genes, (Shapira et al. 1996), 2. PCR assays targeting the *aflP* (*omt-1*), *aflD* (*nor-1*), *aflM* (*ver-1*) genes individually (Färber et al. 1997) and 3. PCR assays amplifying individual sequences of the *aflRS*, *aflJ* and *aflO* (*omtB*) genes (Rahimi et al. 2008). Real-time quantitative PCR (qPCR) moreover provides a tool for accurate and sensitive quantification of target DNA (Mulé et al. 2006; González-Salgado et al. 2009; Rodríguez et al. 2011), that could be applied to quantify aflatoxins producing molds. In addition, qPCR has greatly simplified the procedure relative to conventional culturing techniques, with the continuous monitoring of samples through amplification which allows their easy identification using either the fluorescence of non-specific dyes, such as SYBR Green, which can also give a signal for primer-dimers and non-specific amplified products (Kubista et al. 2006), or a sequence specific hydrolysis probe (TaqMan) (Rodríguez et al. 2012).

A microarray based technique has also been developed recently which was used succesfully to study the effect of various factors on aflatoxin production in *A. flavus* (Schmidt-Heydt et al. 2009; Abdel-Hadi et al. 2012).

Acknowledgements

The research of S.K., N.B. and Cs.V. was supported by the European Union and the State of Hungary, co-financed by the European Social Fund in the framework of TÁMOP 4.2.4.A/2-11-1-2012-0001 'National Excellence Program'. The relating research groups were also supported by the Hungarian Scientific Research Fund (OTKA; grant reference number No. K84122 and K84077) and by the European Union through the Hungary-Serbia IPA Cross-border Cooperation Programme (ToxFreeFeed, HU-SRB/1002/122/062) providing infrastructure.

References

Abdel-Hadi A, Schmidt-Heydt M, Parra R, Geisen R, Magan N (2012) A systems approach to model the relationship between aflatoxin gene cluster expression, environmental factors, growth and toxin production by *Aspergillus flavus*. J Royal Soc Interface 9:757-767.

Adrio JL, Demain AL (2003) Fungal biotechnology. Int Microbiol 6:191-199.

Baquião AC, de Oliveira MM, Reis TA, Zorzete P, Diniz Atayde D, Correa B (2013) Polyphasic approach to the identification of *Aspergillus* section *Flavi* isolated from Brazil nuts. Food Chem 139:1127-1132.

Baranyi N, Kocsubé S, Szekeres A, Raghavan A, Narendran V, Vágvölgyi C, Selvam KP, Babu Singh YR, Kredics L, Varga J, Manikandan P (2013) Keratitis caused by *Aspergillus pseudotamarii*. Med Mycol Case Rep 2:91-94.

Bennett JW, Christiansen SB (1983) New perspectives on aflatoxin biosynthesis. Adv Appl Microbiol 29:53-92.

Bennett JW, Klich M (2003) Mycotoxins. Clin Microbiol Rev 16:497–516.

Bhatnagar D, Cleveland TE, Kingston DGI (1991) Enzymological evidence for separate pathways for aflatoxin B_1 and B_2 biosynthesis. Biochemistry 30:4343-4350.

Bhatnagar D, Ehrlich K, Cleveland T (2003) Molecular genetic analysis and regulation of aflatoxin biosynthesis. Appl Microbiol Biotech 61:83–93.

Bhatnagar D, Ehrlich KC, Cleveland TE (1992) Oxidation-reduction reactions in biosynthesis of secondary metabolites. In Bhatnagar D ed., Handbook of Applied Mycology. Vol. V. Mycotoxins in Ecological Systems. Marcel Dekker, New York, pp. 255-285.

Bhatnagar D, Ehrlich KC, Cleveland TE (1993) Biochemical characterization of an aflatoxin B_2 producing mutant of *Aspergillus flavus*. FASEB J 7:A1234.

Bilandzić N, Varenina I, Solomun B (2010) Aflatoxin M_1 in raw milk in Croatia. Food Control 21:1279-1281.

Blout WP (1961) Turkey "X" disease. Turkeys 9:52-77.

Borbély M, Sipos P, Pelles F, Győri Z (2010) Mycotoxin contamination in cereals. J Agroalim Proc Techn 16:96-98.

Bradshaw RE (2004) *Dothistroma* (red-band) needle blight of pines and the dothistromin toxin: a review. Forest Pathol 34:163-185.

Bradshaw RE, Slot JC, Moore GG, Chettri P, de Wit PJ, Ehrlich KC, Ganley AR, Olson MA, Rokas A, Carbone I, Cox MP (2013) Fragmentation of an aflatoxin-like gene cluster in a forest pathogen. New Phytol 198:525-535.

Cai J, Zeng H, Shima Y, Hatabayashi H, Nakagawa H, Ito Y, Adachi Y, Nakajima H, Yabe K (2008) Involvement of the *nadA* gene in formation of G-group aflatoxins in *Aspergillus parasiticus*. Fungal Genet Biol 45:1081-1093.

Calderari TO, Iamanaka BT, Frisvad JC, Pitt JI, Sartori D, Pereira JL, Fungaro MH, Taniwaki MH (2013) The biodiversity of *Aspergillus* section *Flavi* in brazil nuts: from rainforest to consumer. Int J Food Microbiol 160:267-272.

Cary JW, Linz JE, Bhatnagar D (2000) Aflatoxins: biological significance and regulation of biosynthesis. In Cary JW ed., Microbial foodborne diseases: mechanisms of pathogenesis and toxin synthesis. Technomic, Lancaster, 317-361.

Cary JW, Wright M, Bhatnagar D, Lee R, Chu FS (1996) Molecular characterization of an *Aspergillus parasiticus* gene, norA, located on the aflatoxin biosynthesis gene cluster. Appl Environ Microbiol 62:360-366.

Chang PK, Cary JW, Bhatnagar D, Cleveland TE, Bennett JW, Linz JE, Woloshuk CP, Payne GA (1993) Cloning of the *Aspergillus parasiticus* apa-2 gene associated with the regulation of aflatoxin biosynthesis. Appl Environ Microbiol 59:3273-3279.

Chang PK, Ehrlich KC, Yu J, Bhatnagar D, Cleveland TE (1995) Increased expression of *Aspergillus parasiticus aflR*, encoding a sequence-specific DNA binding protein, relieves nitrate inhibition of aflatoxin biosynthesis. Appl Environ Microbiol 61:2372–2377.

Chang PK, Skory CD, Linz JE (1992) Cloning of a gene associated with aflatoxin B_1 biosynthesis in *Aspergillus parasiticus*. Curr Genet 21:231-233.

Chang PK, Yu J, Bhatnagar D, Cleveland TE (1999) Repressor-AflR interaction modulates aflatoxin biosynthesis in *Aspergillus parasiticus*. Mycopathologia 147:105-112.

Chang PK, Yu J, Ehrlich KC, Boue SM, Montalbano BG, Bhatnagar D, Cleveland TE (2000) The aflatoxin biosynthesis gene *adhA* in *Aspergillus parasiticus* is involved in the conversion of 5'-hydroxyaverantin to averufin. Appl Environ Microbiol 66:4715-4719.

Chettri P, Ehrlich KC, Cary JW, Collemare J, Cox MP, Griffiths SA, Olson MA, de Wit PJ, Bradshaw RE (2013) Dothistromin genes at multiple separate loci are regulated by *AflR*. Fungal Genet Biol 51:12-20.

Cole RJ, Schweikert MA (2003) Handbook of Secondary Fungal Metabolites. Vol. 1. Academic Press, San Diego.

Cotty PJ, Jaime-Garcia R (2007) Influences of climate on aflatoxin producing fungi and aflatoxin contamination. Int J Food Microbiol 119:109-115.

Curtui V, Usleber E, Dietrich R, Lepschy J, Märtlbauer E (1998) A survey on the occurrence of mycotoxins in wheat and maize from western Romania. Mycopathologia 143:97-103.

Degola F, Berni E, Dall'Asta C, Spotti E, Marchelli R, Ferrero I, Restivo FM

(2007) A multiplex RT-PCR approach to detect aflatoxigenic strains of *Aspergillus flavus*. J Appl Microbiol 103:409-417.

Dobolyi C, Sebők F, Varga J, Kocsubé S, Szigeti G, Baranyi N, Szécsi Á, Lustyik G, Micsinai A, Tóth B, Varga M, Kriszt B, Kukolya J (2011) Occurrence of aflatoxin producing *Aspergillus flavus* isolates on maize kernel in Hungary (Aflatoxin-termelő *Aspergillus flavus* törzsek előfordulása hazai kukorica szemtermésben). Növényvédelem 47:125-133 (in Hungarian).

Dobolyi C, Sebők F, Varga J, Kocsubé S, Szigeti G, Baranyi N, Szécsi Á, Tóth B, Varga M, Kriszt B, Szoboszlay S, Krifaton C, Kukolya J (2013) Occurrence of aflatoxin producing *Aspergillus flavus* isolates in maize kernel in Hungary. Acta Aliment 42:451-459.

Dutton MF (1988) Enzymes and aflatoxin biosynthesis. Microbiol Rev 52:274-295.

Ehrlich KC (2009) Predicted roles of the uncharacterized clustered genes in aflatoxin biosynthesis. Toxins 1:37-58.

Ehrlich KC, Cotty PJ (2002) Variability in nitrogen regulation of aflatoxin production by *Aspergillus flavus* strains. Appl Microbiol Biotechnol 60:174-178.

Ehrlich KC, Chang PK, Yu J, Cary JW, Bhatnagar D (2011) Control of aflatoxin biosynthesis in Aspergilli. In Guevara-Gonzalez RG, ed., Aflatoxins-biochemistry and molecular biology. Intech Open: Rijeka, 21-40.

Ehrlich KC, Chang PK, Yu J, Cotty PJ (2004) Aflatoxin biosynthesis cluster gene *cypA* is required for G aflatoxin formation. Appl Environ Microbiol 70:6518-6524.

Ehrlich KC, Mack BM, Wei Q, Li P, Roze LV, Dazzo F, Cary JW, Bhatnagar D, Linz JE (2012) Association with *aflR* in endosomes reveals new functions for *aflJ* in aflatoxin biosynthesis. Toxins 4:1582-1600.

Ehrlich KC, Montalbano BG, Bhatnagar D, Cleveland TE (1998) Alteration of different domains in AflR affects aflatoxin pathway metabolism in *Aspergillus parasiticus* transformants. Fungal Genet Biol 23:279-287.

Ehrlich KC, Scharfenstein LL Jr, Montalbano BG, Chang PK (2008) Are the genes *nadA* and *norB* involved in formation of aflatoxin G_1? Int J Mol Sci 9:1717-1729.

El Mahgubi A, Puel O, Bailly S, Tadrist S, Querin A, Ouadia A, Oswald IP, Bailly JD (2013) Distribution and toxigenicity of *Aspergillus* section *Flavi* in spices marketed in Morocco. Food Control 32:143-148.

Endo A, Kuroda M, Tanzawa K (1976) Competitive inhibition of 3-hydroxy-3-methylglutaryl coenzyme A reductase by ML-236A and ML-236B fungal metabolites, having hypocholesterolemic activity. FEBS Lett 72:323-326.

Färber P, Geisen R, Holzapfel W (1997) Detection of aflatoxigenic fungi in figs by a PCR reaction. Int J Food Microbiol 36:215-220.

Flaherty JE, Payne GA (1997) Overexpression of *aflR* leads to upregulation of pathway gene transcription and increased aflatoxin production in *Aspergillus flavus*. Appl Environ Microbiol 63:3995-4000.

Frisvad JC, Houbraken J, Samson RA (1999) *Aspergillus* species and aflatoxin production: a reappraisal. In Tuijtelaars ACJ ed., Food microbiology and food safety into the next millennium, Foundation Food Micro '99. Zeist, the Netherlands, pp. 125-126.

Frisvad JC, Samson RA (2004) *Emericella venezuelensis*, a new species with stellate ascospores producing sterigmatocystin and aflatoxin B_1. System Appl Microbiol 27:672-680.

Frisvad JC, Samson RA, Smedsgaard J (2004) *Emericella astellata*, a new producer of aflatoxin B_1, B_2 and sterigmatocystin. Lett Appl Microbiol 38:440-445.

Frisvad JC, Skouboe P, Samson RA (2005) Taxonomic comparison of three different groups of aflatoxin producers and a new efficient producer of aflatoxin B_1, sterigmatocystin and 3-O-methylsterigmatocystin, *Aspergillus rambellii* sp. nov. System Appl Microbiol 28:442-453.

Geiser DM, Dorner JW, Horn BW, Taylor JW (2000) The phylogenetics of mycotoxin and sclerotium production in *Aspergillus flavus* and *Aspergillus oryzae*. Fungal Genet Biol 31:169-179.

Georgianna DR, Payne GA (2009) Genetic regulation of aflatoxin biosynthesis: from gene to genome. Fungal Genet Biol 46:113-125.

Gonçalves SS, Stchigel AM, Cano JF, Godoy-Martinez PC, Colombo AL, Guarro J (2012) *Aspergillus novoparasiticus*: a new clinical species of the section *Flavi*. Med Mycol 50:152-160.

González-Salgado A, Patiño B, Gil-Serna J, Vázquez C, González-Jaén MT (2009) Specific detection of *Aspergillus carbonarius* by SYBR Green and TaqMan quantitative PCR assays based on the multicopy ITS2 region of the rRNA gene. FEMS Microbiol Lett 295:57-66.

Groopman JD, Johnson D, Kensler, TW (2005) Aflatoxin and hepatitis B virus biomarkers: a paradigm for complex environmental exposures and cancer risk. Cancer Biomark 1:5-14.

Guezlane-Tebibel N, Bouras N, Mokrane S, Benayad T, Mathieu F (2012) Aflatoxigenic strains of *Aspergillus* section *Flavi* isolated from marketed peanuts (*Arachis hypogaea*) in Algiers (Algeria). Ann Microbiol 62:1-11.

Haberle V (1988) Aflatoxin M_1 determination in samples of market milk produced in Croatia. Hrana I Ishrana 29:195-196 (in Croatian).

Halt M (1994) *Aspergillus flavus* and aflatoxin B_1 in flour production. Eur J Epidemiol 10:555-558.

Halt M, Klapec T, Subaric D, Macura M, Bacani S (2004) Fungal contamination of cookies and the raw materials for their production in Croatia. Czech J Food Sci 22:95-98.

Hawksworth DL (2011a) Naming *Aspergillus* species: progress towards one name for each species. Med Mycol 49:70-76.

Hawksworth DL (2011b) A new dawn for the naming of fungi: impacts of decisions made in Melbourne in July 2011 on the future publication and regulation of fungal names. IMA Fungus 2:155-162.

Hawksworth DL, Crous PW, Redhead SA, Reynolds DR, Samson RA, Seifert KA, Taylor JW, Wingfield MJ, Abaci O, Aime C, Asan A, Bai FY, de Beer ZW, Begerow D, Berikten D, Boekhout T, Buchanan PK, Burgess T, Buzina W, Cai L, Cannon PF, Crane JL, Damm U, Daniel HM, van Diepeningen AD, Druzhinina I, Dyer PS, Eberhardt U, Fell JW, Frisvad JC, Geiser DM, Geml J, Glienke C, Gräfenhan T, Groenewald JZ, Groenewald M, de Gruyter J, Guého-Kellermann E, Guo LD, Hibbett DS, Hong SB, de Hoog GS, Houbraken J, Huhndorf SM, Hyde KD, Ismail A, Johnston PR, Kadaifciler DG, Kirk PM, Kõljalg U, Kurtzman CP, Lagneau PE, Lévesque CA, Liu X, Lombard L, Meyer W, Miller A, Minter DW, Najafzadeh MJ, Norvell L, Ozerskaya SM, Oziç R, Pennycook SR, Peterson SW, Pettersson OV, Quaedvlieg W, Robert VA, Ruibal C, Schnürer J, Schroers HJ, Shivas R, Slippers B, Spierenburg H, Takashima M, Taşkın E, Thines M, Thrane U, Uztan AH, van Raak M, Varga J, Vasco A, Verkley G, Videira SI, de Vries RP, Weir BS, Yilmaz N, Yurkov A, Zhang N (2011) The Amsterdam declaration on fungal nomenclature. IMA Fungus 2:105-112.

Hedayati MT, Mayahi S, Denning DW (2010) A study on *Aspergillus* species in houses of asthmatic patients from Sari City, Iran and a brief review of the health effects of exposure to indoor *Aspergillus*. Environ Monit Assess 168:481-487.

Hedayati MT, Mayahi S, Movahedi M, Shokohi T (2011) Study on fungal flora of tap water as a potential reservoir of fungi in hospitals in Sari city, Iran. J Mycol Med 21:10-14.

Hedayati MT, Pasqualotto AC, Warn PA, Bowyer P, Denning DW (2007) *Aspergillus flavus*: human pathogen, allergen and mycotoxin producer. Microbiology 153:1677-1692.

IARC (International Agency for Research on Cancer) (2012) A review of human carcinogens. Vol. 100F: Chemical agents and related occupations. IARC Working Group on the Evaluation of Carcinogenic Risks to Humans, Lyon, France.

Ito Y, Peterson SW, Wicklow DT, Goto T (2001) *Aspergillus pseudotamarii*, a new aflatoxin producing species in *Aspergillus* section *Flavi*. Mycol Res 105:233-239.

Jakić-Dimić D, Nesić K, Petrović M (2009) Contamination of cereals with aflatoxins, metabolites of fungi *Aspergillus flavus*. Biotechnol Anim Husband 25:1203-1208.

Jaksić SM, Prunić Z, Milanov DS, Jajić M, Abramović F (2011) Fumonisins and co-occurring mycotoxins in North Serbian corn. Proc Natl Sci Matica Srpska Novi Sad 120:49-59.

Jurjević Z, Peterson SW, Horn BW (2012) *Aspergillus* section *Versicolores*: nine new species and multilocus DNA sequence based phylogeny. IMA

Fungus 3:61–81.

Jurjević Z, Peterson SW, Solfrizzo M, Peraica M (2013) Sterigmatocystin production by nine newly described species in section *Versicolores* grown on two different media. Mycotoxin Res 29:141-145.

Keller NP, Dischinger HC Jr, Bhatnagar D, Cleveland TE, Ullah AH (1993) Purification of a 40-kilodalton methyltransferase active in the aflatoxin biosynthetic pathway. Appl Environ Microbiol 59:479–484.

Keller NP, Watanabe CMH, Kelkar HS, Adams TH, Townsend CA (2000) Requirement of monooxygenase-mediated steps for sterigmatocystin biosynthesis by Aspergillus nidulans. Appl Environ Microbiol 66:359-362.

Klich MA, Mullaney EJ, Daly CB, Cary JW (2000) Molecular and physiological aspects of aflatoxin and sterigmatocystin biosynthesis by *Aspergillus tamarii* and *A. ochraceoroseus*. Appl Microbiol Biotechnol 53:605-609.

Klich MA, Tang S, Denning DW (2009) Aflatoxin and ochratoxin production by *Aspergillus* species under *ex vivo* conditions. Mycopathologia 168:185-191.

Kobayashi T, Abe K, Asai K, Gomi K, Juvvadi PR, Kato M, Kitamoto K, Takeuchi M, Machida M (2007) Genomics of *Aspergillus oryzae*. Biosci Biotechnol Biochem 71:646-670.

Kos JJ, Janić Hajnal EJ, Mastilović S, Milovanović L, Kokić M (2013) The influence of drought on the occurrence of aflatoxins in maize. J Natl Sci Matica Srpska Novi Sad 124:59-65.

Kubista M, Andrade JM, Bengtsson M, Forootan A, Jonák J, Lind K, Sindelkae R, Sjöbacka R, Sjögreend B, Strömboma L, Ståhlberga A, Zorica N (2006) The real-time polymerase chain reaction. Mol Aspects Med 27:95-125.

Kurtzman CP, Horn BW, Hesseltine CW (1987) *Aspergillus nomius*, a new aflatoxin- producing species related to *Aspergillus flavus* and *Aspergillus parasiticus*. Antonie van Leeuwenhoek 53:147-158.

Levin RE (2012) PCR detection of aflatoxin producing fungi and its limitations. Int J Food Microbiol 156:1-6.

Liu BH, Chu FS (1998) Regulation of *aflR* and its product, AflR, associated with aflatoxin biosynthesis. Appl Environ Microbiol 64:3718-3723.

Manikandan P, Varga J, Kocsubé S, Samson RA, Anita R, Revathi R, Dóczi I, Németh TM, Narendran V, Vágvölgyi C, Manoharan C, Kredics L. Mycotic keratitis due to *Aspergillus nomius*. J Clin Microbiol 47:3382-3385.

Matasyoh JC, Dittrich B, Schueffler A, Laatsch H (2011) Larvicidal activity of metabolites from the endophytic *Podospora* sp. against the malaria vector *Anopheles gambiae*. Parasitol Res 108:561-566.

Matsushima K, Ando Y, Hamasaki T, Yabe K (1994) Purification and characterization of two versiconal hemiacetal acetate reductases involved in aflatoxin biosynthesis. Appl Environ Microbiol 60:2561-2567.

McGuire SM, Silva JC, Casillas EG, Townsend CA (1996) Purification and characterization of versicolorin B synthase from *Aspergillus parasiticus*. Catalysis of the stereodifferentiating cyclization in aflatoxin biosynthesis essential to DNA interaction. Biochemistry 35:11470-11486.

McNeill J, Barrie FR, Buck WR, Demoulin V, Greuter W, Hawksworth DL, Herendeen PS, Knapp S, Marhold K, Prado J, Prud'homme van Reine WF, Smith GF, Wiersema JH, Turland N (eds. & comps.) (2012) International Code of Nomenclature for algae, fungi, and plants (Melbourne Code), adopted by the Eighteenth International Botanical Congress Melbourne, Australia, July 2011. Koeltz Scientific Books, Königstein.

Minto RE, Townsend CA (1997) Enzymology and molecular biology of aflatoxin biosynthesis. Chem Rev 97:2537-2555.

Miraglia M, Marvin HJ, Kleter GA, Battilani P, Brera C, Coni E, Cubadda F, Croci L, De Santis B, Dekkers S, Filippi L, Hutjes RW, Noordam MY, Pisante M, Piva G, Prandini A, Toti L, van den Born GJ, Vespermann A (2009) Climate change and food safety: an emerging issue with special focus on Europe. Food Chem Toxicol 47:1009-1021.

Moore GG, Elliott JL, Singh R, Horn BW, Dorner JW, Stone EA, Chulze SN, Barros GG, Naik MK, Wright GC, Hell K, Carbone I (2013) Sexuality generates diversity in the aflatoxin gene cluster: evidence on a global scale. PLoS Pathog 9:1003574.

Motomura M, Chihaya N, Shinozawa T, Hamasaki T, Yabe K (1999) Cloning and characterization of the O-methyltransferase I gene (dmtA) from *Aspergillus parasiticus* associated with the conversion of demethylsterigmatocystin to sterigmatocystin and dihydrodemethylsterigmatocystin to dihydrosterigatocystin in aflatoxin biosynthesis. Appl Environ Microbiol 65:4987-4994.

Mulé G, Susca A, Logrieco A, Stea G, Visconti A (2006) Development of a quantitative real-time PCR assay for the detection of *Aspergillus carbonarius* in grapes. Int J Food Microbiol 111:28-34.

Nierman WC, Pain A, Anderson MJ, Wortman JR, Kim HS, Arroyo J, Berriman M, Abe K, Archer DB, Bermejo C, Bennett J, Bowyer P, Chen D, Collins M, Coulsen R, Davies R, Dyer PS, Farman M, Fedorova N, Fedorova N, Feldblyum TV, Fischer R, Fosker N, Fraser A, García JL, García MJ, Goble A, Goldman GH, Gomi K, Griffith-Jones S, Gwilliam R, Haas B, Haas H, Harris D, Horiuchi H, Huang J, Humphray S, Jiménez J, Keller N, Khouri H, Kitamoto K, Kobayashi T, Konzack S, Kulkarni R, Kumagai T, Lafon A, Latgé JP, Li W, Lord A, Lu C, Majoros WH, May GS, Miller BL, Mohamoud Y, Molina M, Monod M, Mouyna I, Mulligan S, Murphy L, O'Neil S, Paulsen I, Peñalva MA, Pertea M, Price C, Pritchard BL, Quail MA, Rabbinowitsch E, Rawlins N, Rajandream MA, Reichard U, Renauld H, Robson GD, Rodriguez de Córdoba S, Rodríguez-Peña JM, Ronning CM, Rutter S, Salzberg SL, Sanchez M, Sánchez-Ferrero JC, Saunders D, Seeger K, Squares R, Squares S, Takeuchi M, Tekaia F, Turner G, Vazquez de Aldana CR, Weidman J, White O, Woodward J, Yu JH, Fraser C, Galagan JE, Asai K, Machida M, Hall N, Barrell B, Denning DW (2005) Genomic sequence of the pathogenic and allergenic filamentous fungus *Aspergillus fumigatus*. Nature 438:1151-1156.

Nyikal J, Misore A, Nzioka C, Njuguna C, Muchiri E, Njau J, Maingi S, Njoroge J, Mutiso J, Onteri J, Langat A, Kilei IK, Nyamongo J, Ogana G, Muture B, Tukei P, Onyango C, Ochieng W, Tetteh C, Likimani S (2004) Outbreak of aflatoxin poisoning - Eastern and Central Provinces, Kenya, January–July 2004. Morbid Mortal Week Rep 53:790-793.

Okano K, Tomita T, Ohzu Y, Takai M, Ose A, Kotsuka A, Ikeda N, Sakata J, Kumeda Y, Nakamura N, Ichinoe M (2012) Aflatoxins B and G contamination and aflatoxigenic fungi in nutmeg. Shokuhin Eiseigaku Zasshi 53:211-216.

Olsen M, Johnsson P, Möller T, Paladino R, Lindblad M (2008) *Aspergillus nomius*, an important aflatoxin producer in Brazil nuts? World Mycotox J 1:123-126.

Paterson RRM, Lima N (2010) How will climate change affect mycotoxins in food? Food Res Int 43:1902-1914.

Paterson RRM, Kelley J, Gallagher M (1997) Natural occurrence of aflatoxins and *Aspergillus flavus* (Link) in water. Lett Appl Microbiol 25:435-436.

Payne GA, Nystrom GJ, Bhatnagar D, Cleveland TE, Woloshuk CP (1993) Cloning of the *afl-2* gene involved in aflatoxin biosynthesis from *Aspergillus flavus*. Appl Environ Microbiol 59:156-162.

Peterson SW, Ito Y, Horn BW, Goto T (2001) *Aspergillus bombycis*, a new aflatoxigenic species and genetic variation in its sibling species, *A. nomius*. Mycologia 93:689-703.

Pildain MB, Frisvad JC, Vaamonde G, Cabral D, Varga J, Samson RA (2008) Two novel aflatoxin-producing *Aspergillus* species from Argentinean peanuts. Int J System Evol Microbiol 58:725-735.

Pitt JI, Hocking AD (2010) Fungi and food spoilage. Springer, Dordrecht.

Polovinski-Horvatovic M, Juric V, Glamocic D (2009) Two year study of incidence of aflatoxin M_1 in milk in the region of Serbia. Biotechnol Anim Husband 25:713-718.

Price MS, Yu J, Nierman WC, Kim HS, Pritchard B, Jacobus CA, Bhatnagar D, Cleveland TE, Payne GA (2006) The aflatoxin pathway regulator AflR induces gene transcription inside and outside of the aflatoxin biosynthetic cluster. FEMS Microbiol Lett 255:275-279.

Prieto R, Woloshuk CP (1997) *Ord1*, an oxidoreductase gene responsible for conversion of O-methylsterigmatocystin to aflatoxin in *Aspergillus flavus*. Appl Environ Microbiol 63:1661-1666.

Probst C, Callicott KA, Cotty PJ (2012) Deadly strains of Kenyan *Aspergillus* are distinct from other aflatoxin producers. Eur J Plant Pathol 132:419-429.

Rahimi KP, Sharifnabi B, Bahar M (2008) Detection of aflatoxin in *Aspergillus* species isolated from pistachio in Iran. J Pathol 156:15-20.

Rank C, Nielsen KF, Larsen TO, Varga J, Samson RA, Frisvad JC (2011) Distribution of sterigmatocystin in filamentous fungi. Fungal Biol 115:406-420.

Richard JL, Bhatnaga, D, Peterson S, Sandor G (1992) Assessment of aflatoxin and cyclopiazonic acid production by *Aspergillus flavus* isolates from Hungary. Mycopathologia 120:183-188.

Rodríguez A, Rodríguez M, Luque MI, Justensen AF, Córdoba JJ (2011) Quantification of ochratoxin A-producing molds in food products by SYBR Green and TaqMan real-time PCR methods. Int J Food Microbiol 149:226-235.

Rodríguez A, Rodríguez M, Luque MI, Martín A, Córdoba JJ (2012) Real-time PCR assays for detection and quantification of aflatoxin-producing molds in foods. Food Microbiol 31:89-99.

Rokas A, Payne G, Fedorova ND, Baker SE, Machida M, Yu J, Georgianna DR, Dean RA, Bhatnagar D, Cleveland TE, Wortman JR, Maiti R, Joardar V, Amedeo P, Denning DW, Nierman WC (2007) What can comparative genomics tell us about species concepts in the genus Aspergillus? Stud Mycol 59:11-17.

Samson RA, Houbraken J, Thrane U, Frisvad JC, Andersen B (2010) Food and airborne fungi. CBS, Utrecht.

Sargeant K, Sheridan A, O'Kelley J, Carnaghan RBA (1961) Toxicity associated with certain samples of groundnut. Nature 192:1096-1097.

Schmidt-Heydt M, Abdel-Hadi A, Magan N, Geisen R (2009) Complex regulation of the aflatoxin biosynthesis gene cluster of *Aspergillus flavus* in relation to various combinations of water activity and temperature. Int J Food Microbiol 135:231-237.

Sepahvand A, Shams-Ghahfarokhi M, Allameh A, Razzaghi-Abyaneh M (2013) Diversity and distribution patterns of airborne microfungi in indoor and outdoor hospital environments in Khorramabad, Southwest Iran. Jundishapur J Microbiol 6:186-192.

Shapira R, Paster N, Eyal O, Menasherov M, Mett A, Salomon R (1996) Detection of aflatoxigenic molds in grains by PCR. Appl Environ Microbiol 62:3270-3273.

Silva JC, Townsend CA (1996) Heterologous expression, isolation, and characterization of versicolorin B synthase from *Aspergillus parasiticus*. J Biol Chem 272:804-813.

Silva JC, Minto RE, Barry CE III, Hollandand KA, Townsend CA (1996) Isolation and characterization of the versicolorin B synthase gene from *Aspergillus parasiticus*: expansion of the aflatoxin B1 biosynthetic cluster. J Biol Chem 271:13600-13608.

Skory CD Chang PK, Cary J, Linz JE (1992) Isolation and characterization of a gene from *Aspergillus parasiticus* associated with the conversion of versicolorin A to sterigmatocystin in aflatoxin biosynthesis. Appl Environ Microbiol 58:3527-3537.

Slot JC, Rokas A (2011) Horizontal transfer of a large and highly toxic secondary metabolic gene cluster between fungi. Curr Biol 21:134-139.

Soares C, Rodrigues P, Peterson SW, Lima N, Venâncio A (2012) Three new species of *Aspergillus* section *Flavi* isolated from almonds and maize in Portugal. Mycologia 104:682-697.

Squire RA (1981) Ranking animal carcinogens: a proposed regulatory approach. Science 214:877-880.

Tabuc C, Marin D, Guerre P, Sesan T, Bailly JD (2009) Molds and mycotoxin content of cereals in southeastern Romania. J Food Prot 72:662-665.

Taniwaki MH, Pitt JI, Iamanaka BT, Sartori D, Copetti MV, Balajee A, Fungaro MH, Frisvad JC (2012) *Aspergillus bertholletius* sp. nov. from Brazil nuts. PLoS One 7(8):42480.

Tirado MC, Clarke R, Jaykus LA, McQuatters-Gollop A, Frank JM (2010) Climate change and food safety: A review. Food Res Int 43:1745-1765.

Torkar KG, Vengust A (2007) The presence of yeasts, moulds and aflatoxin M_1 in raw milk and cheese in Slovenia. Food Control 19:570-577.

Tóth B, Kótai É, Varga M, Pálfi X, Baranyi N, Szigeti G, Kocsubé S, Varga J (2013) Climate change and mycotoxin contamination in Central Europe: an overview of recent findings. Rev Agricult Rural Devel 2:461-466.

Tóth B, Török O, Kótai É, Varga M, Toldiné Tóth É, Pálfi X, Háfra E, Varga J, Mesterházy Á (2012) Role of Aspergilli and Penicillia in mycotoxin contamination of maize in Hungary. Acta Agronom Hung 60:143-149.

Trail F, Chang PK, Cary J, Linz JE (1994) Structural and functional analysis of the nor-1 gene involved in the biosynthesis of aflatoxins by *Aspergillus parasiticus*. Appl Environ Microbiol 60:4078-4085.

Van der Zijden ASM, Blanche Koelensmid WAA, Boldingh J, Barrett CB, Ord WO, Philip J (1962) *Aspergillus flavus* and Turkey X disease: isolation in crystalline form of a toxin responsible for Turkey X disease. Nature 195:1060-1062.

van Egmond HP, Schothorst RC, Jonker MA (2007) Regulations relating to mycotoxins in food: perspectives in a global and European context. Anal Bioanal Chem 389:147-157.

Varga J, Frisvad JC, Samson RA (2009) A reappraisal of fungi producing aflatoxins. World Mycotoxin J 2:263-277.

Varga J, Frisvad JC, Samson RA (2011) Two new aflatoxin producing species, and an overview of *Aspergillus* section *Flavi*. Stud. Mycol. 69:57-80.

Wicklow DT, Vesonder RF, Mcalpin CE, Cole RJ, Roquebert MF (1989) Examination of *Stilbothamnium togoense* for *Aspergillus flavus* group mycotoxins. Mycotaxon 34:249-252.

Woloshuk CP, Foutz KR, Brewer JF, Bhatnagar D, Cleveland TE, Payne GA (1994) Molecular characterization of *aflR*, a regulatory locus for aflatoxin biosynthesis. Appl Environ Microbiol 60:2408-2414.

Yabe K, Nakamura Y, Nakajima H, Ando Y, Hamasaki T (1991a) Enzymatic conversion of norsolorinic acid to averufin in aflatoxin biosynthesis. Appl Environ Microbiol 57:1340-1345.

Yabe K, Ando Y, Hamasaki T (1991b) Desaturase activity in the branching step between aflatoxins B_1 and G_1 and aflatoxins B_2 and G_2. Agric Biol Chem 55:1907-1911.

Yabe K, Ando Y, Hashimoto J, Hamasaki T (1989) Two distinct *O*-methyltransferases in aflatoxin biosynthesis. Appl Environ Microbiol 55:2172-2077.

Yabe K, Chihaya N, Hamamatsu S, Sakuno E, Hamasaki T, Nakajima H, Bennett JW (2003) Enzymatic conversion of averufin to hydroxyversicolorone and elucidation of a novel metabolic grid involved in aflatoxin biosynthesis. Appl Environ Microbiol 69:66-73.

Yabe K, Hamasaki T (1993) Stereochemistry during aflatoxin biosynthesis: cyclase reaction in the conversion of versiconal to versicolorin B and racemization of versiconal hemiacetal acetate. Appl Environ Microbiol 59:2493-2500.

Yabe K, Nakajima H (2004) Enzyme reactions and genes in aflatoxin biosynthesis. Appl Microbiol Biotechnol 64:745-755.

Yabe K, Nakamura M, Hamasaki T, (1999) Enzymatic formation of G-group aflatoxins and biosynthetic relationship between G and B-group aflatoxins. Appl Environ Microbiol 65:3867-3872.

Yu J (2012) Current understanding on aflatoxin biosynthesis and future perspective in reducing aflatoxin contamination. Toxins 4:1024-1057.

Yu J, Cary JW, Bhatnagar D, Cleveland TE, Keller NP, Chu FS (1993) Cloning and characterization of a cDNA from *Aspergillus parasiticus* encoding an O-methyltransferase involved in aflatoxin biosynthesis. Appl Environ Microbiol 59:3564-3571.

Yu J, Chang PK, Bhatnagar D, Cleveland TE (2000b) Genes encoding cytochrome P450 and monooxygenase enzymes define one end of the aflatoxin pathway gene cluster in *Aspergillus parasiticus*. Appl Microbiol Biotechnol 53:583-590.

Yu J, Chang PK, Cary JW, Bhatnagar D, Cleveland TE (1997) *avnA*, a gene encoding a cytochrome P-450 monooxygenase, is involved in the conversion of averantin to averufin in aflatoxin biosynthesis in *Aspergillus parasiticus*. Appl Environ Microbiol 63:1349-1356.

Yu J, Chang PK, Ehrlich KC, Cary JW, Bhatnagar D, Cleveland TE, Payne GA, Linz JE, Woloshuk CP, Bennett JW (2004) Clustered pathway genes in aflatoxin biosynthesis. Appl Environ Microbiol 70:1253-1262.

Yu J, Chang PK, Ehrlich KC, Cary JW, Montalbano B, Dyer JM, Bhatnagar D, Cleveland TE (1998) Characterization of the critical amino acids of an *Aspergillus parasiticus* cytochrome P-450 monooxygenase encoded by ordA that is involved in the biosynthesis of aflatoxins B_1, G_1, B_2, and G_2. Appl Environ Microbiol 64:4834-4841.

Yu J, Woloshuk CP, Bhatnagar D, Cleveland TE (2000a) Cloning and char-

acterization of *avfA* and *omtB* genes involved in aflatoxin biosynthesis in three *Aspergillus* species. Gene 248:157-167.

Yu JH, Butchko RAE, Fernandes M, Keller NP, Leonard TJ, Adams TH (1996). Conservation of structure and function of the aflatoxin regulatory gene aflR from *Aspergillus nidulans* and A. *flavus*. Curr Genet 29:549-555.

Zalar P, Frisvad JC, Gunde–Cimerman N, Varga J, Samson RA (2008) Four new species of *Emericella* from the Mediterranean region of Europe. Mycologia 100:779-795.

Volume 57(2):109-112, 2013
Acta Biologica Szegediensis
http://www.sci.u-szeged.hu/ABS

ARTICLE

Mass spectrometric investigation of alamethicin

Tamás Marik*, Csaba Várszegi, László Kredics, Csaba Vágvölgyi, András Szekeres

Department of Microbiology, University of Szeged, Szeged, Hungary

ABSTRACT The peptaibols, such as alamethicin are secondary metabolites belonging to the family of fungal peptide antibiotics. These compounds are linear, amphipathic oligopeptides classified into 4 subfamilies and composed of 5-20 amino acids. Their backbones usually contain several nonproteinogenic amino acid residues representing characteristic building blocks of the structure. In our present work, the mass spectrometric analysis of alamethicin has been investigated by on-line reversed-phase high performance liquid chromatography (HPLC) coupled to electrospray ionization tandem mass spectrometry (ES-MS). Initially, the parameters of the MS were optimized by the continuous infusion of an alamethicin standard solution directly into the ESI source. Then, the proper HPLC method was developed for the analysis of the alamethicin components, which was capable to separate the peaks of F50-5, F50-6a, F50-7 and F50-8b from each other, which could be identified based on their mass spectra.
Acta Biol Szeged 57(2):109-112 (2013)

KEY WORDS

alamethicin
mass spectrometry
peptaibol
α-aminoisobutyric acid
RP-HPLC-UV/ESI-IT-MS

A number of economically important antibiotics, secondary metabolites and extracellular enzymes are produced by species of the genus *Trichoderma*, including a unique peptide group of antibiotics (Sivasithamparam and Ghisalberti 1998). Although these peptide-type molecules are produced by other organisms as well, most of them are produced by this genus or by species from closely related genera (Degenkolb et al. 2003). They have characteristic molecular weights of 500-2200 Da and contain numerous non-proteinogenic, α,α-dialkylated amino acids like isovaline (Iva) and α-aminoisobutyric acid (Aib), an acetylated N-terminus, and an amino alcohol, mostly phenylalaninol at the C-terminal end (Szekeres et al. 2005). The name peptaibol comes from the words peptide, Aib, and amino alcohol. The peptaibols produced by *Trichoderma* species regularly contain 18-20 amino acid residues, and their unusal amino acid content is synthesized through non-ribosomal biosynthesis (Marahiel et al. 1997). The bioactivities of peptaibols are mainly related to formation of channels in lipid membranes, which are containing several hydrophobic transmembrane helices surrounding a central pore (Duclohier 2004; Whitmore et al. 2004).

The first described peptaibol was reported in 1967, which was isolated from the ferment broth of *Trichoderma viride* (later reidentified as *T. arundinaecum*) and named alamethicin (ALM) (Meyer and Reusser 1967; Leitgeb et al. 2007; Kredics et al. 2013). Based on their retention factor values in thin layer chromatography (TLC), ALM is composed of two major classes, an acidic and a neutral group distinguished by Glu/Gln18 exchange and named ALM F30 (85%) and ALM F50 (12%), respectively, and an additional minor component (ALM F20) (Kirschbaum et al. 2003; Degenkolb et al. 2007). Moreover, some further groups of ALM (ALM-F40, ALM-F60 and ALM-F70) were also recognised by TLC in low concentrations (Melling and McMullen1975).

In our earlier work we described a sensitive and low-cost biological pre-screening for the detection of peptaibol compounds (Marik et al. 2013). The present study is dealing with the establishment of a proper analytical method enabling the sensitive detection and identification of these fungal peptides.

Materials and Methods

Materials

Methanol, acetonitrile for sample preparation and eluents were purchased from VWR (Hungary). The trifluoroacetic acid (TFA) and ALM standards were obtained from Sigma-Aldrich (Hungary). Membrane-filtered, deionized water for HPLC runs was produced by Millipore water purification equipment (Merck, Hungary) with a resistivity of 18MΩ. Reversed phase (RP) – high performance liquid chromatography (HPLC)-UV/electrospray ionization (ESI) – mass spectrometric (MS) investigations were performed on an Agilent 1100 (Palo Alto, USA) modular HPLC system coupled to a Varian 500 (Agilent, USA) ion trap (IT)-MS. The HPLC system was equipped with a degasser (G1379A), a binary pump (G1376A), a micro-well plate autosampler (G1229A) and a diode array detector (G1315B). The HPLC and the MS were controlled by the Chemstation B.02.01 and MS Workstation 6.6 softwares, respectively.

Accepted March 3, 2014
*Corresponding author. E-mail: mariktamas88@gmail.com

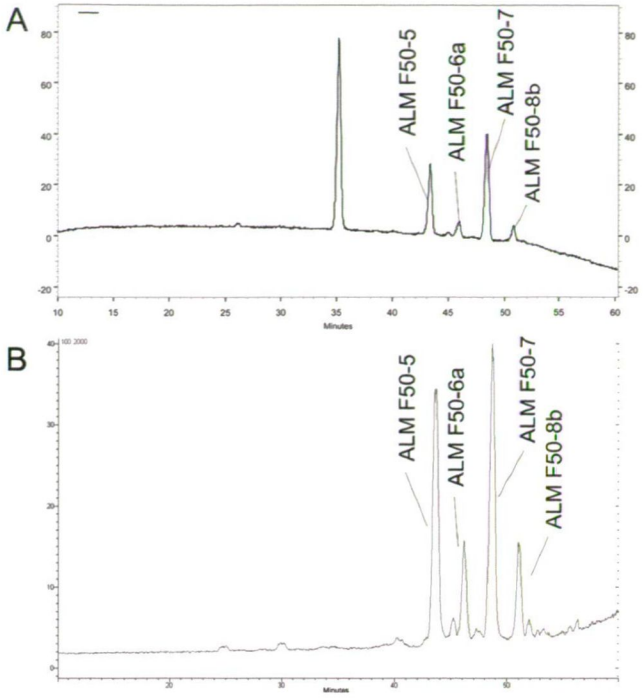

Figure 1. HPLC-UV (A) and HPLC-ESI-MS chromatogram of ALM components.

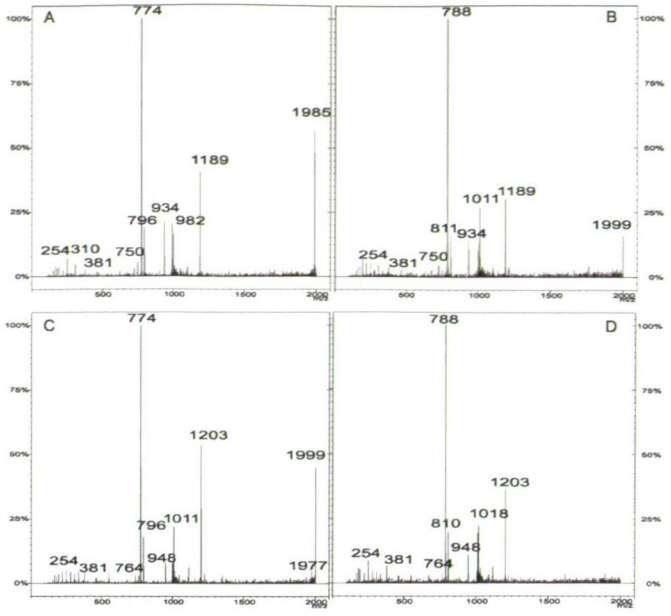

Figure 2. HPLC-ESI-MS spectra of ALM-F50-5 (A), ALM-F50-6a, ALM-F50-7 and ALM-F50-8b.

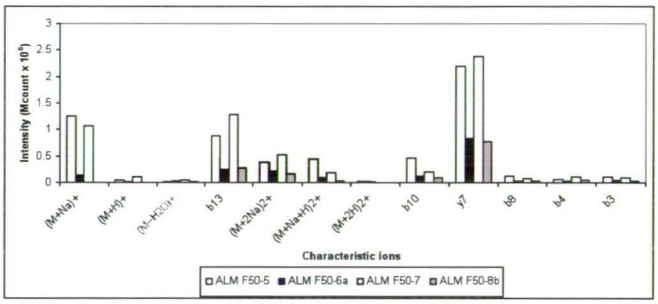

Figure 3. Abundances of the characteristic fragments of ALM components appearing on the HPLC-ESI-MS spectra.

HPLC parameters

The HPLC system solvent A was water with 0.05% (v/v) TFA, while solvent B was MeCN/MeOH 1/1 (v/v) with 0.05% (v/v) TFA. Separations were performed using a Phenomenex Gemini NX-C18 (Gen-Lab Kft., Hungary) (150 mm x 2.0 mm, 3 µm) HPLC column with mobile phase flow rate of 0.2 mL/min. The column temperature was maintained at 40°C using a Jones Model 7990 Space column heater (Jones Chromatography, UK). The length of the connecting capillaries (127 µm ID) between injector and column and column to MS nebulizer were mineralized by placing the column heater in optimal position. The gradient elution started with 65% B held for 5 min and increased linearly to 80% B at 45 min, and then to 100% B at 70 min, which was decreased to the initial percentage until the pressure stabilized. The injection volume was 5 µl.

Ion trap mass spectrometric conditions

The MS examinations were made with a Varian 500MS Ion Trap mass spectrometer equipped with an atmospheric-pressure ESI source in scan mode at normal scan speed. Positive and negative ESI Parameters were: spray chamber temperature, 50°C; drying gas (N_2) pressure and temperature, 30 psi and 350°C, respectively; nebulizer gas (N_2) pressure, 50 psi; needle voltage, 5704 V/-5000 V; spray shield voltage, 600 V/-600 V. General Parameters were: maximum scan times, 2.78; µScans averaged, 2 µScans; data rate, 0.36 Hz; multiplier offset, 0. Ionization Control Parameters were: target TIC, 100%; max ion time, 250000 µsec. The full scan parameters were: capillary voltage, 66 V; RF loading, 147%; Low mass, 100 *m/z*; High mass, 2000 *m/z* high.

Results and Discussion

Initially, in order to optimize the ESI-IT-MS, the mass spectrometric parameters including RF loading, capillary- and needle voltages were tuned in both positive and negative modes by continuous infusion (5 µl/min) of an ALM standard solution (100 ng/µl) with the built-in syringe pump of the instrument. Based on the reported data the purchased standard mainly represents definitely the neutral ALM F50 peptides (Kirschbaum et al. 2003), thus during the optimization, the

Table 1. Identifications of characteristic ions (*m/z*) of ALM components acquired in positive mode.

	ALM components			
	5	6a	7	8b
R_t (min)	43.7	46.2	48.5	51.1
$(M+H)^+$	1963	1977	1977	1991
$(M+Na)^+$	1985	1999	1999	Out of range
$(M+2Na)^{2+}$	1004	1011	1011	1018
$(M+Na+H)^{2+}$	993	1000	1000	1007
$(M+2H)^{2+}$	982	989	989	996
$(M-H_2O)^+$	1945	1959	1959	1973
b_{13}	1189	1189	1203	1203
b_{10}	934	934	948	948
b_8	750	750	764	764
b_4	381	381	381	381
b_3	310	310	310	310
y_7	774	788	774	788

following protonated/deprotonated molecular ions ($(M+H)^+$/$(M-H)^-$) of microheterogenity mixture of ALM components were monitored in positive/negative mode: *m/z* 1963/1961 for ALM F50-5, *m/z* 1977/1975 for ALM F50-6a/6b/7 and *m/z* 1991/1989 for ALM F50-8b/8c. After the setup of ion optic parameters, the optimal ion source conditions such as nebulizer gas- and drying gas pressures and source temperatures were estimated via flow injection analysis in the mobile phase constitution 1/1 (v/v) of eluent A/B.

For further investigations, ALM was separated by HPLC on an analytical ODS column equivalent to the stationary phase used by Krause et al. (2006) as the general method for the peptaibol analysis, but other than applied by Kirschbaum et al. (2003) specifically for the ALM separation (Fig. 1).

Mass spectrometric measurements of peptaibols usually generate molecular ions and more or less complete series of characteristic fragment ions (Kirschbaum et al. 2003; Krause et al. 2006). However, in our case, the molecular ions showed much lower abundance due to their easily disintegration than the sodium adduct form in positive mode with exception of ALM-F50-8b falling its correspondent *m/z* value out of the examined mass range (Fig. 2, Fig. 3), which could make the identification of the unknown peptaibols difficult in our further screening studies. With the ESI negative mode ionization the $(M-H)^-$ masses were visible only with moderate intensity.

The most abundant ions were the y_7 and b_{13} fragment ions resulting from cleavage of the extremely labile Aib-Pro bond of the 20 residue peptides at position 6-7 from the carboxyl terminus in positive mode. Thus, the summation of the proper y and b ions could serve the mass of hydrogen adduct of the molecular ion. It is interesting that the double charged adduct ions showed high intensity in the used MS instrument such as $(M+2Na)^{2+}$ and $(M+Na+H)^{2+}$ (Fig. 2, Fig. 3), which was not observed earlier. Relatively high were the signals of the b_{10} fragments due to the break of the Aib-Gly bond, although their y_{10} counter-fragments were not detected. At the lower *m/z* values with lower intensity, but detectable level, the series of shorter b fragments were recorded including b_{10}, b_8, b_4 and b_3 ions (Fig. 2, Fig. 3). From the mass differences (Δm) of fragment ions, the presence of the marker amino acid Aib, characterized by *m/z* 85.1 Da (Krause et al. 2006) could not be deduced. The fragment ions and the acquired corresponding masses are shown in Table 1.

The resulting peaks were in accordance with the ALM components reported previously (Kirschbaum et al. 2003), eluted with proper resolutions (Fig. 1). Furthermore, based on the mass spectra acquired from certain peaks, the different components could be identified, some of which were denoted earlier only as mixture of isomers including ALM-F50-4b/5, ALM-F50-6a/6b and ALM-F50-8b/8c (Kirschbaum et al. 2003). In the case of ALM-F50-4b/5 eluted at 43.7 min, the characteristic ions of the 4b component were not presented regarding to the single charged and double charged sodium adducts at the *m/z* 1971 and 998, respectively (Fig. 2A). The peak of ALM-F50-6a/6b at 46.2 min contains also only the 6a component, because of the absence of *m/z* 930 (b_{10} fragment) regarding the ALM-F50-6b (Fig. 2B). Similarly, in the case of ALM-F50-8b/8c at 51.1 min, only the ALM-F50-8b was involved due to the lack of y_7 (*m/z* 744) and b_{10} (*m/z* 962) fragments originated from the fragmentation of ALM-F50-8c (Fig. 2D) while the ALM-F50-8c eluted at 48.5 min showing the highest peak area (Fig. 2C). There was a peak with a remarkable area on the UV chromatogram at approx. 35 min, but it was not active mass spectrometrically.

The results achieved in this study could contribute to the identification of other unknown peptaibol molecules isolated from ferment broth of different *Trichoderma* species based on the gathered data about the MS fragmentation properties, which are in the scope of our further research activities.

Acknowledgement

This research was supported by the European Union and the State of Hungary, co-financed by the European Social Fund in the framework of TÁMOP-4.2.4.A/ 2-11/1-2012-0001 'National Excellence Program'.

References

Degenkolb T, Berg A, Gams W, Schlegel B, Gräfe U (2003) The occurrence of peptaibols and structurally related peptaibiotics in fungi and their mass spectrometric identification via diagnostic fragment ions. J Peptide Sci 9:666-678.

Degenkolb T, Kirschbaum J, Brückner H (2007) New sequences, constituents, and producers of peptaibiotics: an updated review. Chem Biodivers 4:1052-1067.

Duclohier H (2004) Helical kink and channel behaviour: a comparative study with the peptaibols alamethicin, trichotoxin and antiamoebin. Eur Biophys J 33:169-174.

Kirschbaum J, Krause C, Winzheimer RK, Brückner H (2003) Sequences of alamethicins F30 and F50 reconsidered and reconciled. J Peptide

Sci 9:799-809.

Krause C, Kirschbaum J, Brückner H (2006) Sequence diversity of the peptaibol antibiotic suzukacillin-A from the mold *Trichoderma viride*. Amino Acids 30:435-443.

Kredics L, Szekeres A; Czifra D; Vágvölgyi Cs, Leitgeb B (2013) Recent results in alamethicin research. Chem Biodivers 10:744-771.

Leitgeb B, Szekeres A, Manczinger L, Vágvölgyi Cs, Kredics L (2007) The history of alamethicin: a review of the most extensively studied peptaibol. Chem Biodivers 4:1027-1051.

Marahiel MA, Stachelhaus T, Mootz HD (1997) Modular peptide synthetases involved in nonribosomal peptide synthesis. Chem Rev 97:2651-2673.

Marik T, Szekeres A, Várszegi C, Czifra D, Vágvölgyi Cs, Kredics L (2013) Rapid bioactivity-based pre-screening method for the detection of peptaibiotic-producing *Trichoderma* strains. Acta Biol Szeged 57:1-7.

Melling J, McMullen AJ (1975) Separation, purification and characterisation of alamethicins produced from *Trichoderma viride*. ISC-IAMS Proceedings Science Council of Japan 5:446-452.

Meyer CE, Reusser F (1967) A polypeptide antibacterial agent isolated from *Trichoderma viride*. Experientia 23:85-86.

Sivasithamparam K, Ghisalberti EL (1998) Secondary Metabolism in *Trichoderma* and *Gliocladium*. In Kubicek, C. P., Harman, G. E. (Ed.), *Trichoderma* and *Gliocladium*: Basic Biology, Taxonomy and Genetics, London, UK, Taylor & Francis, pp. 139-191.

Szekeres A, Leitgeb B, Kredics L, Antal Z, Hatvani L, Manczinger L, Vágvölgyi C (2005) Peptaibols and related peptaibiotics of *Trichoderma*. A review. Acta Microbiol Immunol Hung 52:137-168.

Whitmore L, Wallace BA (2004) The peptaibol database: a database for sequences and structures of naturally occurring peptaibols. Nucl Acid Res 32:593-594.

Volume 57(2):113-116, 2013
Acta Biologica Szegediensis
http://www.sci.u-szeged.hu/ABS

ARTICLE

Evaluation of five essential oils for the control of food-spoilage and mycotoxin producing fungi

Csilla Gömöri[1]*, Elvira Nacsa-Farkas[1], Erika Beáta Kerekes[1], Sándor Kocsubé[1], Csaba Vágvölgyi[1], Judit Krisch[2]

[1]Department of Microbiology, University of Szeged, Szeged, Hungary, [2] Institute of Food Engineering, University of Szeged, Szeged, Hungary

ABSTRACT The inhibition of growth and aflatoxin production by essential oils (EOs) of cinnamon, clary sage, juniper, lemon and marjoram were investigated on food-spoilage fungi *Aspergillus parasiticus var.globosus, Fusarium graminearum* and *Fusarium culmorum.* The antifungal effect of the EOs was observed by determination of growth-rate (mm/day) and antifungal index (%) using reversed Petri-dish method. Aflatoxin production of *A. parasiticus* was monitored by thin layer chromatography (TLC). The growth of *A. parasiticus* was significantly decreased (P<0,001) by marjoram and clary sage EOs. TLC results revealed only a slight effect on aflatoxin production: cinnamon and clary sage EOs found to decrease the amount of aflatoxin B1 and G2. *F. graminearum* and *F. culmorum* showed almost similar response to the EOs. In both cases cinnamon EO caused a total inhibition of growth, while lemon EO was ineffective. Juniper significantly (P<0,003) inhibited the growth of *F. culmorum* but had no effect on *F. graminearum*. The EOs tested in this study may be potential antimicrobial compounds for use as food preservatives and anti-aflatoxin agents. **Acta Biol Szeged 57(2):113-116 (2013)**

KEY WORDS

essential oils
growth- inhibition
aflatoxin
Aspergillus
Fusarium

Many fungal species produce mycotoxins contaminating various foods and feed (Naeini et al. 2010). Among them, aflatoxin synthetised by several fungal species from which *Aspergillus flavus* and *Aspergillus parasiticus* are the most important ones. This toxin is produced during plant growth, harvest, storage, and food processing. Aflatoxin is extremely hazardous: it has a hepatotoxic, carcinogenic and immunosuppressive effect. It may also affect the epidemiology of many diseases and it poses serious health risks in those countries where the toxin content of food and feed commodities are not properly monitored and controlled (Williams et al. 2004). *Fusarium culmorum*, and more recently, *F. graminearum* are the most common causes of Fusarium ear blight and both of them produce trichothecenes and *F. graminearum* also produces zearalenone. Many of these mycotoxins are possible immunosuppressants (Hope et al. 2005).

Global warming may strongly influence the occurrence and distribution of mycotoxin producing fungi. Climate change can lead to the increasing abundance of thermotolerant species (especially in extremely hot years) in regions with temperate climate, including Central Europe. This is accompanied with the appearance of their mycotoxins in agricultural products (Tóth et al. 2013). From all these reasons, mycotoxins are in the focus of food safety concerns today. There is an increasing need to find efficient and easy-to-use mycotoxin-reducing strategies (Naeini et al. 2010).

Several authors demonstrated that, most of the essential oils extracted from aromatic plants, have antimicrobial, antifungal effect and/or antioxidant properties. That means they have also a potential to act against mycotoxin-producing fungi. There are some results which suggest that in an experimental system the extent of inhibition of fungal growth and aflatoxin production depends on the concentration of essential oils used (Atanda et al. 2006; Sindhu et al. 2011). A great advantage of EOs is their bioactivity in the vapour-phase, a characteristic that makes them attractive as feasible fumigants for stored product protection (Tripati and Dubey 2004). It is also worth to mention that EOs proved their potential as antimicrobial compounds in food preservation (Nguefack et al. 2004). The recent study has the aim to investigate the antifungal and anti-aflatoxin production activity of five essential oils on three mycotoxin-producing fungi, *A. parasiticus, F. culmorum* and *F. graminearum.*

Materials and Methods

Microorganisms

Aspergillus parasiticus CBS 260.67 was obtained from the Centralbureau voor Schimmelcultures (CBS, Utrecht, The Netherlands). *Fusarium graminearum* NRRL 28436 and *Fusarium culmorum* NRRL 29379 were provided by the

Accepted March 17, 2014
*Corresponding author. E-mail: gmri.csilla@gmail.com

Table 1. Chemical composition (%) of the essential oils tested.

Essential oil	Compound	Chemical composition (%)
Lemon	limonene	83.20
	β-pinene	9.54
	γ-terpinene	5.60
Juniper	α-pinene	40.70
	β-pinene	36.00
	o-cymene	18.90
Marjoram	terpinen-4-ol	33.58
	γ-terpinene	19.53
	β-phellandrene	8.00
Clary sage	linalyl acetate	84.00
	linalool	13.60
Cinnamon	cinnamic aldehyde	93.10
	cinnamyl- acetate	2.50

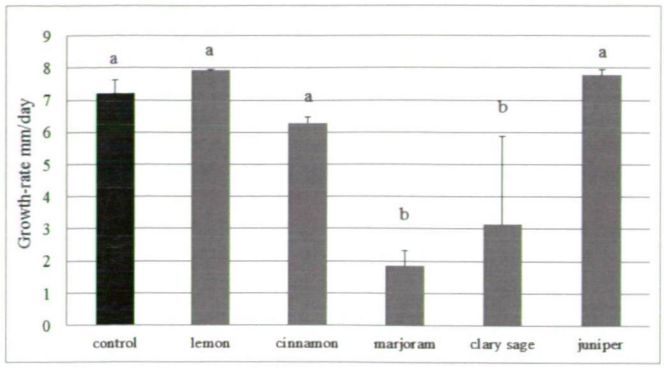

Figure 1. Average growth rate ± SD of *A. parasiticus* after treatment with different EOs (20 mg). Different letters on the top of columns represent significantly different results (P<0,05).

Table 2. Antifungal index of the investigated essential oils (20 mg/paper disc).

	Antifungal index (%)				
	Cinna-mon	Lemon	Marjo-ram	Clary sage	Juniper
A. parasiticus	14,93	-3,17	76,47	28,05	-0,45
F. graminearum	96,67	0	43,33	9,26	0
F. culmorum	96,67	0	68,7	73,7	0

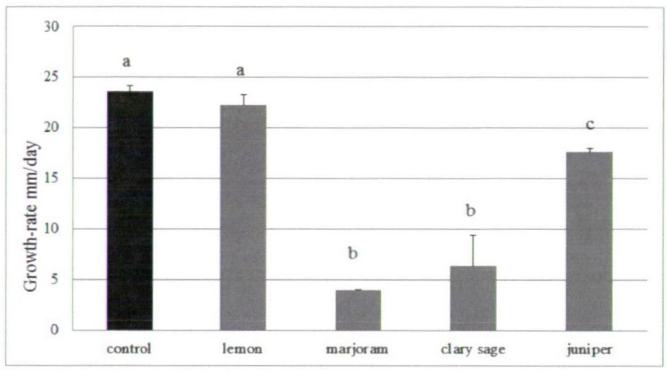

Figure 2. Average growth rates ± SD of *F. culmorum* after treatment with different EOs (20 mg). Different letters on the top of columns represent significantly different results (P<0,05).

National Center for Agricultural Utilization Research (NRRL, Peoria, Illinois). Potato dextrose agar (PDA, Difco) was used for the cultivation of *Fusarium* species and malt extract agar (0,5% malt extract, 0,5% yeast, 0,5% glucose, 2% agar) for *A. parasiticus*.

Essential oils

Five essential oils – cinnamon *(Cinnamomum zeylanicum)*, clary sage *(Salvia sclarea)*, juniper *(Juniperus communis)*, lemon *(Citrus lemon)* and marjoram *(Origanum majorana)* - were used in the experiments. They were purchased from Aromax Natural Products Zrt. (Budapest, Hungary). The composition of the oils was determined by GC-MS (Agilent; GC: 6850 Series II; MS: 5975C VL MSD) using an Agilent 19091S-433E colonna at the laboratory of Aromax. EOs were prepared by steam distillation of leaves or bark of the plants, except lemon EO; that was cold-pressed from lemon peel. Table 1 presents the chemical compositions of these essential oils.

Antifungal activity of EOs

To investigate the antifungal effect of the EOs reversed Petri-dish method was used. Petri-dishes (9 cm diameter) contained malt extract agar (for *A. parasiticus*) or potato dextrose agar (for *Fusarium* species) were inoculated at the centre with a mycelial disc (3 mm diameter) taken from the periphery of a fungus colony grown for 72 h.

Paper discs (10 mm in diameter) were fixed to the inner top of the Petri-dish with a drop of agar and impregnated with different amounts of EOs (5 mg, 20 mg or 40 mg). Control plates contained discs with distilled water. Plates were closed with parafilm and were incubated in reversed position at 25°C for 10 days. The colony diameter was recorded each day.

The growth-rate was calculated by linear regression of the linear phase of colony growth curves. The growth of fungal cultures containing different concentrations of the investigated EOs was compared with the control culture growing without any EOs (Passone et al. 2012).

Antifungal index was calculated by the following formula:

Antifungal index (%) = $(1- (D_t/D_c))x\ 100$

Dt diameter of EO treated mould colonies (mm)

Dc diameter of control mould colonies (mm) (Shukla et al. 2012).

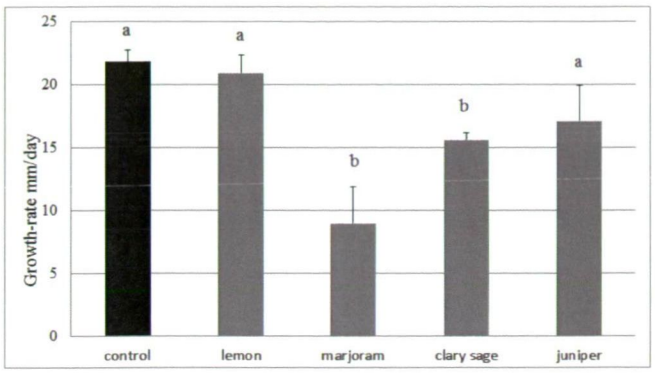

Figure 3. Average growth rates ± SD of *F. graminearum* after treatment with different EOs (20 mg). Different letters on the top of columns represent significantly different results (P<0,05).

Determination of aflatoxin production

Effect of the EOs on aflatoxin production was investigated at 5 and 40 mg/paper disk concentration of the EOs. At the 10th day of growth 10 round discs (12 mm diameter) were cut from the colony of *A. parasiticus* and were extracted with 10 mL chloroform. 1 mL extract was evaporated to dryness and redisolved in 100 µL chloroform.

Aflatoxin standard (B1, B2, G1, G2) produced by Trilogy Analytical Laboratory (Washington MO, Missouri, USA ((TS-108 (P86) was used in 5 µg/ml concentration.

One µl of each sample and 20 µl of the standard were used to the thin-layer chromatography on silica gel F60 aluminium sheets. The chromatogram was developed in a mixture of toluene-ethyl acetate-formic acid in 6:3:1 ratio. The bands were visualized and photographed under UV light. Colour intensity of bands representing aflatoxin types were compared visually.

All experiments were made in three replicates per treatment, except for the identification of aflatoxins which was carried out once.

Statistical analysis

Results were analysed using the Windows R-2.8 programme. One-way ANOVA was used to determine the differences between the control and treated samples.

Results and Discussion

For the proper comparability of the results, fungal growth-rates and antifungal indexes are presented using 20 mg/paper disk EO concentration. In most cases there were no inhibitory effect at lower concentrations and no growth at higher concentrations.

The growth rate of *A. parasiticus* compared to the untreated sample showed a minimal enhancement by juniper and lemon oil but these changes were not significant (P>0,05). Marjoram and clary sage decreased the growth rate significantly (P<0,05) (Fig. 1). Marjoram EO showed the best growth inhibition with the antifungal index of 76.4% (Table 2). The inhibitory effect of clary sage also differed significantly (P<0,001) from the control sample.

F. graminearum and *F. culmorum* showed almost similar response after treatment with the EOs (Figs. 2-3). Both of the controls grew very quick: the colony diameter of the control sample of *F. graminearum* has reached 90 mm (diameter of the Petri dish) on the 5th day and the control *of F. culmorum* on the 4th day. Lemon EO was ineffective in both cases. Juniper significantly (P<0,003) inhibited the growth of *F. culmorum* but had no effect on *F. graminearum* (Table 2).

In cases of *Fusarium* strains cinnamon EO was the best inhibitor, a total inhibition of growth was obtained with this EO. Marjoram significantly inhibited the growth of *F. culmorum* (p<0.001, antifungal index: 68.7%) and *F. graminearum* (p<0.001, antifungal index: 43.33%). Clary sage inhibited the growth of both *Fusarium* species, having an antifungal index of 73.7% for *F. culmorum* and an antifungal index of 9.26% for *F. graminearum (*Table 2).

Results regarding aflatoxin production can be seen on Figure 4. Results of TLC show that mycotoxin production of *A. parasiticus* was slightly influenced by the EOs. Compared to the control samples there seems to be a difference in B1, G1 production in the case of treatment with 5 mg cinnamon, and 5 mg and 40 mg of clary sage but further quantitative studies are needed to confirm this examination.

This study has reported the antifungal properties of five essential oils tested against three food spoilage and mycotoxin producing fungi. Higher antifungal activity was found in the EOs from cinnamon, marjoram and clary sage. Cinnamon EO caused complete inhibition of the growth of the tested fungi.

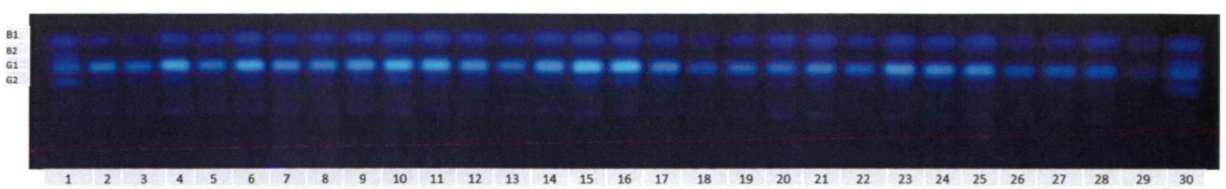

Figure 4. Thin layer chromatography of aflatoxin production by *A. parasiticus.* Standard (1, 30), control samples (2, 3, 4), juniper 5 mg (5,6,7), juniper 40 mg (8, 9, 10), lemon 5 mg (11, 12, 13), lemon 40 mg (14, 15, 16), cinnamon 5 mg (17, 18, 19), cinnamon 40 mg (20, 21), marjoram 5 mg (22, 23, 24), clary sage 5 mg (25, 26, 27), clary sage 40 mg (28, 29).

This result is similar to the findings of Soliman and Badeaa (2002) where the effect of cinnamon EO was tested on *A. flavus, A. parasiticus, A. ochraceus* and *F. moniliforme*. Many previous studies had verified cinnamon oil as a fungicide agent against a lot of fungi and showed its high fungicidal activity (Sinha et al. 1993; Mukherjee and Nandi 1994). This activity of cinnamon EO is mainly due to its major component, cinnamaldehyde which is a powerful fungistatic agent (Burt 2004; Bakkali et al. 2008).

Further studies in connection with the mycotoxin-reducing effect of these EOs will be necessary to reveal all the circumstances of this process.

Acknowledgement

This research was supported by the grants of the Hungarian-Romanian Intergovernmental S&T Cooperation Programme TÉT_10-1-2013-0019.

References

Atanda OO, Akpan I, Oluwafemi F (2006) The potential of some spice essential oils in the control of *A. parasiticus* CFR 223 and aflatoxin production. Food Control 18:601-607.

Bakkali F, Averbeck S, Averbeck D, Idaomar M (2008) Biological effects of essential oils – a review. Food Chem Toxicol 46:446-475.

Burt S (2004) Essential oils: their antibacterial properties and potential applications in foods – a review. Int J Food Microbiol 94:223-253.

Hope R, Aldred D, Magan N (2005) Comparison of environmental profiles for growth and deoxynivalenol production by *Fusarium culmorum* and *F. graminearum* wheat grain. Lett Appl Microbiol 40:295-300.

Mukherjee PS, Nandi B (1994) Poultry feed preservation from fungal infection by cinnamon oil. J Mycopathol Res 32(1):1-5.

Naeini A, Ziglari T, Shokri H, Khosravi AR (2010) Assessment of growth-inhibiting effect of some plant essential oils on different *Fusarium* isolates. J Mycol Médic 20: 174-178.

Nguefack J, Leth V, Amvan Zollo PH, Mathur SB (2004) Evaluation of five essential oils from aromatic plants of Cameroon for controlling food spoilage and mycotoxin producing fungi. Int J Food Microbiol 94:329-334.

Passone AM, Girardi SN, Ferrand AC, Etcheverry M (2012) In vitro evaluation of five essential oils as botanical fungitoxicants for the protection of stored peanuts from *Aspergillus flavus* and *A. parasiticus* contamination. Int Biodeter 70:82-88.

Shukla R, Singh P, Prakash B, Dubey NK (2012) Efficacy of *Acorus calamus* L. essential oil as a safe plant-based antioxidant, Aflatoxin B_1 suppressor and broad spectrum antimicrobial against food-infesting fungi. Food Sci Technol 48:128-135.

Sindhu S, Chempakam B, Leela NK, Suseela Bhai R (2011) Chemoprevention by essential oil of turmeric leaves (*Curcuma longa* L.) on the growth of *Aspergillus flavus* and aflatoxin production. Food Chem Tox, 49:1188-1192.

Sinha KK, Sinha AK, Ggajendra P, Prasad G (1993) The effect of clove and cinnamon oils on growth of and aflatoxin production by *A. flavus*. Lett Appl Microbiol 16(3):114-117.

Soliman KM, Badeaa RI (2002) Effect of oil extracted from some medicinal plants on different mycotoxigenic fungi. Food Chem Toxicol 40:1669-1675.

Tóth B, Kótai É, Varga M, Pálfi X, Baranyi N, Szigeti Gy, Kocsubé S, Varga J (2013) Climate change and mycotoxin contamination in Central Europe: an overview of recent findings. Rev Agric Rural Develop 2(1):461-466.

Williams JH, Phillips TD, Jolly PE, Stiles JK, Jolly CM, Aggarwal D (2004) Human aflatoxicosis in developing countries: a review of toxicology, exposure, potential health consequences, and interventions. Am J Clin Nutr 80:1106-1122.

Volume 57(2):117-120, 2013
Acta Biologica Szegediensis
http://www.sci.u-szeged.hu/ABS

ARTICLE

The complete degradation of acetanilide by a consortium of microbes isolated from River Maros

Lóránt Hatvani[1]*, László Manczinger[1], Tamás Marik[1], Szilvia Bajkán[2], Lívia Vidács[2], Ottó Bencsik[1], András Szekeres[1], Isidora Radulov[3], Lucian Nita[3], Csaba Vágvölgyi[1]

[1]Department of Microbiology, University of Szeged, Szeged, Hungary, [2]Lower Tisza District Water Directorate (ATI-VIZIG), Szeged, Hungary, [3]Banat University of Agricultural Sciences and Veterinary Medicine, Timişoara, Romania

ABSTRACT Chemical pollutants occurring in rivers may have severe effects on human health along with being harmful to the environment. Bioaugmentation is a potential tool for the removal of xenobiotics from soil and water therefore the objectives of this study were the isolation, identification and characterization of microbes with acetanilide- and aniline-degrading properties from the River Maros. Microbes isolated on minimal media containing acetanilide or aniline-HCl as a sole carbon and nitrogen source were considered as acetanilide- or aniline-degraders. The decomposition of acetanilide and aniline were followed by High Pressure Liquid Chromatography (HPLC). An acetanilide-degrading bacterium, identified as *Rhodococcus erythropolis*, was able to convert acetanilide to aniline, which was further decomposed by the fungal isolate *Aspergillus ustus* when the two microbes were co-cultivated in a minimal medium containing acetanilide as a sole carbon and nitrogen source. The strains isolated in this study might be used in approaches addressing the biodegradation of acetanilide and aniline in the environment.
Acta Biol Szeged 57(2):117-120 (2013)

KEY WORDS

xenobiotics
bioaugmentation
Aspergillus ustus
Rhodococcus erythropolis

Numerous chemical pollutants frequently occurring in rivers, such as heavy metals, polycyclic aromatic hydrocarbons (PAHs) or pesticides and their degradation products may have serious effects on environment and human health. Wang et al. (2012) observed great metal carcinogenic risk in drinking water sources in China, where the co-occurrence of PAHs with Cr represented the highest risk factor. Eleven different PAHs were detected in water and sediment in Mexico with the dominance of phenantrene. Toxicity tests revealed the potential harmful effect of the observed PAHs on aquatic organisms (Jaward et al. 2012). Liu et al. (2012) identified sixteen human-originated PAHs in water bodies in China. These examples indicate that human activities seriously affect water resources and contaminated drinking water represents a potential risk factor for human health due to the mutagenic and carcinogenic effect of PAHs. Numerous widely-used pesticides are acetanilide- and aniline-derivatives (Stamper and Tuovinen 1998; Sanyal and Kulshrestha 2002; Munoz et al. 2011; Milan et al. 2012; Sondhia 2012; Chatterjee et al. 2013), which may affect human health seriously, including for instance methemoglobinemia (Kusin et al. 2012) and various types of cancer (Hanley et al. 2012).

Biodegradation of xenobiotics by microorganisms represents an alternative way for the removal of chemical pollutants from surface and groundwater. Decomposition of phenantrene by *Vibrio parahaemolyticus* was reported by Smith et al. (2012), whereas Ellegaard-Jensen et al. (2013) documented the biodegradation of the phenylurea herbicide diuron by *Mortierella* sp.

Based on the above statements, the aim of this study was the isolation, identification and characterization of acetanilide- and aniline-degrading microbes from River Maros.

Materials and Methods

Materials

For isolating acetanilide- and aniline-degrading microorganisms solid minimal medium (SMM: 1 g KH_2PO_4, 3 g Na_2HPO_4, 1 g $MgSO_4$, 20 g agarose per liter) supplemented with 1 g acetanilide or aniline-HCl per liter as a sole carbon and nitrogen source, was used. The isolated acetanilide-degrading bacteria and fungi were examined throughout the study.

For polymerase chain reaction (PCR), bacterial strains were grown in liquid yeast extract-glucose medium (YEGM: 2 g yeast extract, 5 g glucose per liter).

The aniline- and acetanilide-degrading ability of the isolates was tested following cultivation in liquid minimal medium (LMM: 1 g KH_2PO_4, 3 g Na_2HPO_4, 1 g $MgSO_4$ per liter) supplemented with 50 mg acetanilide per liter as a sole carbon and nitrogen source.

Accepted March 3, 2014
*Corresponding author. E-mail: lorant.hatvani@gmail.com

Unless specified, all chemicals used in the study were purchased from Sigma-Aldrich.

Methods

Water sampling and isolation of acetanilide- or aniline-degrader microorganisms

Water samples were collected at 10 different locations of the Romanian (Arad, Bodrog, Munar, Periam Port, Igris) and Hungarian parts (Nagylak, Magyarcsanád, Apátfalva, Makó, Deszk) of River Maros (Mures) in April, July and October 2012, as well as in January 2013. Fifty µl of the water samples were spread onto the surface of SMM and the plates were incubated at 25°C for 7 days. The appearing colonies were considered as potential acetanilide- or aniline-degraders. These were reinforced with sub-culturing to the same medium.

Degradation of acetanilide- or aniline by mixed microbial cultures

Each acetanilide-degrading bacterial isolate were inoculated together with the aniline-degrading fungal isolate SZMC 20913 into LMM in a final concentration of 10^7 bacterial cells/ml and the same concentration of fungal conidia. The shaken (100 rpm) cultures were incubated at 25°C for 7 days. After the incubation period, 5 ml of each culture was centrifuged (3000 g, 15 min) and the supernatants were subjected to HPLC analysis.

Sequence-based species identification

For species identification, the bacterial strains were grown overnight in 20 ml YEGM medium at 25°C on a rotary shaker (100 rpm). One µl of each culture was diluted with 50 µl distilled water and used as DNA template for the subsequent PCR-amplification. A fragment of the rDNA region was amplified by PCR using the primers Eub-8F (5`-agagtttgatCCtggctcag-3`) (Baker et al. 2003) and Eub-534R (5`-ATTACCGCGGCTGCTGG-3`) (Muyzer et al. 1993). For each reaction, the mixture (50 µl) contained 5 µl 10x Taq Buffer with KCl and 15 mmol/L $MgCl_2$, 5 µl 25 mmol/L $MgCl_2$, 5 µl 2 mmol/L dNTP Mix, 0.2 µl 5U/µl Taq DNA Polymerase (Fermentas), 1-1 µl 10 µmol/L primers, 33 µl double distilled water and 5 µl template DNA. Amplification was performed in a Biometra T3 Thermocycler as follows: 1 cycle of 94°C 2 min, 30 cycles of 94°C 30 s, 51°C 45 s and 68°C 1 min, and 1 cycle of 68°C 10 min. The amplicons were sequenced using an external service (LGC Genomics). The sequences were subjected to NCBI BLAST analysis (http://blast.ncbi.nlm.nih.gov/).

In the case of the fungal isolate, DNA extraction, PCR-amplification and sequencing of the internal transcribed spacer (ITS) region of the ribosomal DNA was carried out as described previously (Kredics et al. 2009).

Table 1. Acetanilide- and aniline-degrader microorganisms isolated in the study.

Code	Degraded compound (1 g/L)	Species
SZMC[a] 20918	acetanilide	*Pseudomonas mendocina*
SZMC 21052	acetanilide	*Rhodococcus erythropolis*
SZMC 21053	acetanilide	*Rhodococcus erythropolis*
SZMC 21056	acetanilide	*Rhodococcus erythropolis*
SZMC 20913	aniline	*Aspergillus ustus*

[a]SZMC: Szeged Microbiological Collection (WDCM 987)

High pressure liquid chromatography (HPLC) analysis

The degradation of acetanilide and aniline was quantified by high pressure liquid chromatography (HPLC) analysis, using a modular HPLC system (Merck-Hitachi) including system controller (D-7000), degasser (L-7612), HPLC pump (L-7100), autosampler (L-7200), and equipped with a reversed phase Prodigy C_{18} column (250 x 4.6 mm 5 µm; Phenomenex); a Prodigy guard (Phenomenex) with 5 µm pore size was also applied.

Detection of the selected compounds was carried out by a diode array detector (L-7455, Merck-Hitachi) in the range of 220 nm to 400 nm. Fixed wavelength was set to 233 nm. The optimal mobile phase proved to be the mixture of water and methanol (55:45) at a flow rate of 1 ml/min. Ambient column temperature was used during the analysis and the injection volume was 10 µl. Aniline and acetanilide standards (50 mg/L) were used to determine the degradation efficiency of the selected isolates. The retention time of aniline and acetanilide were 5.63 min and 6.95 min, respectively. For quantification, 9-step calibration curves were used in the range of 2 - 500 mg/L. The concentration-signal functions were $f(x) = -7.947*10^{-1} + 8.25*10^{-5}X$ for aniline and $f(x) = -4.787*10^{-1} + 7.232*10^{-5}X$ for acetanilide. The R^2 values proved to be 1.0000 for both aniline and acetanilide.

Results and Discussion

The aims of this study were the isolation, identification and characterization of microbes with acetanilide- and aniline-degrading ability from the River Maros. Four bacteria and a single fungal strain were isolated with the ability of utilizing acetanilide and aniline-HCl, respectively, as sole carbon and nitrogen source. The isolates were deposited in the Pollutant-Degrading Microorganism Collection (PDMC) of the SZMC (Szeged Microbiological Collection, University of Szeged, Szeged, Hungary) (Table 1).

The bacterial isolates SZMC 20918, 21052, 21053 and 21056, showing high acetanilide-decomposing ability, were identified as *Pseudomonas mendocina* and *Rhodococcus erythropolis* (1 and 3 strains, respectively), while the aniline-

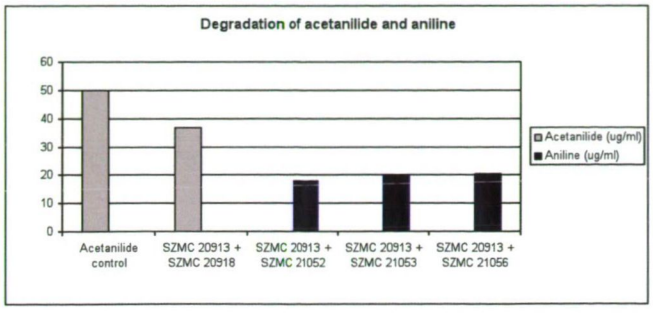

Figure 1. Concentrations of acetanilide and aniline (mg/L) in the culture supernatants of the consortia of acetanilide- (*Pseudomonas mendocina* SZMC 20918, *Rhodococcus erythropolis* SZMC 21052, 21053 and 21056) and aniline-degrading (*Aspergillus ustus* SZMC 20913) isolates. The initial acetanilide concentration was 50 mg/L.

degrader fungus SZMC 20913 proved to be *Aspergillus ustus* (Table 1). The degradation of aniline-derivatives has been examined by numerous authors. The decomposition of alachlor by a bacterial consortium was reported by Dehghani et al. (2013), whereas Sanyal and Kulshrestha (2002) documented the degradation of metolachlor by a mixed fungal culture. Munoz et al. (2011) published the degradation of both compounds by *Candida xestobii*, whereas in the study of Ellegaard-Jensen et al. (2013) a diuron-degrading strain was identified as *Mortierella* sp. These data suggest that the ability to degrade PAHs is present in a wide taxonomical range of microscopic fungi. Among acetanilide degrading bacteria, *Bacillus cereus* and *B. thuringiensis* showed the highest alachlor, propachlor and metolachlor degrading potential in previosu studies (Wang et al. 2008). The biodegradation of 2-chloro-4 nitroaniline by *Rhodococcus* sp. was examined by Khan et al. (2013), while Liu et al. (2013) documented the decomposition of the mixture of nitrobenzene and aniline by a consortium of cold tolerant microbes.

Degradation of acetanilide and aniline was examined by HPLC. When the isolated bacteria were grown in the presence of 50 mg/L acetanilide as the sole carbon and nitrogen source, no acetanilide could be detected in the samples by HPLC, indicating that the entire amount was degraded during the incubation period. The *A. ustus* strain with aniline-degrading ability was able to reduce the concentration of aniline in the culture medium from the initial 50 mg/L to 24.3 mg/L during the 7-day period examined. Combinations of the isolated acetanilide- and aniline-degrading microbial strains were cultivated in the presence of acetanilide as a sole carbon and nitrogen source. Substantial inhibition of the acetanilide-degrading potential of *P. mendocina* SZMC 20918 by *A. ustus* SZMC 20913 was observed, while a synergistic effect was detected between *A. ustus* SZMC 20913 and the *R. erythropolis* isolates tested (Fig. 1), resulting in the complete conversion of acetanilide to aniline and the further degradation of the latter compound.

The microbial strains isolated in this study are expected to provide a good basis for future approaches addressing the bioaugmentation of acetanilide, aniline and their derivatives in environmental samples.

Acknowledgements

This work was supported in part by the project MARIVMIC-COLL (HURO/1001/129/2.2.2), which is implemented under the Hungary-Romania Cross-Border Co-operation Programme 2007-2013 and is part-financed by the European Union through the European Regional Development Fund, Hungary and Romania.

References

Baker GC, Smith JJ, Cowan DA (2003) Review and re-analysis of domain-specific 16S primers. J Microbiol Methods 55(3):541–545.

Chatterjee NS, Gupta S, Varghese E(2013) Degradation of metaflumizone in soil: impact of varying moisture, light, temperature, atmospheric CO_2 level, soil type and soil sterilization. Chemosphere 90(2):729-736.

Dehghani M, Nasseri S, Zamanian Z (2013) Biodegradation of alachlor in liquid and soil cultures under variable carbon and nitrogen sources by bacterial consortium isolated from corn field soil. Iranian J Environ Health Sci Engineer 10(1):21.

Ellegaard-Jensen L, Aamand J, Kragelund BB, Johnsen AH, Rosendahl S (2013) Strains of the soil fungus *Mortierella* show different degradation potentials for the phenylurea herbicide diuron. Biodegradation 24(6):765-774.

Hanley KW, Viet SM, Hein MJ, Carreón T, Ruder AM (2012) Exposure to o-toluidine, aniline, and nitrobenzene in a rubber chemical manufacturing plant: a retrospective exposure assessment update. J Occup Environ Hyg 9(8):478-490.

Khan F, Pal D, Vikram S, Cameotra SS (2013) Metabolism of 2-chloro-4-nitroaniline via novel aerobic degradation pathway by *Rhodococcus* sp. strain MB-P1. PLoS One 8(4):e62178.

Kredics L, Kocsubé S, Nagy L, Komoń-Zelazowska M, Manczinger L, Sajben E, Nagy A, Vágvölgyi C, Kubicek CP, Druzhinina IS, Hatvani L (2009) Molecular identification of *Trichoderma* species associated with *Pleurotus ostreatus* and natural substrates of the oyster mushroom. FEMS Microbiol Lett 300(1):58-67.

Kusin S, Tesar J. Hatten B, Horowitz ZB, Hendrickson R, Leman R (2012) Severe methemoglobinemia and hemolytic anemia from aniline purchased as 2C-E (4-ethyl-2,5-dimethoxyphenethylamine), a recreational drug, on the Internet - Oregon, 2011. Morbid Mortal Week Rep 61(5):85-88.

Liu N, Li H, Ding F, Xiu Z, Liu P, Yu Y (2013) Analysis of biodegradation by-products of nitrobenzene and aniline mixture by a cold-tolerant microbial consortium. J Hazard Mat 260:323-329.

Liu Y, Shen J, Chen Z, Ren N, Li Y (2012) Distribution of polycyclic aromatic hydrocarbons in surface water and sediment near a drinking water reservoir in Northeastern China. Environ Sci Poll Res 20(4):2535-2545.

Milan M, Vidotto F, Piano S, Negre M, Ferrero A (2012). Dissipation of propanil and 3,4 dichloroaniline in three different rice management systems. J Environ Quality 41(5):1487-1496.

Munoz A, Koskinen WC, Cox L, Sadowsky MJ (2011) Biodegradation and mineralization of metolachlor and alachlor by *Candida xestobii*. J Agricult Food Chem 59(2):619-627.

Muyzer G, Dewaal EC, Uitterlinden AG (1993) Profiling of complex microbial populations by denaturing gradient gel electrophoresis analysis of polymerase chain reaction amplified genes coding for 16S ribosomal RNA. Appl Environ Microbiol 59(3):695-700.

Sanyal D, Kulshrestha G (2002) Metabolism of metolachlor by fungal cultures. J Agricult Food Chem 50(3):499-505.

Smith CB, Johnson CN, King GM (2012) Assessment of polyaromatic hydrocarbon degradation by potentially pathogenic environmental *Vibrio parahaemolyticus* isolates from coastal Louisiana, USA. Marine Poll Bullet 64(1):138-143.

Sondhia S (2012) Dissipation of pendimethalin in soil and its residues in chickpea (*Cicer arietinum* L.) under field conditions. Bullet Environ Contam Toxicol 89(5):1032-1036.

Stamper DM, Tuovinen OH (1998) Biodegradation of the acetanilide herbicides alachlor, metolachlor, and propachlor. Crit Rev Microbiol 24(1):1-22.

Wang RS, Xu QJ, Zhang X, Wei QS, Yan CZ (2012) Health risk assessment of heavy metals in typical township water sources in Dongjiang River basin. Chinese J Environ Sci 33(9):3083-3088.

Wang YS, Liu JC, Chen WC, Yen JH (2008) Characterization of acetanilide herbicides degrading bacteria isolated from tea garden soil. Microbial Ecol 55(3):435-443.

Volume 57(2):121-129, 2013
Acta Biologica Szegediensis
http://www.sci.u-szeged.hu/ABS

ARTICLE

A modified method of total RNA isolation and quantitative analysis of superoxide dismutase gene expression from different organs of *Ipomoea carnea*

Panchanand Mishra, Surendra C. Sabat*

Gene Function and Regulation, Stress Biology Laboratory, Institute of Life Sciences, Bhubaneswar-751023, Odisha, India

ABSTRACT *Ipomoea carnea* (*I. carnea*) has unique biological features for the study of cellular and molecular adaptation mechanisms due to presence of diverse alkaloid and its cadmium tolerance capacity. The present study was directed to quantify total SOD content in different organs of the plant and further extended to relative quantification of cytosolic CuZn-SOD, Fe-SOD and Mn-SOD mRNA. A modified method of total RNA isolation from the plant *I. carnea* which is rich in alkaloids has been described. Total SOD content of apical and lateral bud was highest, but transcript abundance of cytosolic CuZn-SOD was much lower as compared to root and leaves. In these cases Mn- and Fe-SOD mRNA was relatively higher and perhaps that was contributing to the high SOD activity. However, less photosynthetically active organs like root and petal show less SOD activity but mRNA level of cytosolic CuZn-SOD was competitive in these cases. The results showed that SODs in different compartments are differently regulated and each SOD isoenzyme must be performing specific function related to its cellular localization and expression of the protein isoforms depend upon local accumulation of superoxide.

Acta Biol Szeged 57(2):121-129 (2013)

KEY WORDS

differential expression
Ipomoea carnea
real time PCR
superoxide dismutase

Superoxide dismutase (SOD, EC 1.15.1.1) in plant, a key enzyme in reactive oxygen metabolism, catalyzes the dismutation of $O_2^{\cdot -}$, forming molecular oxygen and H_2O_2 (Fridovich 1975; Bannister et al. 1987). The H_2O_2 thus produced is quickly scavenged by catalase and peroxidase group of enzymes present in the plant cell (Murai and Murai 1996). The individual member of protein in this group is characterized on the basis of the metal ion cofactor they harbour, and as such four different classes like CuZn-SOD, Mn-, Fe-, and Ni- have been reported to date. In higher plants, distinct immunologically distinguishable CuZn-SODs remain distributed in cytosol, chloroplasts, peroxisomes, and in extracellular space. Mn-SOD is housed in mitochondria. Further, the distribution of cuprozinc and mangano SOD in mitochondria is restricted respectively to inter-membrane space and the mitochondrial matrix (Salin and Bridges 1981). The chloroplast, which is devoid of mangano SOD (Salin and Bridges 1981), harbours Fe-SOD in addition to cuprozinc SOD. Ni-SOD has not been reported from plants (Alscher et al. 2002). Based on the criteria of amino acid sequence, spectral characteristics, and three dimensional fold, CuZn-SODs are believed to be evolutionary distinct from Mn and Fe containing SODs (Perry et al. 2010).

Accepted April 1, 2014
*Corresponding author. E-mail: surendrachandra@gmail.com

Exposure to photo-inhibitory light condition, ozone fumigation, ultraviolate-B radiation or other environmental biotic and abiotic stresses, including metal toxicity impose oxidative stress with steady formation of $O_2^{\cdot -}$ in plants (Kliebenstein et al. 1998). Nevertheless, expression of different iso-forms SOD can also vary in different tissues depending on the local accumulation of $O_2^{\cdot -}$. The existence of three different isoforms of SOD (CuZn, Mn, and Fe), each of which is typically encoded by small but distinct gene family, further complicate the situation as regard to their specific role in view of tissue localization (Alscher et al. 2002), and more importantly the specificity of metabolic activity endowed by the tissue.

To date, the protective role of SOD in plants has been explored mainly by transgenic approaches, primarily through over-expression or by correlation of SOD expression in different stress condition (Gupta et al. 1993). However, the factors which controls the expression of particular iso-forms of SOD in specific tissues along with its metabolic specificity is still an enigma.

Ipomoea carnea (morning glory), subsp. *fistulosa* (Jacq.) is a toxic weed found abundantly in many tropical countries including India. Presence of various nortropane groups of alkaloids in different organ of plants are identified as potent toxic compound (Ikeda et al. 2003; Hueza et al. 2007). Recently, the plant has also gained much attention due to its suitability in phyto-extraction of cadmium (Cd) from

Table1. Oligonucleotide primers used for RT-PCR and Real time PCR analysis. 'F' and 'R' stands respectively for forward and reverse primers used in the experiments. Full length accession number of the corresponding genes has been mentioned in the table.

Name of the oligo	Accession No.	Sequence (5' to 3')	Amplicon length (bp)	T_m
18sF	AK059783	GACTACGTCCCTGCCCTTTGTACAC	128	60°C
18sR		AGGTTCAATGGACTTCTCGCGACGTC		
Cyt CuZn *SOD* F	JQ906095	CGGGCCTTCAAACCTGGTCTT	254	60°C
Cyt CuZn *SOD* R		CATGAACAACAACAGCTCTTCC		
Fe *SOD* F	M55910.1	GCTGCGGCAACACAATTTGGCTCTGG	157	61°C
Fe *SOD* R		AAGTCCAGATAGTAAGCATGCTCCCA		
Mn *SOD* F	JF509743.1	GTACAAGGTTCTGGCTGGGTGTGGCTG	186	61°C
Mn *SOD* R		ACTTCACATGCATATTTCCAGTTCACA		

soil (Ghosh and Singh 2005). The excess of Cd in plant tissue can stimulate the formation of reactive oxygen species (ROS), disturbs the cellular redox balance, suppresses cell expansion, and leads to significant accumulation of H_2O_2, which causes hardening of the cell wall and also activate the formation of phytochelatins and metallothioneins (Metwally et al. 2003; Gill et al. 2013). These cellular events can lead to reprogramming of the antioxidants system in plants, in order to cope with the oxidative stress caused due to the heavy metal toxicity. It is also believed that, SOD plays a dual role in preventing metal toxicity by cleaning the $O_2^{\cdot -}$ radical and preventing the accumulation of free metal (Okamoto and Colepicolo 1998).

Although, SOD has been extensively studied for their role in stress tolerance, development and morphogenesis, organ and tissue specific expression of the different iso-form is lacking in the literature. The objective of the present report is to evaluate the organ specific activity of SOD in a cadmium tolerant plant; *Ipomoea carnea* (*I.carnea*) and further extended to mRNA quantification of Fe, Mn and cytosolic CuZn-SODs. The study also describes a modified method for isolation of high quality total RNA from the plant rich in alkaloids and phenolics.

Materials and Methods

Plant material and reagents

Plant material *I. carnea* was collected from the Institute of Life Sciences campus, Bhubaneswar, India and washed thoroughly with distilled water before use in the experiments.

Unless mentioned, all analytical grade reagents were procured from Sigma. Taq DNA polymerase was obtained from Promega while AffinityScript QPCR cDNA synthesis Kit was from Stratagene. For real time PCR QuantiTect SYBR Green PCR kit from Qiagen was used. All the oligonucleotide primers used in this study were obtained from Ocimum Biosolution, India.

Preparation of crude extract

Crude extract from different organs of mature *I. carnea* plant (200 mg) at flowering stage were prepared by homogenizing in liquid nitrogen and then suspended in 1 ml of ice cold 50 mM K-PO_4 buffer (pH 7.8) containing 0.1 mM Phenylmethanesulfonyl fluoride (PMSF), 8% (w/v) polyvinylpolypyrrolidone (PVPP) and protease inhibitor cocktail (Roche). The homogenate was then centrifuged at 15,000 x g for 30 min at 4°C and the supernatant was used for SOD activity assay. The protein concentration was measured following modified Bradford assay (Zor and Selinger 1996).

SOD activity assay

Spectrophotometric assay of SOD activity was carried out by following (Beauchamp and Fridovich 1971). Assay were performed in a reaction mixture containing 50 mM potassium phosphate buffer (pH 7.8), 1.33 mM Diethylenetriamine pentaacetic acid (DTPA), and 2.45 mM Nitro blue tetrazolium salt (NBT), 1.8 mM xanthine and a suitable concentration of xanthine oxidase (till a linear curve with a slope of 0.025 absorbance per min in time scan was obtained). One unit of SOD activity was defined as the amount of protein which produced one half of the maximum competition against NBT in the specified system. The final activity was recorded after deducting out the non-specific SOD like activity produced by many low molecular compounds (Yamahara et al. 1999; Sharma et al. 2004). This was achieved by measuring the activity in samples following heat inactivation of protein (95°C for 20 min).

All assays were done using three different crude extract preparations and five different concentrations of proteins were used and data are the means of three replicates.

RT- PCR primer design

The sequences of the primer used in this study are given in Table 1. Rice 18S rRNA (AK059783) was used as the

housekeeping genes as an internal control. In order to amplify shorter fragment of *I. carnea* SODs, internal primers were designed on the basis of homology based nucleotide sequence alignment (Fig. 1-Cytosolic CuZn-SOD, Fig. 2-Fe-SOD and Fig. 3-Mn-SOD) using ClustalX (Larkin et al. 2007) taking selected plant species for each class of SODs and degenerate primer pairs (Table 1) were designed from the most conserved sequence (shaded with yellow region, Fig. 1, 2 and 3). Annealing temperature of all the primers was kept constant at ~ 60°C.

Isolation of total RNA and cDNA preparation

Isolation of total RNA from different organs of I. *carnea* was carried with some modifications from the protocol described by Natalia et al.,(Kolosova et al. 2004). Prior to isolation of RNA, all the plant material were kept in 0.1% Diethyl pyrocarbonate (DEPC)-treated water for 30-60 min. Since the plant is rich in phenolic and alkaloid compounds, concentration of PVPP was increased to 8% (w/v) in the extraction buffer [200 mM Tris-HCl, pH 8.5, 1.5% lithium dodecylsulfate, 300 mM LiCl, 10 mM disodium salt EDTA, 1% (w/v) sodium deoxycholate, 1% (w/v), Nonidet P-40 (NP-40)]. 5 mM thiourea, 1 mM aurintricarboxylic acid, 10 mM dithiothreitol, and 2% (w/v) PVPP were added to the extraction buffer just before use.

Plant tissue (1 g) was grounded to fine powder in liquid nitrogen using a mortar and pestle and the powder was transferred to a 50-mL polypropylene tube. 20ml of extraction buffer per gram tissue was added and vigorously shaken to uniformly suspend the sample. The suspension was then frozen at -80°C for 1 h and the extracts were centrifuged at 5000×g for 30 min at 4°C. One-thirtieth volume of 3.3 M sodium acetate (pH 6.1) and 0.1 volume 100% ethanol were added to the supernatant, and the mixture was chilled on ice for 10 min to precipitate polysaccharides. Polysaccharides were pelleted by centrifugation at 5000×g for 30 min at 4°C. In order to precipitate nucleic acids, one-tenth volume of 3.3 M sodium acetate and 0.6 volume of ice-cold isopropanol were added to the supernatant, and the solution was left at -80°C for 1 h. Nucleic acid pellets were collected by centrifugation for 45 min at 5000×g at 4°C. The supernatant was removed, and the pellet was resuspended in 2 mL of TE ((10 mM Tris-HCl, pH 8.0, 1 Mm Ethylenediaminetetraacetic acid (EDTA)) and 2 mL 5 M NaCl and kept on ice for 30 min with periodic vortex mixing. The samples were mixed with 4 mL of 10% Cetyltrimethylammonium bromide (CTAB) at room temperature, vortex mixed, and incubated for 5 min at 65°C to remove residual polysaccharides. Mixtures were then extracted twice with an equal volume of chloroform/isoamylalcohol (24:1, v/v). One-fourth volume of 5 M LiCl was added to the supernatant, mixed, and kept at 4°C overnight. RNA was pelleted by centrifugation at 5000×g for 30 min at 4°C. The supernatant was poured off, and the residual

```
CLUSTAL 2.1 multiple sequence alignment-Cytosolic CuZn-SOD

Ipomoea         ATGGTGAAGGCTGTCGCAGTTCTTAGCAGTAGTGAAGGTGTCAGCGGCACCATTTTCTTC 60
Populus         ATGGTGAAGGCTGTAGCTGTTCTTAATAGCAGTGAAGGTGTGAGTGGCACCATCTTCTTT 60
Oryza           ATGGTGAAGGCTGTTGTTGTGCTTGGTAGCAGTGAGATTGTTAAGGGCACTATCCACTTT 60
Malus           ATGGTGAAGGGTGTTGCTGTTCTCGGCTCCAGTGAGGGCGTTAAAGGAACCATCAGCTTT 60
Arachis         ------------------------------------------------------------
Brassica        ATGGGCAAGGGAGTGGCAGTCTTGAACAGCGGTGAGGGTGTTAAGGGGACTATCTTTTTC 60

Ipomoea         AGCCAAGAAGGAGATGGTCCAACCACAGTCACTGGAAACGTTTCGGGCCTCAAACCTGGT 120
Populus         ACCCAAGAAGGAGATGGCCCAACTACTGTAACTGGAAACCTTTCTGGTCTTAAGCCAGGC 120
Oryza           GTCCAAGAGGGAGATGGTCCCACCACTGTGACTGGAAGTGTCTCTGGCCTCAAGCCTGGT 120
Malus           GTCCAGGAGGGAGATGGCCCAACTACTGTGACTGGAAGTGTCTCTGGCCTCAAGCCTGGA 120
Arachis         ----AGGAAGGAAATGGTCCAACCACTGTGACTGGAAATCTTGCTGGCCTTAAGCCTGGT 56
Brassica        ACCCAGGAAGGAGACGGTGTGACCACTGTGACTGGAACAGTTTCTGGACTTAAACCTGGT 120
                    * ** *** * **    ** ** ** *******   *  * ** ** ** ** **

Ipomoea         CTTCATGGCTTCCATGTCCATGCCCTAGGTGACACAACAAATGGATGCATGTCTACTGGA 180
Populus         CTTCATGGCTTCCACGTCCATGCCCTTAGAGACACCACAAATGGCTGCATGTCAACTGGG 180
Oryza           CTCCATGGGTTCCATATTCATGCACTTGGTGACACCACCAATGGTTGCATCTCAACTGGG 180
Malus           CTTCATGGTTTCCATGTCCATGCTCTTGGAGACACAACAAACGGTTGCATGTCAACTGGG 180
Arachis         CTTCATGGGTTCCATGTCCATGCCCTTGGAGACACCACAAATGGTTGCCTGTCAACTGGA 116
Brassica        CTACATGGTTTCCATGTCCATGCTCTTGGTGACACCACTAACGGTTGCATGTCCACCGGT 180
                ** ***** *****  * ***** **  * ***** ** ** ** *** * ** ** **

Ipomoea         CCACATTTCAATCCTGCTGGAAAGGAGCATGGAGCTCCTGGAGACGATAACCGCCATGCC 240
Populus         CCGCATTTTAATCCTGTAGGCAAGGAGCATGGTGCCCCTGAGGATGAGAATCGTCATGCT 240
Oryza           CCACACTACAATCCTGCCGGAAAGGAGCATGGAGCACCAGAAGATGAGACCCGCCATGCT 240
Malus           CCACACTTCAATCCTGCTGGAAAAGAGCATGGTGCCCCTGAAGATGAGCTTCGCCATGCT 240
Arachis         CCGCATTTCAATCCTAACAACAAGGAGCATGGTGCCCCTGAAGATGAGAACCGCCATGCT 176
Brassica        CCACATTTCAACCCTGATGGTAAACAACACGGTGCCCCTGAGGATGCTAATCGTCATGCT 240
                ** ** *  ** ***       **  * ** ** ** ** ** *  ** *      ** *****

Ipomoea         GGTGATCTTGGAAACATCACGGTTGGAGAAGATGGTACTGCTT-CATTCACCATCACTGA 299
Populus         GGTGATCTGGGAAATGTCACTGTTGGTGATGATGGCACTGCTA-CTTTCACAATCATTGA 299
Oryza           GGTGATCTTGGAAATGTCACCGCTGGAGAAGATGGTGTTGCTAATATCCATG-TTGTTGA 299
Malus           GGCGATCTTGGAAACATCACTGCTGGGGACGATGGAACTGC-AACCTTCACGATTGTTGA 299
Arachis         GGTGATTTAGGAAATGTTAATGTTGGAGATGATGGAACTGTTAGC-TTCTCCATTTCCGA 235
Brassica        GGCGATCTAGGAAACATCATTGTTGGAGATGATGGAACTGCCA-CCTTCACAATCACTGA 299
                ** *** * ******  * *  * *** ** *****   **      * *   *    **

Ipomoea         CAAGCAGATTCCGCTTACTGGAGCAAATTCTGTTATTGGAAGAGCTGTTGTTGTTCATGG 359
Populus         CAAACAGATTCCTCTTACTGGACCACATTCCATTATTGGAAGGGCTGTTGTTGTTCATGG 359
Oryza           CAGTCAGATTCCACTTACTGGACCAAATTCAATCATTGGCAGAGCCGTCGTTGTCGCATGC 359
Malus           CAAGCAGATTCCTCTCGCTGGACCACACTCTATCATTGGTAGGGCGGTTGTTGTCCACGC 359
Arachis         CAGTCAGATCCCTCTTAGTGGGCCAAACTCCATTGTTGGAAGGGCTGTTGTTGTCCATGC 295
Brassica        CTGCCAGATTCCTCTTAGTGGACCAAACTCTATTGTCGGAAGGGCTGTTGTTGTCCACGC 359
                *   ***** ** **   ***  ** * ** *  * ** ** ** ** ** ***** ** *

Ipomoea         TGATCCCGATGATCTTGGTAAAGGTGGCCATGAGCTCAGCAAAAGCACTGGAAATGCTGG 419
Populus         AGATCCTGATGATCTTGGCAAGGGAGGACATGAACTCAGCAAAACCACCGGTAATGCTGG 419
Oryza           CGATCCTGATGATCTTGGAAAGGGTGGGCACGAGCTGAGCAAGACCACCGGAAACGCTGG 419
Malus           AGACCCTGATGACCTTGGCAAGGGTGGACATGAGCTTAGCAAATCCACAGGAAATGCTGG 419
Arachis         TGATCCTGATGATCTTGGGAAAGGTGGGCATGAGCTTAGCAAATCCACTGGAAATGCTGG 355
Brassica        AGACCCTGATGACCTCNGAAAGGGAGGCCATGAACTCAGCTTGGCTACCGGAAATGCANG 419
                 ** ** ***** **  * ** ** ** ** ** ** ***       ** ** ** **  *

Ipomoea         CGGGAGGGTTGCCTGCGGTATCATTGGCCTGCAGGGTTAA 459
Populus         CGGCAGAGTAGCATGCGGTATTATTGGTCTGCAAGGTTGA 459
Oryza           TGGCCGTGTTGCTTGCGGGATCATCGGACTTCAAGGCTGA 459
Malus           TGGCAGGGTGGCTTGCGGTATTATTGGTCTGCAAGGATGA 459
Arachis         TGGCAGAGTAGCTTGTGGGATTATTGGTTTGCAAGGCTAG 395
Brassica        TGGCCGTGTTGCTTGTGGCATTATTGGTCTTCANGGCTAA 459
                 **  * ** ** ** ** ** ** ** **  * ** ** *
```

Figure 1. Nucleotide sequence alignment of the cytosolic CuZn-SOD gene from different species using Clustal W. Representative plant species are *Ipomoea batatas* (JQ906095), *Populus suaveolens* (DQ481231), *Brassica juncea* (AF540558), *Oryza sativa* (L36320), *Arachis hypogaea* (DQ499511) and *Malus xiaojinensis* (AY646367). Degenerate primers (Table 1) for real time PCR were designed from sequences shaded in yellow.

liquid was carefully removed with a pipet. The RNA pellet was dissolved in 1 mL TE buffer and 0.9 volume of chilled isopropanol and 0.1 volume of 3.3 M sodium acetate were added, followed by precipitation at -80°C for 1 h RNA pellets were collected by centrifugation in a microcentrifuge at 16,000×g at 4°C for 30 min, washed twice with 200 µl of 70% ethanol, and collected by centrifugation at 16,000×g at 4°C for 20 min. Pellets were dried at room temperature, and RNA was resuspended in 200 µl of autoclaved DEPC-treated water. The quality and quantity of the isolated RNA were verified by 1% formaldehyde denaturing agarose gel electrophoresis and spectrophotometry.

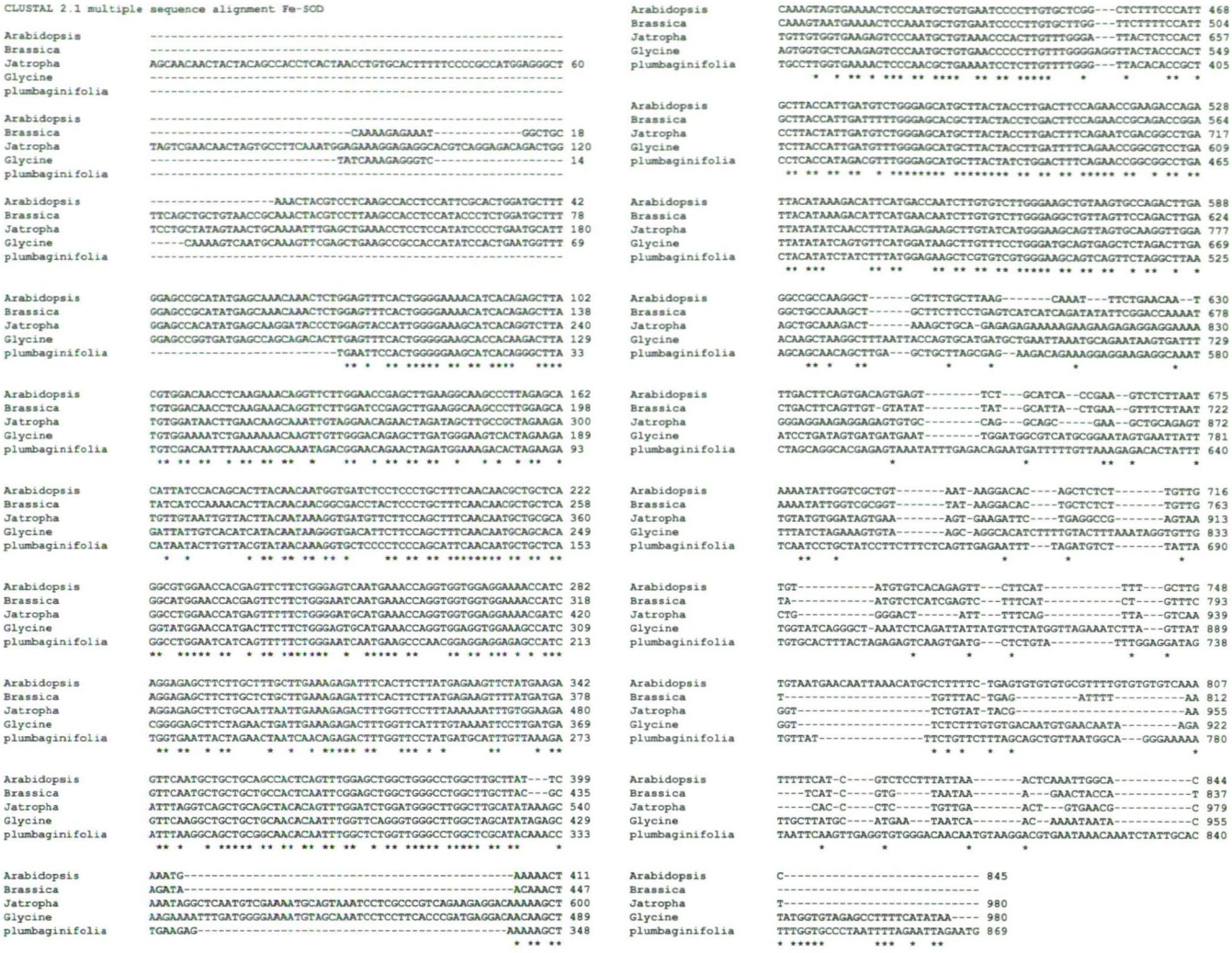

Figure 2. Nucleotide sequence alignment of the Fe-SOD gene from different species using Clustal W. Representative plant species are *Arabidopsis thaliana* (M55910.1), *Glycine max* (AAA33960.1), *Jatropha curcas* (JF509742.1), *Brassica oleracea* (JF720320.1), *Nicotiana plumbaginifolia* (M55909.1). Degenerate primers (Table 1) for real time PCR were designed from sequences shaded in yellow.

First-strand cDNA from 200 ng of total RNA was synthesized using AffinityScript QPCR cDNA Synthesis Kit following manufacturer's instruction using equimolar (10 pmole) concentration of oligo(dt) and random primer. In order to assess the integrity of cDNA prepared, Reverse transcription-polymerase chain reaction (RT-PCR) analysis was performed taking 18s and SOD primers (Table 1).

Real-Time PCR analysis

Real-Time PCR reactions were performed in using Quanti-Tect SYBR Green PCR to detect dsDNA synthesis. Reactions were done according to kit instruction in 25 µl volumes containing 10 pmole of each primer and 50 ng of starting RNA. Three replications were done for each gene analysis of Real-time PCR. Dissociation curves for each amplicon were then analyzed to verify the specificity of each amplification reaction.

Relative gene expression data were analyzed using real-time quantitative PCR by $2^{-\Delta\Delta CT}$ method (Livak and Schmittgen 2001). Expression levels (fold change) were determined as the number of amplification cycles needed to reach a fixed threshold in the exponential phase of the PCR reaction (CT). To assess the sensitivity and amplification efficiencies of the method three different template dilutions were checked. The amount of target were normalized to the housekeeping reference (18s rRNA) and used for $2^{-\Delta\Delta CT}$ calculation.

For relative quantification, expression of all the SOD isoform in root was taken as unity for fold change calculations.

```
CLUSTAL 2.1 multiple sequence alignment Mn-SOD

Jatropha        --CGGGCTCTTT-CACTC-CCTACACTATTCGACTC-CTGT---CGA---------CGAA 43
Zea             CACACACTCCGCATACGCACCTACGAGAGTCGAGTGACAGTGAGCGAGCGAGCGAGCGAA 60
Arabidopsis     ---GCGACCACTAGA-------AGGAGAAACAAATCTTCAT---------------TCCA 35
Ipomoea         ------------------------------------------------------------
Solanum         ------------------------------------------------------------G 1

Jatropha        TCAATGGCTCTCCGTTCTCTGGCCACCAGAACCGCCCTAGGCGCCGCTGTCAAGGCGGAT 103
Zea             GCCATGGCTCTCCGCACCCTGGCATCGAAGAACGCCCTATCCTTCGCGCTC--GGTGGAG 118
Arabidopsis     GCAATGGCGATTCGTTGTGTAGCGAGTAGAAAAACCCTAGCCG----GCTTGAAGGAGAC 91
Ipomoea         ------------------------------------------------------------
Solanum         GACAAAGAGCTTAAGCGCCTGGTGGTTGAAACCACTGCA---------------------- 40

Jatropha        TCTAATCTTTTCCTAGGCTTAGGATTAAGTCAACTTCGAGGATTGAAAACCTTCTCTCTC 163
Zea             --CGGCCCGGCCGTCGGC---GGAGTCCGCGA-----GGGGGGTGACGACGGTCGCGCTC 168
Arabidopsis     ATCATCGAGGCTATTGA----GGA-----TCA-----GAGGGATTCAGACTTTTACGCTT 137
Ipomoea         ------------------------------------------------------------
Solanum         ---AATCAGGTGATTGA-----------------------------------TGCATGTTC 63

Jatropha        CCCGATCTTGCCTACGACTATTCAGCTCTTGAGCCCGTGATTAGTGCCGAGATAATGCAG 223
Zea             CCCGACCTCTCCTACGACTTCGGCGCGCTGGAGCCGGTCATCTCGGGGGAGATCATGCGC 228
Arabidopsis     CCTGATCTTCCTTACGATTATGGCGCATTGGAACCGGCCATTAGTGGAGAGATCATGCAG 197
Ipomoea         ------------------------------------------------------------
Solanum         T---ATTTATCCTA-------------------------GATGAATAGATAGAT-ATGT-T 94

Jatropha        CTTCATCACCAAAAGCACCACCAGACTTATATTACTAACTATAATAAGTCTCTTGAGCTG 283
Zea             CTGCACCACCAGAAGAACCACGCCACCTACGTCGTCAACTACAACAAGGCGCTTGAGCAG 288
Arabidopsis     ATTCATCACCAGAAGCATCACCAGGCTTATGTTACTAATTACAATAATGCTCTTGAGCAG 257
Ipomoea         ------------------------------------------------------------
Solanum         CTATTTATCCTAAATTAATAGATAGCTGAG--CATCATCTTCAACAAG------------ 140

Jatropha        CTCAATGAAGCTATGAATAAGGGGGACTCTGCTTCT--GTTGTCAAGTTGCAGAGCGCCA 341
Zea             ATCGACGATGTCGTCGTCAAGGGCGACGACTCCGCT--GTCGTCCAGCTCCAGGGCGCCA 346
Arabidopsis     CTTGATCAAGCTGTGAACAAGGGAGATGCTTCCACT--GTTGTTAAGTTGCAGAGCGCCA 315
Ipomoea         ------------------------------------------------------------
Solanum         -----TGAAGTT------------GATTCCTCCACTTTGTTGCCTTGACTTAGAGGTTAA 183

Jatropha        TCAAGTTCAATGGTGGAGGTCATATCAACCACTCCATTTTCTGGAAGAATCTCGCCCCTG 401
Zea             TCAAGTTCAACGGCGGCGGTCATGTGAACCATTCAATCTTTTGGAAGAACCTCAAGCCTA 406
Arabidopsis     TCAAATTCAACGGCGGAGGTCATGTCAACCATTCGATTTTCTGGAAGAACCTTGCTCCTT 375
Ipomoea         ------------------------------------------------------------
Solanum         TACTATCCAA-----GAAAGCGTGAAAA--------------GAAAATGCATAAGACTG 223

Jatropha        TTCGTGAAGGAGGTGGTGAACCTCCGCATGGTTCCCTTGGTTGGGCGATTGATGAA--GA 459
Zea             TTAGCGAAGGTGGTGGGGAGCCGCCACATGGGAAACTTGGCTGGGCCATCGATGAG--GA 464
Arabidopsis     CCAGTGAAGGTGGTGGAGAGCCACCAAAAGGATCTCTTGGTAGTGCCATTGACGCT--CA 433
Ipomoea         ----------------------CCGAAGAGTTCTTTTGGCTGGGAGATTGACAAT--CA 35
Solanum         CTAAT--------TTCTTGATTGCT-TAGAAGTCTTTAAGTTGTAGACTAAATAATTTGA 274

Jatropha        TTTTGGTTCTTTGGAAAAGTTGATCC--AGAAAATCAGC-------ACAGAA-GGTGCTG 509
Zea             TTTTGGTTCATTTGAGGCACTTGTAA--AGAGGATGAAT-------GCAGAA-GGCGCTG 514
Arabidopsis     CTTTGGCTCCCCTTGAAGGTCTGGTGA--AAAAGATGAGT-------GCTGAG-GGTGCTG 483
Ipomoea         CTTTGGCTCTTTAGATGCTCTGATAC--AAAAGATGTCT-------GCAGAA-GGTGCTG 85
Solanum         CTTCCATTTCTTATTAGCTGCCATGATTGAGAGATGTATTTTTTATGTTAATTGATGCTG 334

Jatropha        GTTGAGACAACTGCAAACCAGGACCCATTG-GTAACTAAAGGACCAACTTTAGTTCCTTT 627
Zea             GTTGAAACTACAGCTAATCAGGATCCTCTG-GTGACTAAAGGTGCAAGCTTGGTTCCGCT 632
Arabidopsis     GTTGACACAACTGCCAATCAGGATCCATTA-GTGACAAAAGGAGGAAGCTTGGTACCTCT 601
Ipomoea         GTTGAAACCACCCCAAATCAGGACCCTTTG-GTTACTAAAAATCCAAACAAGGTTCCTCT 203
Solanum         ACCGGTCCT---------TTAGAATTATTTGCATTTCCCCACCTC----CTTGGT----CT 424

Jatropha        GCTTGGCATT--GATGTTTGGGAGCATGCATACTA--CTT--ACAGTACAAGAATGTCAG 681
Zea             GTTGGGGATT--GATGTCTGGGAACATGCGTACTA--CCT--GCAGTACAAGAATGTTAG 686
Arabidopsis     GGTGGGTATA--GATGTTTGGGAGCACGCCTACTA--CTT--GCAGTACAAAAATGTGAG 655
Ipomoea         ACTGGGCATA--GATGTTTGGGAACATGCGTACTA--CTT--ACAGTACAAGAATGTGAG 257
Solanum         G-TCAGCATTCTGCAGTCTAC-ATCATAYGGCCCAGGCTTCAACTGTAGATAGGTCTTAT 482

Jatropha        ACCTGATTATCTAAAGAACATATGGAAGGTAATAAATTGGA--AGTATGCAAGTG-AAGT 738
Zea             GCCGGATTACCTGAACAACATCTGGAAGGTGATGAACTGGA--AATATGCTGGAG-AGGT 743
Arabidopsis     GCCTGAGTATCTGAAGAATGTATGGAAAGTGATCAACTGGA--AATATGCAAGCG-AGGT 712
Ipomoea         GCCGGATTACTTGAAGAATATATGGAAAGTTGTGAACTGGA--AATATGCATGTG-AAGT 314
Solanum         TTTTGTCTATTTTGACAATCCTTTTTATATGTGGGATTGCATAAGAACGTTGGCATATGC 542

Jatropha        GTA---------------------TGCAAATGAATGCCCTTCAGCTTAGAGCGCTCACCA 777
Zea             GTA---------------------CGAAAATG---------------------------- 754
Arabidopsis     TTA---------------------TGAGAAGGAAAG------------------------- 727
Ipomoea         TTACCAACAATTTACACCATTGCCTGCAAGCAGAGACTGATCAGACCAGGTGATCCAACA 374
Solanum         TTT---------------------TGCAATAGT---------------------------- 554

Jatropha        CTCTT----ATGATTG---AAATAAAATGATGTGTTAATG------TATTATAAAATATT 824
Zea             TTCT------TGCTTG---AAT--------TGTCTTAATG------GACAATA------- 784
Arabidopsis     ----------CAACTG---AAT--------CGTTTACACGAT----GAC-ATAAGGAGAT 761
Ipomoea         CTCATCAAGGTGCCCG---AGT--------TTCTTTAATCTCGTGGGATAAAATAATGCT 423
Solanum         ----------TGCTTGTCAGGT--------TGTCTT-ATG------AATTATGG------ 583

Jatropha        AAGGGCCCCTTCTCTCCACCGAGCTGTTCACAGGTTGTCTGCA------CTAGTGTGTGC 878
Zea             --------CTCATCTGCGCGGGTTTGTTTTCGGGCTG---------------------- 813
Arabidopsis     GAACCAGTTCCAGCTCAGCT--TTTGTTTTAAGGTTGTCTGAAACAAACTTACAGTGTCT 819
Ipomoea         AAGTTAACTTTGCTTCGGCTT-TCTGCTGAACTGTTGT-------------------TGC 463
Solanum         --------------TAGG--GATCATTTTTGGGATTAT---------------------- 605

Jatropha        TTTTGTTCATTTCTTCTTTGTCAGTC--------CTATCATGGAACATATTGCTCT-TGA 929
Zea             -TTTGACCAT---------------------------GTGAAATAAA---------GA 834
Arabidopsis     CTTTGGTTTTTAAGATTTGCTCAACT--------CAGCTGTGTGGTACGTTGTTTTACAA 871
Ipomoea         TTCTGTTTTCTGTGTAGTGGTAAATAAATTGTTGTATTTGTGAATTTTGTTGCTTT-TAG 522
Solanum         -TTTGTTCTT---------------------------GCAGGACCCTTTGGTTTCTAA 635

Jatropha        TGTC------CTGTTATATGGATCTTCTAATAACAACAATT----------TGGGCACTA 973
Zea             TGGA------CT----TGTGTACCTGC---------------------------------- 851
Arabidopsis     TGAAAGTTTTSAAGAATAAAAATTTGCTATTATTGTCAG------------AAAGCGCTA 919
Ipomoea         CACACTGTCACTGTGATGTGAAACTTATCACTTCAACAGAGTTAAAATTGAAAAATGCAG 582
Solanum         AGGA------------GCAAATTTGGTACCTCTTATGGGT---------ATAGACGTTT 673

Jatropha        GATTTTATTCAAAAAAAAAAAAAAAAAAAA 1004
Zea             ------------------------------
Arabidopsis     TTGTTTATTCT------------------- 930
Ipomoea         GAGTTTTTCTGCT----------------- 595
Solanum         GGGAACACGCAT------------------ 685
```

Figure 3. Nucleotide sequence alignment of the Mn-SOD gene from different species using Clustal W. Representative plant species are *Jatropha curcas* (JF509743.1), *Ipomoea batatas*(L36676.1), *Solanum bulbocastanum* (HQ856192.1), *Zea mays* (L19462.1), *Arabidopsis thaliana* (AY085319.1). Degenerate primers (Table 1) for real time PCR were designed from sequences shaded in yellow.

Results

SOD activity in crude extracts

A comparative analysis of total SOD activity in the crude extract of different organs of *I. carnea* is presented in Figure 4. SOD activity assays were performed with increasing protein concentration (Fig. 4A) and specific activity (units/ mg of protein) was calculated (Fig. 4B) in the linear range of increase in SOD activity with increase in protein concentration. SOD specific activity was maximum in case of apical and lateral bud, while root and petal show comparatively lesser activity. Leaf and stem showed moderate SOD activity as compared to other plant parts.

Higher SOD activities in the meristematic tissue like apical and lateral buds are obvious also. It is well documented that these fast dividing cells produces large amount of reac-

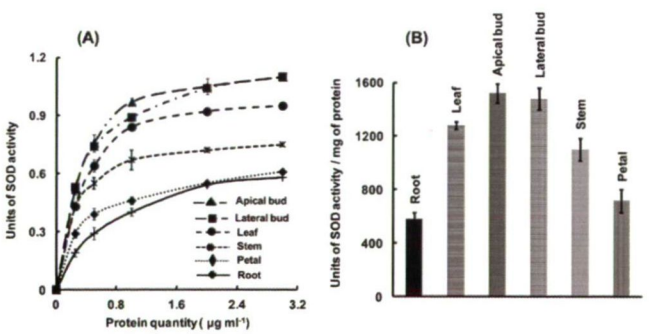

Figure 4. SOD activity in crude extracts of I.carnea. (A) as a function of increase in protein concentration (B) specific activity of the protein in terms of Units of SOD activity/ mg of protein.

tive oxygen species due to higher metabolic rate (Samis et al. 2002 ; Bi et al. 2011). Thus, increase in SOD activity in these tissues is physiologically essential in order to tolerate flux of ROS and hence prevent the plant from oxidative damage. Lesser SOD activity in non green tissues like root and petals could be argued for lack of photosynthesis machinery, the process which is accountable for largest production of superoxide is plant cells (Perl-Treves and Galun 1991; Murai and Murai 1996; Asada 1999). Therefore, these plants organs represent differential accumulation $O_2^{\cdot-}$ and plants are adapted to regulate the SOD activity based on local accumulation of $O_2^{\cdot-}$.

Purification and quality detection of total RNA

Electrophoresis of isolated RNA on 1% denaturating agarose gel stained with ETBR showed distinct 28S and 18S rRNA bands (Fig. 5A). Only those RNA samples with 260/280 ratio between 1.9 and 2.1 and 260/230 ratio greater than 2.0 were used for the cDNA preparation (Jain et al. 2006).

RT-PCR of the cDNA prepared using the housekeeping 18S rRNA and all three SOD isoform show a single distinct band in agarose gel (Fig. 5B-C) and hence proceeded for real time analysis.

Real time PCR analysis and quantification of relative gene expression

Presence of single sharp peak for both 18S rRNA and SOD as reflected in the dissociation curves (melting curves) ascertain the absence of primer dimers and non-specific amplification products. It also showed that the amplification has good reproducibility in each sample for all genes. However, both RT PCR and amplification curve (data not shown) of Fe-SOD shows slightly less efficiency, which might be due to higher degeneracy of the Fe-SOD sequence with the designed primer.

The quantitative expression cytosolic CuZn-SOD gene in different organs was evaluated by taking the amount of expression in root as unity (Fig. 6A). The relative expression level of the gene compared to root was highest in leaf (1.3 times), while expression was about 0.35-fold and 0.22-fold lower in case of apical and lateral bud respectively. The transcript abundance in stem and petals as compared to root was about 0.54 and 0.37.

Although, it was shown in earlier section that the total SOD activity was highest in buds, relative mRNA expression of the cytosolic CuZn-SOD gene was found to be least in these cases. These anomalous gene expression profiles suggest that distributions of different SOD isoforms in different organs of the plants are different. This is also supported by previous reports (Kliebenstein et al. 1998; Corpas et al. 2006) where it was found that the cytosolic CuZn-SOD plays a more important role in oxidative stress tolerance in roots as compared with the chloroplastic isoform. It is most likely

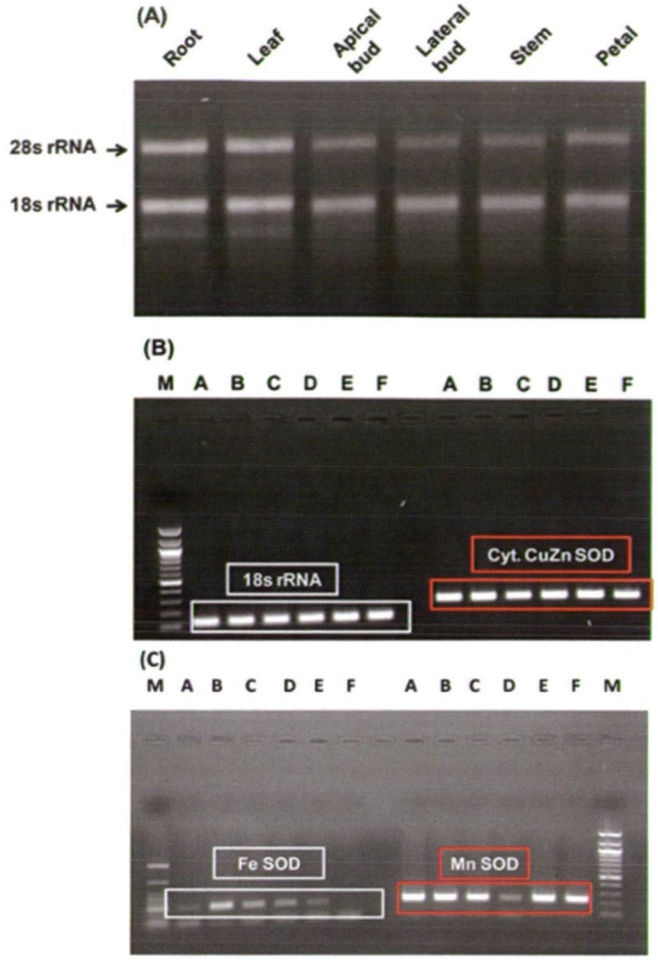

Figure 5. Purification of total RNA and reverse transcriptase PCR. (A) Resolution of total RNA on formaldehyde agarose gel. (B) PCR of the corresponding cDNA using 18s rRNA and CuZn-SOD primer and (C) Fe-SOD and Mn-SOD. Sequence of representative cDNA from A-F is root, leaf, apical bud, lateral bud, stem and petal.

that, others isoforms of SOD like chloroplastic CuZn-SOD, Fe-SOD and Mn-SOD might be contributing to the higher activity of the buds.

Evaluation of transcript level of Fe and Mn-SOD isoforms also advocate this fact. The relative expression level of the Fe-SOD was highest in leaf (6.3 times), followed by apical bud and lateral bud while expression was comparable in case of stem and petal (Fig. 6B). Variation in Fe-SOD transcript abundance in these organs primarily represent the presence of chloroplast and those organs where chloroplast is absent shows lower level of expression, which is primarily basal level only.

The expression level of Mn-SOD gene was highest in apical bud followed by lateral bud while transcript abundance of the gene was average in root, leaf, stem and petal (Fig. 6C). These observations suggest that both apical and lateral bud

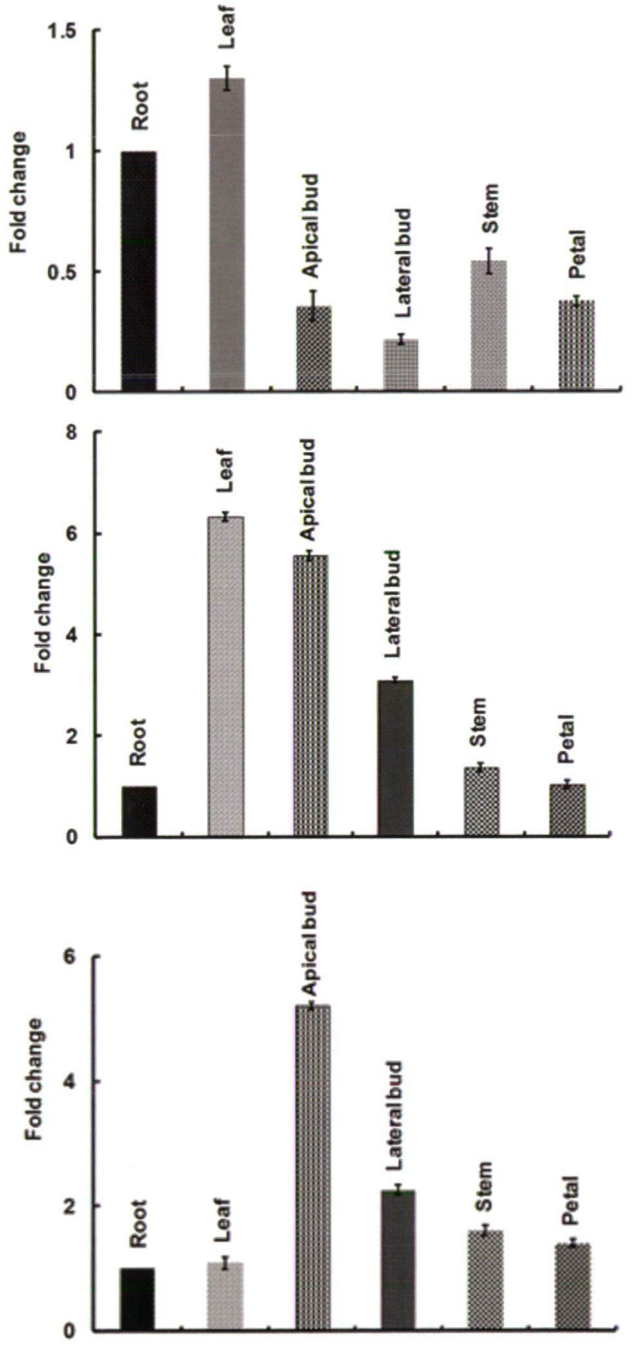

Figure 6. Relative quantification of SOD expressions in different organs of *I.carnea*. Quantification of gene expression was evaluated by taking the amount of expression in root as unity and expressed in terms of fold change. (A) CuZn-SOD (B) Fe-SOD (C) Mn-SOD.

have higher accumulation $O_2^{\cdot-}$ which might be due to high rate of metabolism and since Mn-SOD is the major isoform present in mitochondria, so higher expression of Mn-SOD in these meristematic organs strongly advocate its higher abundance to prevent plant from oxidative injury. So, perhaps Mn-SOD contributes towards higher SOD activity of buds as shown in earlier section.

Discussion

Reactive oxygen species (ROS) are produced as a normal product of plant cellular metabolism. ROS are always formed by the inevitable leakage of electrons onto O_2 from the electron transport activities of chloroplasts, mitochondria, and plasma membranes or as a by product of various metabolic pathways operating in different cellular compartments (Bannister et al. 1987a). Various Environmental stresses such as drought, salinity, chilling, metal toxicity, and UV-B radiation as well as pathogens attack can lead to enhanced production of ROS within plant tissues due to disruption of cellular homeostasis (Bowler et al. 1994). Scavenging of excess ROS is achieved by highly efficient antioxidative machinery comprising of both nonenzymatic and enzymatic antioxidants. The enzymatic components include superoxide dismutase (SOD), catalase (CAT), guaiacol peroxidase (GPX), enzymes of ascorbate-glutahione (AsA-GSH) pathway such as ascorbate peroxidase (APX), monodehydroascorbate reductase (MDHAR), dehydroascorbate reductase (DHAR), and glutathione reductase (GR). Ascorbate (AsA), glutathione (GSH), carotenoids, tocopherols, and phenolics serve as potential nonenzymatic antioxidants within the plant cell (Noctor and Foyer 1998). However, plants rely upon the unique enzyme superoxide dismutase (SOD) to detoxify superoxide. That's why SODs are ubiquitous enzymes present in all phyla and various isoforms of this class of enzymes are distributed in different cellular compartments. The presence of multiple SOD isoforms raises the possibility that each protein may protect plants against a subset of oxidative stresses and that a variety of SODs are deployed to fully combat environmental stresses (Bowler et al. 1994; Alscher et al. 2002).

There have been several studies showing the importance of SODs in combating environment stresses by developing plants overexpressing different isoforms of the enzyme. However, there are some disparities among transgenic plants overexpressing SOD (Tepperman and Dunsmuir 1990; Gupta et al. 1993). It is also essential to obtain deeper insights into the relationship between cellular localization and specific function of each SOD isoforms. However, tissue and organ specific expression of SOD activity and relative expression of different isoforms are still lacking in literature.

In some cases, tissue specific expression were analysed by fusing the 5' upstream regulatory region of these genes to the beta-glucuronidase reporter gene and differential tissue specificity were checked in transgenic plants. Those studies were confined only to one gene at a time (Van Camp et al. 1996). Therefore, in this study we report the total SOD activity in different organs of *Ipomoea carnea* and further extended to analysis of transcript abundance of cytosolic CuZn-SOD,

Fe-SOD and Mn-SOD by real time PCR. Our observations demonstrate that expression of different isoforms of SODs are developmentally regulated and hence provide a valuable clue about the existence of a specific isoform of SODs in particular organ of the plant.

The comparison of total SOD activity in the crude extract of different organs of *I. carnea* showed clear discrepancies. Our observation reveals that activity was maximum in case of apical and lateral bud. These buds of plant represent the highly meristematic region. Hence, it is apparent that the high metabolic rate might result in higher production of ROS; an event which might be responsible for higher SOD activity. However, Root and petal shows least activity which might be due to lack of photosynthesis and/or lesser metabolic rate in these organs. These data emphasize the critical role of subcellular superoxide dismutase location and strongly advocate that enzymatic activity of SOD is differentially regulated at different organs of the plant depending upon its developmental and physiological conditions.

CuZn SOD is the most abundant SOD isoenzyme in many plant species (Bowler et al. 1994; Alscher et al. 2002). In this report, we have analysed the relative expression of major isoform of CuZn-SOD which is localised in cytosol. Our observations reveal that expression of cytosolic CuZn-SOD is slightly higher in leaf while other organs show less abundance of the gene. This also supports previous reports which suggest that cytosolic CuZn-SOD plays major role in scavenging $O_2^{\cdot-}$ (Perl-Treves and Galun 1991; Murai and Murai 1996) and hence this isoforms is uniformly distributed in different tissues of the plant.

On the other hand, expression level of Fe-SOD was found to be highest in leaf followed by apical bud and lateral bud, while expression was least non photosynthetic organs like root, stem and petal. To date most of the Fe-SODs found are chloroplastic, so abundance of chloroplast in organs probably determine abundance of Fe-SOD mRNA abundance in these organs (Bowler et al. 1994; Okamoto and Colepicolo 1998; Alscher et al. 2002). In addition to Fe-SOD, CuZn-SOD is also present in chloroplast and both of these enzymes are responsible for the efficient removal of the superoxide formed during photosynthetic electron transport and hence function in reactive oxygen species metabolism. The availability of copper is believed to be a major determinant of CuZn-SOD and Fe-SOD expression (Pilon et al. 2011). However, in our case since all the plant organs belongs to same condition (copper present in the soil), expression pattern of Fe-SOD/ CuZn-SOD represent the true value and copper is not a detrimental factor here. Rather, presence/ absence of chloroplast are the sole determinant of the gene expression.

Mn-SODs are found in mitochondria; with only exceptions are watermelon and pea, where it is found in peroxisomes also (del Río et al. 2003; Rodríguez-Serrano et al. 2007). Decrease in Mn-SOD may leads to reduced root growth and affects Tricarboxylic Acid Cycle (TCA) Flux and mitochondrial redox homeostasis (Morgan et al. 2008). Thus, regulation of Mn-SOD is critical in those tissue where generation $O_2^{\cdot-}$ from mitochondria is very high. The transcript abundance of Mn-SOD gene in apical bud and lateral bud suggests higher accumulation $O_2^{\cdot-}$ in these meristematic tissues which might be due to high rate of metabolism and Mn-SOD play critical role here to prevent plant from oxidative injury (Seguí-Simarro et al. 2008).

In conclusion, expression patterns of SOD isoenzymes give insights into their probable functions in different tissues and development stages. The SODs in different compartments must be differently regulated at the level of gene expression by site-specific oxidative stress. Our findings demonstrate that distinct regulation mechanisms might be involved in the expression of SODs in different organs of *Ipomoea carnea*. All these cases provide evidence of the heterogeneous distribution of SOD isozymes in higher plant species, and suggest that each SOD isoenzyme must have a specific function probably related to its cellular and subcellular localization.

Acknowledgement

The authors are thankful to The Director, Institute of Life Sciences for providing financial support. The authors would like to acknowledge Adyasha Bharati for real time PCR data analysis and Sudhir Baral and Rashmirekha Satapati for their technical support.

References

Alscher RG, Erturk N, Heath LS (2002) Role of superoxide dismutases (SODs) in controlling oxidative stress in plants. J Exp Bot 53:1331-1341.

Asada K (1999) The water-water cycle in chloroplast: scavenging of active oxygens and dissipation of excess photons. Annu Rev Plant Physiol Plant Mol Biol 50:601-639.

Bannister JV, Bannister WH, Rotilio G (1987a) Aspects of the structure, function, and applications of superoxide dismutase. Crit Rev Biochem Mol Biol 22:111-180.

Beauchamp C, Fridovich I (1971) Superoxide dismutase: Improved assays and an assay applicable to acrylamide gels. Anal Biochem 44:276-287.

Bi YD, Wei ZG, Shen Z, Lu TC, Cheng YX, Wang BC, Yang CP (2011) Comparative temporal analyses of the *Pinus sylvestris* L. var. mongolica litv. apical bud proteome from dormancy to growth. Mol Biol Rep 38:721-729.

Bowler C, Van Camp W, Van Montagu M, Inzé D, Asada K (1994) Superoxide dismutase in plants. Crit Rev Plant Sci 13:199-218.

Corpas FJ, Fernández-Ocaña A, Carreras A, Valderrama R, Luque F, Esteban FJ, Rodríguez-Serrano M, Chaki M, Pedrajas JR, Sandalio LM, del Río LA, Barroso JB (2006) The expression of different superoxide dismutase forms is cell-type dependent in olive (*Olea europaea* L.) leaves. Plant Cell Physiol 47:984-994.

del Río LA, Sandalio LM, Altomare DA, Zilinskas BA (2003) Mitochondrial and peroxisomal manganese superoxide dismutase: differential expression during leaf senescence. J Exp Bot 54:923-933.

Fridovich I (1975) Superoxide dismutases. Annu Rev Biochem 44:147-159.

Ghosh M, Singh SP (2005) A comparative study of cadmium phytoextraction by accumulator and weed species. Environmental Pollution

133:365-371.

Gill SS, Hasanuzzaman M, Nahar K, Macovei A, Tuteja N (2013) Importance of nitric oxide in cadmium stress tolerance in crop plants. Plant Physiol Biochem 63:254-261.

Gupta AS, Webb RP, Holaday AS, Allen RD (1993) Overexpression of superoxide dismutase protects plants from oxidative stress (induction of ascorbate peroxidase in superoxide dismutase-overexpressing plants). Plant Physiol 103:1067-1073.

Hueza IM, Guerra JL, Haraguchi M, Gardner DR, Asano N, Ikeda K, Górniak SL (2007) Assessment of the perinatal effects of maternal ingestion of *Ipomoea carnea* in rats. Exp Toxicol Pathol 58:439-446.

Ikeda K, Kato A, Adachi I, Haraguchi M, Asano N (2003) Alkaloids from the poisonous plant *Ipomoea carnea*: Effects on intracellular lysosomal glycosidase activities in human lymphoblast cultures. J Agri Food Chem 51:7642-7646.

Jain M, Nijhawan A, Tyagi AK, Khurana JP (2006) Validation of housekeeping genes as internal control for studying gene expression in rice by quantitative real-time PCR. Biochem Biophy Res Comm 345:646-651.

Kliebenstein DJ, Monde RA, Last RL (1998) Superoxide dismutase in *arabidopsis*: An eclectic enzyme family with disparate regulation and protein localization. Plant Physiol 118:637-650.

Kolosova N, Miller B, Ralph S, Ellis BE, Douglas C, Ritland K, Bohlmann J (2004) Isolation of high-quality RNA from gymnosperm and angiosperm trees. Biotechniques 36:821-824.

Larkin MA, Blackshields G, Brown NP, Chenna R, McGettigan PA, McWilliam H, Valentin, F, Wallace IM, Wilm A, Lopez R, Thompson JD, Gibson TJ, Higgins DG (2007) Clustal W and Clustal X version 2.0. Bioinformatics 23:2947-2948.

Livak KJ, Schmittgen TD (2001) Analysis of relative gene expression data using real-time quantitative PCR and the $2^{-\Delta CT}$ method. Methods 25:402-408.

Metwally A, Finkemeier I, Georgi M, Dietz KJ (2003) Salicylic acid alleviates the cadmium toxicity in barley seedlings. Plant Physiol 132:272-281.

Morgan MJ, Lehmann M, Schwarzländer M, Baxter CJ, Sienkiewicz-Porzucek A, Williams TCR, Schauer N, Fernie AR, Fricker MD, Ratcliffe RG, Sweetlove LJ, Finkemeier I (2008) Decrease in manganese superoxide dismutase leads to reduced root growth and affects tricarboxylic acid cycle flux and mitochondrial redox homeostasis. Plant Physiol 147:101-114.

Murai R, Murai K (1996) Different transcriptional regulation of cytosolic and plastidic CuZn-superoxide dismutase genes in *Solidago altissima* (Asteraceae). Plant Sci 120:71-79.

Noctor G, Foyer CH (1998) Ascorbate and Glutathione: Keeping active oxygen under control. Annu Rev Plant Physiol Plant Mol Biol 49:249-279.

Okamoto OK, Colepicolo P (1998) Response of superoxide dismutase to pollutant metal stress in the marine dinoflagellate *Gonyaulax polyedra*. Comp Biochem Physiol Part C: Pharmacol, Toxicol and Endocrinol 119:67-73.

Perl-Treves R, Galun E (1991) The tomato Cu,Zn superoxide dismutase genes are developmentally regulated and respond to light and stress. Plant Mol Biol 17:745-760.

Perry JJP, Shin DS, Getzoff ED, Tainer JA (2010) The structural biochemistry of the superoxide dismutases. Biochim Biophys Acta-Prot Proteom 1804:245-262.

Pilon M, Ravet K, Tapken W (2011) The biogenesis and physiological function of chloroplast superoxide dismutases. Biochim Biophys Acta - Bioenerg 1807:989-998.

Rodríguez-Serrano M, Romero-Puertas MC, Pastori GM, Corpas FJ, Sandalio LM, del Río LA, Palma JM (2007) Peroxisomal membrane manganese superoxide dismutase: characterization of the isozyme from watermelon (*Citrullus lanatus* Schrad.) cotyledons. J Exp Bot 58:2417-2427.

Salin ML, Bridgesw SM (1981) Absence of the iron-containing superoxide dismutase in mitochondria from mustard (*Brassica campestris*). Biochemi J 195:229-233.

Samis K, Bowley S, McKersie B (2002) Pyramiding Mn-superoxide dismutase transgenes to improve persistence and biomass production in alfalfa. J Exp Bot 53:1343-1350.

Seguí-Simarro JM, Coronado MJ, Staehelin LA (2008) The mitochondrial cycle of arabidopsis shoot apical meristem and leaf primordium meristematic cells is defined by a perinuclear tentaculate/cage-like mitochondrion. Plant Physiol 148:1380-1393.

Sharma N, Park SW, Vepachedu R, Barbieri L, Ciani M, Stirpe F, Savary BJ, Vivanco JM (2004) Isolation and characterization of an RIP (Ribosome-Inactivating Protein)-Like protein from tobacco with dual enzymatic activity. Plant Physiol 134:171-181.

Tepperman J, Dunsmuir P (1990) Transformed plants with elevated levels of chloroplastic SOD are not more resistant to superoxide toxicity. Plant Mol Biol 14:501-511.

Van Camp W, Herouart D, Willekens H, Takahashi H, Saito K, Van Montagu M, Inze D (1996) Tissue-specific activity of two manganese superoxide dismutase promoters in transgenic tobacco. Plant Physiol 112:525-535.

Yamahara T. Shiono T, Suzuki T, Tanaka K, Takio S, Sato K, Yamazaki S, Satoh T (1999) Isolation of a germin-like protein with manganese superoxide dismutase activity from cells of a moss, *Barbula unguiculata*. J Biol Chem 274:33274-33278.

Zor T, Selinger Z (1996) Linearization of the bradford protein assay increases its sensitivity: theoretical and experimental studies. Anal Biochem 236:302-308.

Volume 57(2):131-144, 2013
Acta Biologica Szegediensis
http://www.sci.u-szeged.hu/ABS

ARTICLE

Calcium and L-histidine interaction on growth improvement of three tomato cultivars under nickel stress

Hossein Mozafari[1]*, Zahra Asrar[1], Farkhondeh Rezanejad[1] Shahram Pourseyedi[2], Mohammad Mehdi Yaghoobi[3]

[1]Biology Department, Shahid Bahonar University of Kerman, Kerman, Iran, [2]Agronomy Department, Shahid Bahonar University of Kerman, Kerman, Iran, [3]Environmental Sciences Institute, International Center for Sciences, High Technology and Environmental Sciences, Mahan, Iran

ABSTRACT Nickel is considered to be an essential micronutrient for many plants; however, it is very toxic at excess concentration. In this investigation the interaction between L-histidine (His) and calcium on improvements of growth and K^+ nutrition was studied under Ni^{2+} stress in hydroponic media in 3 tomato cultivars (*Cal-J N3*, *Early Urbana Y* and *Petoearly CH*) from Iran. The treatments contained Ca^{2+} (400 and 700 µM), L-histidine (0 and 300µM) and $NiSO_4$ (0, 150 and 300 µM). The following parameters were determined: root and shoot length, fresh weight, pigment concentration, leaf area index, K^+ accumulation, reducing sugars, proline, free amino acids (FAA) and leaf relative water content (RWC). The results showed that Ni^{2+} treatments significantly decreased the shoot and root length, the pigment content of leafs and the K^+ content of root and shoot in all cultivars, whilst application of Ca^{2+} and His elevated these growth and nutritional parameters irrespectively of the presence of Ni. The effect of Ca^{2+} on increasing of leaf area and other parameters in *Early Urbana Y* and *Cal-J N3* cultivars was more pronounced than in *Petoearly CH* cultivar. Therefore, application both Ca^{2+} and His can affect on nutrition improvement and increasing of the tolerance and growth of agronomic plants under Ni^{2+} stress.

Acta Biol Szeged 57(2):131-144 (2013)

KEY WORDS

calcium
L-histidine
hydroponic media
nickel stress
tomato

Heavy metals such as nickel, copper, cadmium and mercury are toxic to most organisms and a variety of mechanisms have been evolved for coping with these toxic elements (Scheller et al. 1987). Ni is an essential micronutrient for plants, since it is in the active centre of the enzyme urease, which is required for nitrogen metabolism in higher plants. However, it is also showed that at elevated levels, Ni is a toxic metal in various plant species. The most decisive symptoms of Ni-induced toxicity in plants are the inhibition of growth, photosynthesis, mineral nutrition, sugar transport and water relation (Seregin and Kozhevnikova 2006). During Ni-induced toxicity, plants develop different resistance mechanism to avoid or tolerate Ni stress, including the changes of the lipid composition, the profiles of isozymes and enzyme activity, sugar or amino acid contents, and the level of soluble proteins (Schützendübel and Polle 2002).

Metal chelation by specific low-M_r ligands is one of the major processes that determine metal tolerance of a plant. All plants are able to produce phytochelatins, which can bind and detoxify heavy metals (Ha et al. 1999). In nickel-tolerant plants histidine has been implicated in metal detoxification (Sagner et al. 1998).

Accepted January 17, 2014
*Corresponding author. E-mail: mozafari.hossein@gmail.com

Generally, plants develope a complex network of highly effective homeostatic mechanisms that serve to control the uptake, accumulation, trafficking and detoxification of metals. Chelators are involved in metal detoxification via buffering the cytosolic metal concentration (Clemens 2001). Reactive interaction between metal ions and organic acids or amino acids for metal chelating was reported (Wagner 1993; Delhaize and Ryan 1995; Sagner et al. 1998).

The binding of Ni with His has been confirmed with the analyses of Ni-hyper accumulation and non-accumulation species. Under Ni toxication, increasing of the His content was detected in xylem sap in the Ni-hyper accumulation *Alyssum lesbiacum* (Kramer et al. 1996). When His treatments had been used for non-accumulation plant *A. montanum*, these treatments increased the Ni tolerance (Kramer et al. 1996). Tolerance of yeasts to Ni and other heavy metals has been reported to correlate with high cellular His levels (Joho et al. 1992). Metal chelators like phytosiderophores or organic acids also play an important role in regulating metal uptake by plant cells (Curie et al. 2001). Phytosiderophores have been detected in the xylem sap of barley plants (Alam et al. 2001). Chelators mediate and control the partitioning and translocation of the heavy metal such as Ni between the roots and shoot organs.

Calcium is an essential macronutrient with diverse functions in plants (McLaughlin and Wimmer 1999). Ca plays an important regulatory role in cell division, cell extension, cell wall- and membrane-synthesis and function (Hanson 1984; McLaughlin and Wimmer 1999). Ca also functions as a second messenger at low concentrations in signal transduction between environmental factors and plant responses (Marschner 1995). The concentration of Ca in the cytosol is very low (1 µM approximately), since Ca is cytotoxic in higher concentrations at millimolar range (Marschner 1995). The various roles of Ca in plant systems depend on its unique chemical properties that allow it to exist in a wide variety of binding states (Hepler and Wayne 1985).

In the cell wall, Ca is mainly bound to exchangeable sites in the middle lamella. By binding to carboxylic groups of the polygalacturonic acids (pectins) and cross-linking the pectic chains of the middle lamella, Ca strengthens the cell wall and controls its rigidity (Demarty et al. 1984).

The selective property of cell wall correlates with optimum Ca content in plant tissues and rhizosphere (Girija et al. 2002). The cell wall is important chelator of toxic metals such as Ni, as far as the metal is transported apoplastically especially in root tissue. The cell walls inevitably come into direct contact with the heavy metal-containing medium in the soil and act as a cation exchanger in the plant root (Küpper et al. 2001). It has been described that Ca may decrease the uptake, translocation and accumulation of heavy metals in plants (Österas and Greger 2006).

As hypothesized, metals were found to interact and negatively affecting the accumulation of each other in the stem and roots of plants. Furthermore, in nutrient solutions Ca was found to decrease the accumulation of Cd, Cu, Mn and Zn in stem and roots. Even at low elevated Ca or Cu addition interactions were found (Saleh et al. 1999). Similarly, heavy metals, like Cu and Cd, have been found to reduce the Ca, Mn and Zn contents in roots, shoots and leaves of trees (Arduini et al. 1998).

Heavy metal ions are supposed to enter into plant cells through systems devoted to the uptake of essential cations. The uptakes of many toxic metals are happened via Ca channels by plant cells (Wu and Hendershot 2010). Moreover, it was shown that heavy metals compete with Ca at both Ca channels (Nelson 1986) and intracellular Ca binding proteins (Rivetta et al. 1997). Metals with similar physiochemical properties, such as ion-size and charge, compete with each other for binding sites in plants (Marschner 1995), thereby affecting the uptake, translocation and accumulation of each other.

Supplementing the medium with Ca alleviates growth inhibition under metal stress conditions (Yan et al. 1992; Kinraide 1998). The concentration of different cations in the uptake solution is decisive for the resulting transport across the membrane (Lu et al. 2010). Raising the Ca^{2+} concentration was shown to block heavy metal transport into rice roots as a result of the competition of toxic metals with Ca^{2+} for Ca transporters (Clemens 2006).

Permeability of plasma membrane to toxic ions correlates with cell wall activity and Ca content. The main part of Ca in plant tissues is located in the apoplast, bound to the cell wall, the outer surface of the plasma membrane and other structures (Marshner 1995). Ca blocks the symplastic uptake of Ni in root tissue. Generally, Ca ion plays an important role in regulating ion transfer into plant cells growing in stress conditions, like salinity and toxic metals (Greenway and Munns 1980). In addition, Ca is very effective in detoxifying high concentration of other toxic elements under stress condition (Ashraf and Akhtar 2004). Thus, Ca sustains potassium transport and K^+/Na^+ selectivity in plant membrane. Ca also plays a key role in control of production of proline and glycine-betaine (Charest and Phan 1990; Wu et al. 2009).

This study aimed at analysing the interaction effect between exogenous Ca (as a very important nutrient with diverse functions specially in cell wall and membrane) and His (as a specific Ni ligand) on the probable higher alleviation effect of Ni stress in three cultivars of tomato from Iran and improving growth and nutrition of these plants under Ni^{2+} stress conditions. On the other hand, we attempt to clarify that non-toxic concentration of exogenous Ca with His probably can alleviate Ni toxication in tomato than His application alone. For this reason, we evaluated growth and biochemical parameters, in three tomato cultivars under Ca, His and $NiSO_4$ treatments in hydroponic media under standard conditions and optimized treatments.

Materials and Methods

Plant growth

Seeds of the tomato cultivars (*Solanum lycopersicon* Mill. CVs; *Petoearly CH, Cal-J N3, Early Urbana Y*), that were a gift from Falaat Ghaareh Company (Tehran, Iran), were placed on two sheets filter paper in Petri dishes (9 cm), that contain Hoagland solution for optimum seedling growth. After 7 days and emergence, uniform seedlings of tomato were selected and transferred into dark polyethylene vessels (two plants per vessel), each supplied with 50 ml of a modified Hoagland solution (Hoagland and Arnon 1950) containing 0.5 mM KNO_3, 400 µM $Ca(NO_3)_2$, 10 µM Fe-EDTA, 0.2 mM $MgSO_4$, 0.1 mM KH_2PO_4, 10 µM H_3BO_3, 2 µM $MnCl_2$, 2 µM $ZnSO_4$, 0.1 µM Na_2MoO_4 and 0.2 µM $CuSO_4$ buffered to pH 5.8±0.1. The growth medium was continuously aerated and the nutrient solutions were exchanged once a day. Seedlings and plants were grown in greenhouse with supplementary light provided by sodium vapor lamps at a photon flux density of 10 klx during the day, a photoperiod of 16/8 hours, day and night temperature of 25°C and 22°C respectively, and 60% constant relative humidity.

Experimental treatments

Tomato plants were grown under control conditions in a modified Hoagland solution for 3 weeks that was continuously aerated and exchanged once a day. After this period, the effect of Ni exposure and other compounds (L-histidine and $CaCl_2$) on growth have been studied. Nutritional and physiological parameters were investigated by replacing the nutrient with a fresh solution containing the respective compounds for 10 days that was continuously aerated and was exchanged once a day. The indicated total treatment concentrations were supplied as $NiSO_4$ (0, 150 and 300 µM), as $CaCl_2$ (400 and 700 µM; total Ca^{2+} concentration in nutritional media) and L-histidine (0 and 300 µM; extra pure, Merck Co, Germany), that were solved in the Hoagland solution and adjusted to pH 5.8±0.1 with KOH. In this experiment the root and shoot samples were collected after treatments exposure for growth and physiological analyses. At the end of the treatment period, root and shoot organs were washed in deionised water, blotted dry with tissue paper, measured, frozen in liquid nitrogen and stored at -80°C until analysis.

Morphological analysis

The morphological parameters determined in this research included fresh weight (FW), length of both shoot and root organs and leaf area.

Biochemical analysis

The concentration of the main photosynthetic pigments (chlorophyll a+b and total carotenoids) were measured quantitatively in acetone extract from untreated and Ni-treated (with or without Ca and His) tomato cultivars using absorption coefficient at specific wavelengths (470, 646 and 663 nm) given by Lichtenthaler (1987) and recalculated per gram of fresh weight. The relative water content (RWC) of leaves was determined by the method of Turkan et al. (2005). The method for proline determination was essentially as described by Bates et al. (1973). Free amino acids (FAA) was measured in shoot and root tissues using the method of Hwang and Ederer (1975). For the determination of the reduced carbohydrates the method of Somogyi (1952) was used.

Element analysis

Samples of root and shoot were oven dried at 70 °C for 72 h, and after the determination of dry biomass 0.5 g samples were dissolved in 10 ml 65% (w/v) nitric acid (supra pure, Merck Co, Germany). Total concentration of K^+ was determined by inductively coupled plasma atomic emission spectroscopy (ICP-AES, Varian) by the method of Sagner et al. (1998).

Experimental design and statistical data analysis

The experimental design was a completely randomized design with 12 treatments, 3 cultivars and 4 replications per treatments. Samples were collected from two plants per culture vessels. Data were analysed using analysis of variance (four-way ANOVA), followed by Duncan test. Differences between means were considered significant at confidence level of P 0.05. All statistical analyses were done using the software SPSS package Version 18.0 (SPSS 2009).

Results

The effects of various treatments on root and shoot length in the three tomato cultivars are shown in Figure 1. When the concentrations of the external His and Ca^{2+} were low, an increase from 0 to 150 or 300 µM Ni^{2+} significantly decreased the shoot length in all cultivars compared to the control. A further increase in the concentrations of Ca^{2+} and His from 0 to 300 µM, separately or together, had increasing positive effect on shoot length. In general, both Ca^{2+} and His significantly increased the root growth in two cultivars (*Petoearly CH* and *Early Urbana Y*) under Ni^{2+} toxication, however, *Cal-J N3* cultivar had no improving growth after treatment with 300 µM Ni^{2+} beside Ca^{2+} and His. Ni^{2+} treatment (150 µM) without Ca^{2+} and His decreased the shoot length, while treatments containing Ca^{2+} and His resulted increasing growth compared to the control. Generally, Ca^{2+} and His significantly increased the root growth in all studied cultivars under Ni^{2+} toxication; only it had not observed any improving effect on the growth of *Cal-J N3* cultivar, when 300 µM Ni^{2+} was applied beside Ca^{2+} and His (Figs. 1 and 2).

In the treatment containing 150 µM Ni^{2+} beside Ca^{2+} and His, shoot fresh weight (FW) was not significantly different in *Cal-J N3* cultivar compared to the control. But shoot and root FW was increased under 300 µM Ni^{2+} in the other two cultivars compared to the control. However, in treatments containing only His, root FW was higher than under Ca^{2+} treatments (Fig. 2 D-F). Similar results were found also at the dry weight determination (data not shown).

Figure 3 A-C indicated the leaf RWC at different Ni^{2+} concentrations affected by Ca^{2+} and His treatments. In both cultivars, *Early Urbana Y* and *Cal-J N3*, the Ca^{2+} and His improved the leaf RWC under 150 and 300 µM Ni^{2+} treatments. However, Ca^{2+} and His had negative effects on leaf RWC in tomato *Petoearly CH* cultivar compared to the control (Fig. 3C).

In this research, leaf pigments, especially chlorophylls were also determined (Fig. 4 A-C). The application of Ca^{2+} and His increased the level of chlorophyll pigments under Ni^{2+} stress. Our data indicated that His increased the level of chlorophyll (a+b) under Ni^{2+} stress. In *Cal-J N3* cultivar under 150 µM Ni^{2+} treatment, application 300 µM Ca^{2+} and His increased the level of chlorophyll (a+b) compared to other treatments. Chlorophyll (a+b) content was significantly increased under Ca^{2+} treatment in unstressed conditions (Fig. 4 A-C). On the other hand, this pigment increase shows that

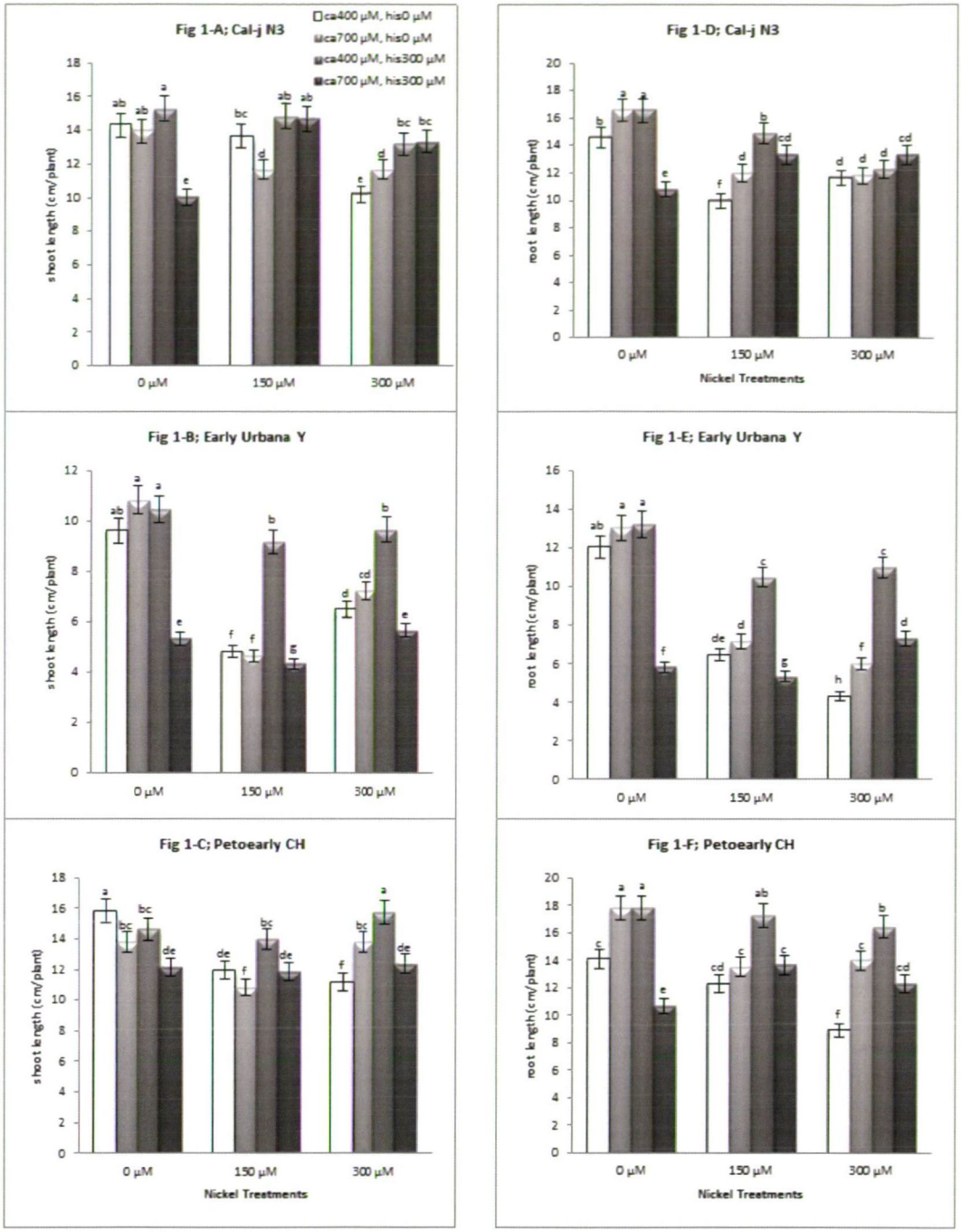

Figure 1. The mean of shoot and root length (A-F) determined and three-way ANOVA with multiple but equal number of observations per test tube for the effects of individual treatments and their interactive effects on the growth prarmeter changes in the tomato cultivars treated with a nutrient solution containing different concentrations of nickel, calcium and histidine ($P<0.05$). Vertical bars indicate the mean of four replications ± SE (n=4). Different letters indicate significantly different values among the experimental treatments.

leaf growth and expanding can depend upon calcium ion. The total carotenoid determination showed that Ca^{2+} and His increased the concentration of this leaf pigment under 150 µM Ni^{2+} treatment. The incubation with Ni^{2+} (300 µM) beside Ca^{2+} and His resulted in a decrease of carotenoid content in leaf tissue in all the tomato cultivars. In two cultivars (*Early Urbana Y* and *Cal-J N3*) leaf area was increased under Ni^{2+}, Ca and His treatments compared to Ni^{2+} treatment without Ca^{2+} and His. In summary, Ca^{2+} with or without His, improved growth and leaf area index in the studied cultivars of tomato. In ad-

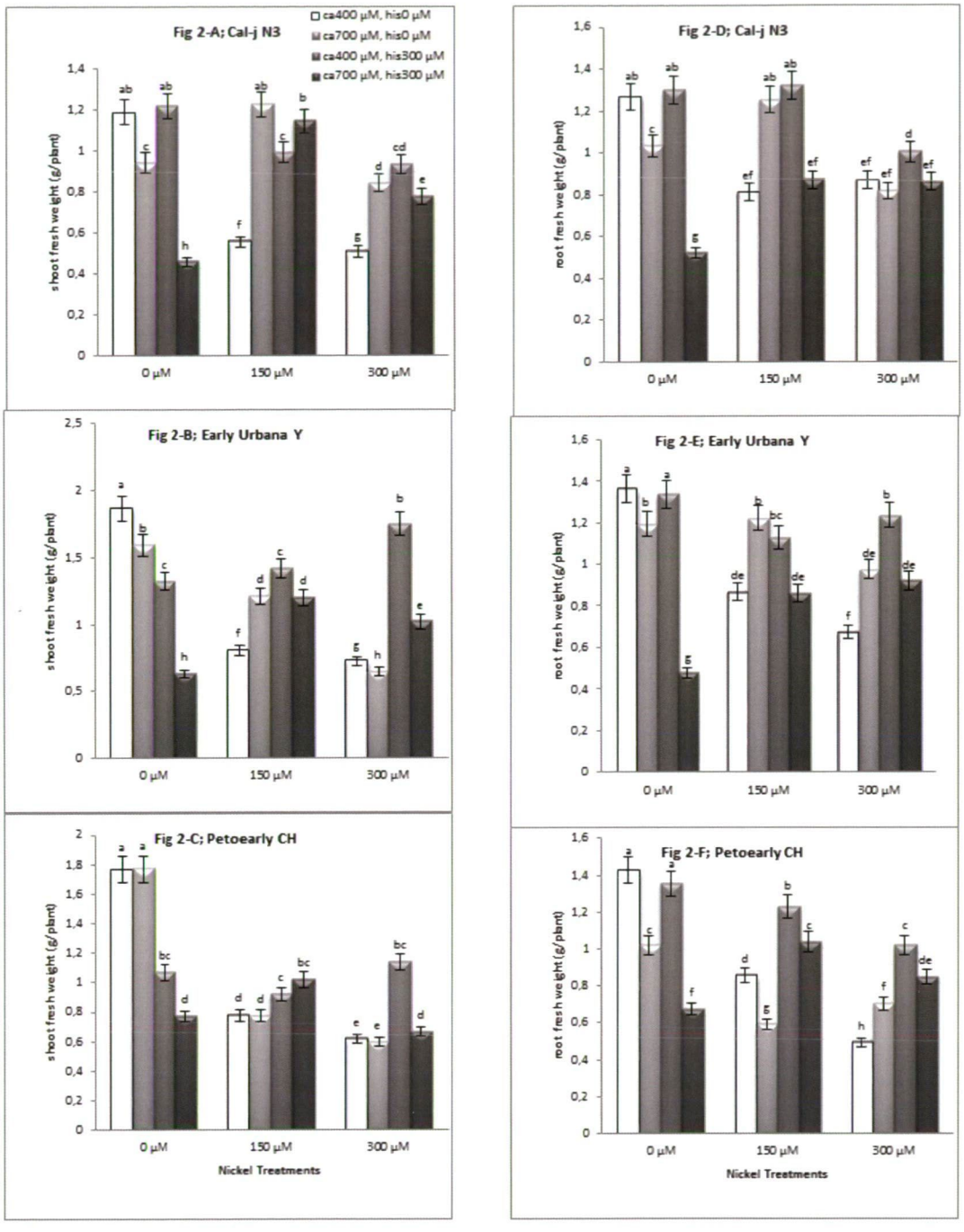

Figure 2. The mean of shoot and root fresh weight (A-F) determined and three-way ANOVA with multiple but equal number of observations per test tube for the effects of individual treatments and their interactive effects on fresh weight changes in the tomato cultivars treated with a nutrient solution containing different concentrations of nickel, calcium and histidine ($P<0.05$). Vertical bars indicate the mean of four replications ± SE (n=4). Different letters indicate significantly different values among the experimental treatments.

dition, it has been observed that His treatments have positive effect on leaf area increase under Ni^{2+} treatments in the *Early Urbana Y* and *Cal-J N3* cultivars of tomato (Fig. 4 D-F).

The proline content in both root and shoot was increased under Ni^{2+} stress and it was the highest in the presence of Ni^{2+} without Ca^{2+} and His in tomato plants. In the root and shoot of *Cal-J N3* cultivar treatment with 300 µM Ni^{2+} increased the proline concentration (Fig. 6 A-F). In the other two cultivars (*Petoearly CH* and *Early Urbana Y*) the effect of 150 µM Ni^{2+} on proline content was significantly higher (Fig. 6

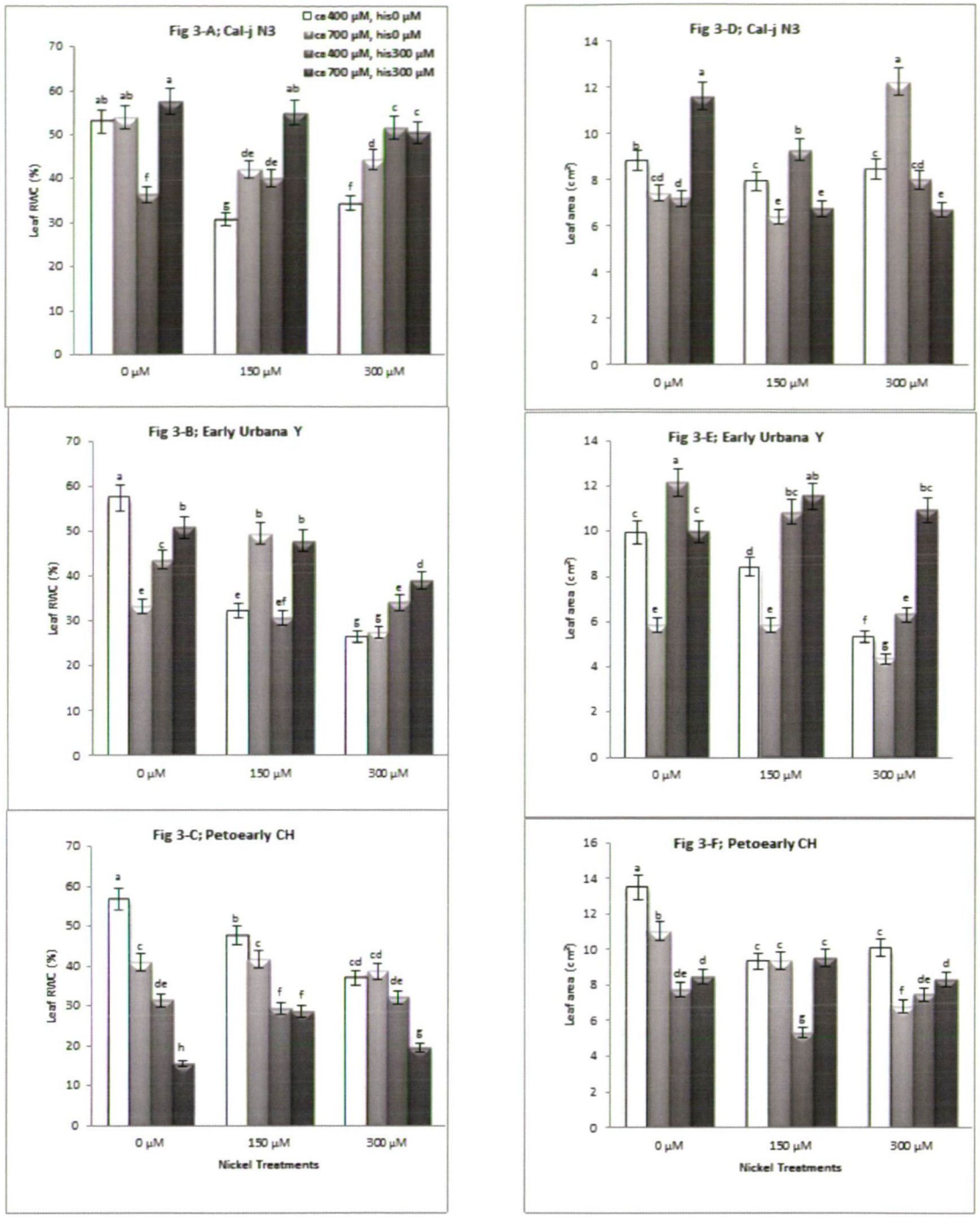

Figure 3. The mean of leaf RWC (A-C) and leaf area (D-F) determined and three-way ANOVA with multiple but equal number of observations per test tube for the effects of individual treatments and their interactive effects on the leaf parameters changes in the tomato cultivars treated with a nutrient solution containing different concentrations of nickel, calcium and histidine ($P<0.05$). Vertical bars indicate the mean of four replications ± SE (n=4). Different letters indicate significantly different values among the experimental treatments.

A-F). The proline content was also the highest in the presence of Ni^{2+} without Ca^{2+} and His in all tomato cultivars. Based on the lower effect of 150 Ni^{2+} µM on proline concentration in *Cal-J N3* cultivar, proline content was not diminished by the addition of Ca^{2+} and His as ligands. Proline content was decreased by the addition of 300 µM His under both concentrations (150 and 300 µM) of Ni^{2+} treatments, while the effect of His combined with Ni^{2+} was similar to the control in *Cal-J N3* cultivar. Interaction effect of His and Ca^{2+} on proline decline was observed in all cultivars under Ni-stress. In the

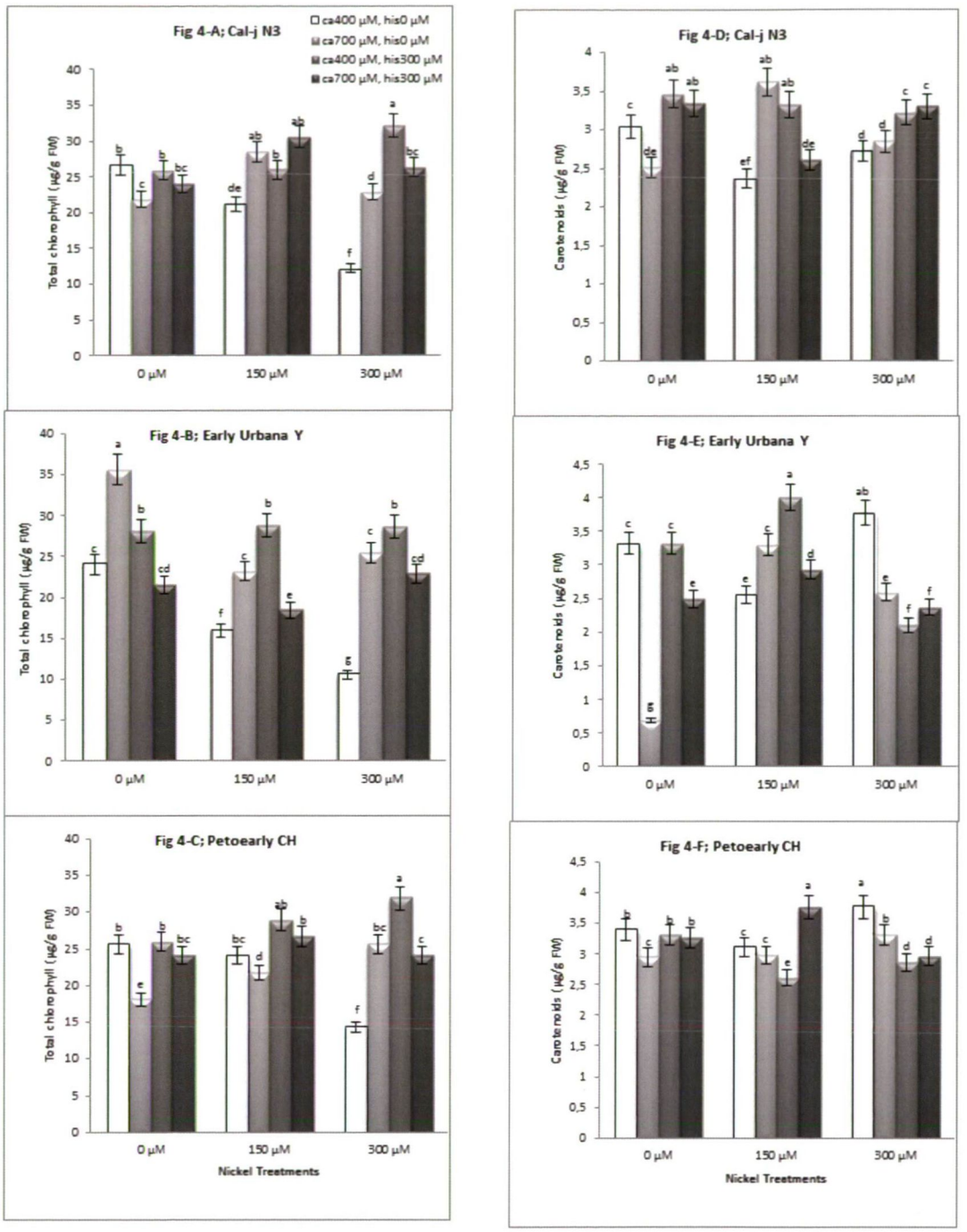

Figure 4. The mean of leaf total chlorophyll (A-C) and carotenoids (D-F) determined and three-way ANOVA with multiple but equal number of observations per test tube for the effects of individual treatments and their interactive effects on the leaf parameters changes in the tomato cultivars treated with a nutrient solution containing different concentrations of nickel, calcium and histidine ($P<0.05$). Vertical bars indicate the mean of four replications ± SE (n=4). Different letters indicate significantly different values among the experimental treatments.

shoot of the *Petoearly CH* cultivar proline accumulation was lower under Ni^{2+}, Ca^{2+} and His treatments than under Ni^{2+} treatment alone.

The interaction effect of Ca^{2+} and His on FAA content was significant compared to the control. The influence of Ca^{2+} and His on the decreasing of FAA content was observed in *Cal-J N3* cultivar under 150 µM Ni^{2+} compared to unstressed conditions. The treatment with 300 µM Ni^{2+} beside Ca^{2+} and His resulted in the decreasing of the FAA content in the root and shoot tissues in all tomato cultivars. It seems that Ca^{2+}

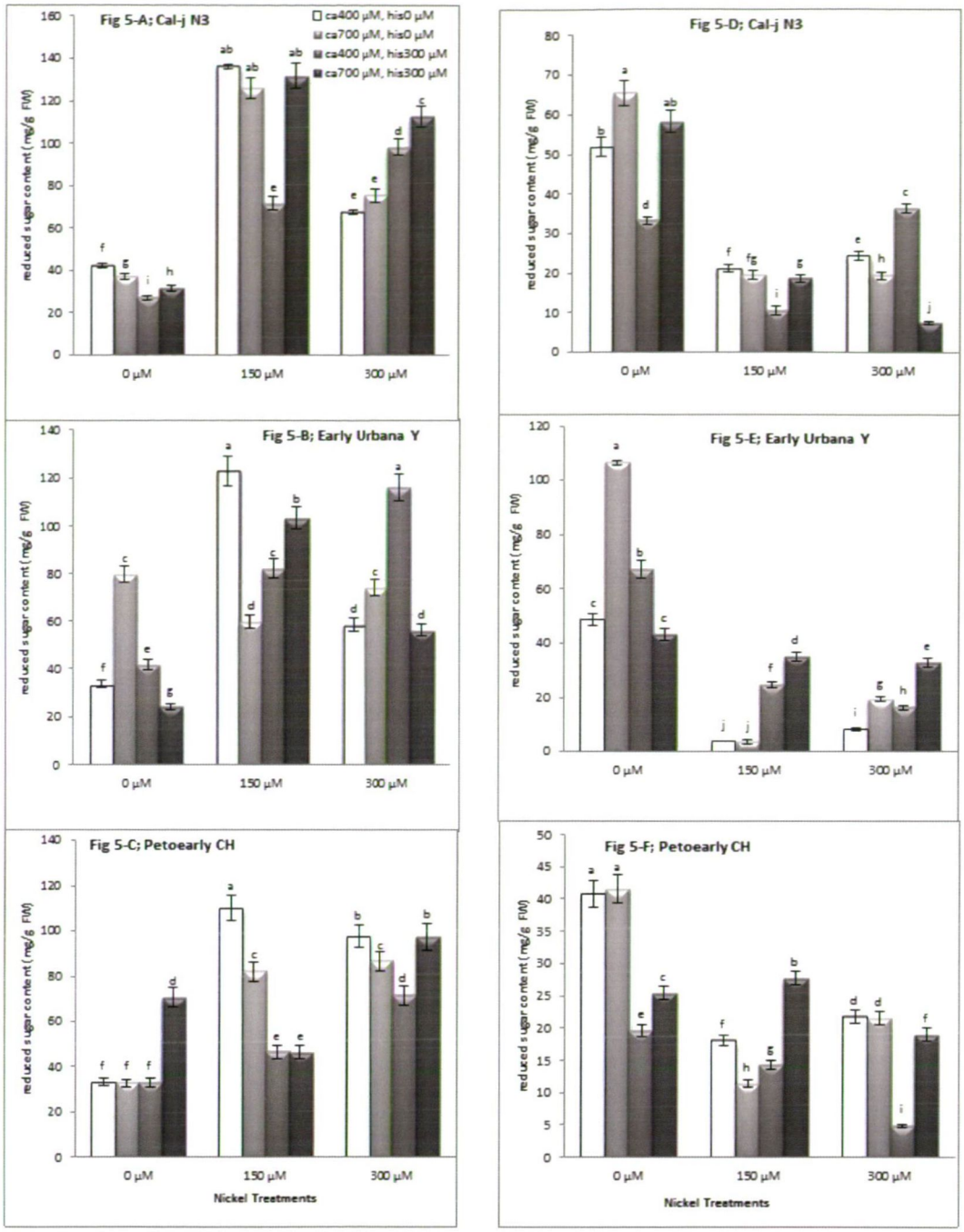

Figure 5. The mean of shoot and root reduced sugars (A-F) determined and three-way ANOVA with multiple but equal number of observations per test tube for the effects of individual treatments and their interactive effects on reduced sugars content changes in the tomato cultivars of treated with a nutrient solution containing different concentrations of nickel, calcium and histidine ($P<0.05$). Vertical bars indicate the mean of four replications ± SE (n=4). Different letters indicate significantly different values among the experimental treatments.

effect on FAA decrease is significant under 150 µM Ni^{2+} and interaction between Ca^{2+} and His on the FAA concentration was found at 300 µM Ni^{2+} treatment (Fig. 7 A-C).

Our data showed that Ni^{2+} stress resulted in the accumulation of the reducing sugars in the shoot of the cultivars, whereas in root tissue they are decreased in comparison to the control (Fig. 5; A-F). The level of the reducing sugar content was considerably greater in the shoot of *Cal-J N3*, than other cultivars treated with Ni^{2+} at toxic levels. However, sugar concentration was lower in root of *Cal-J N3*, than in other

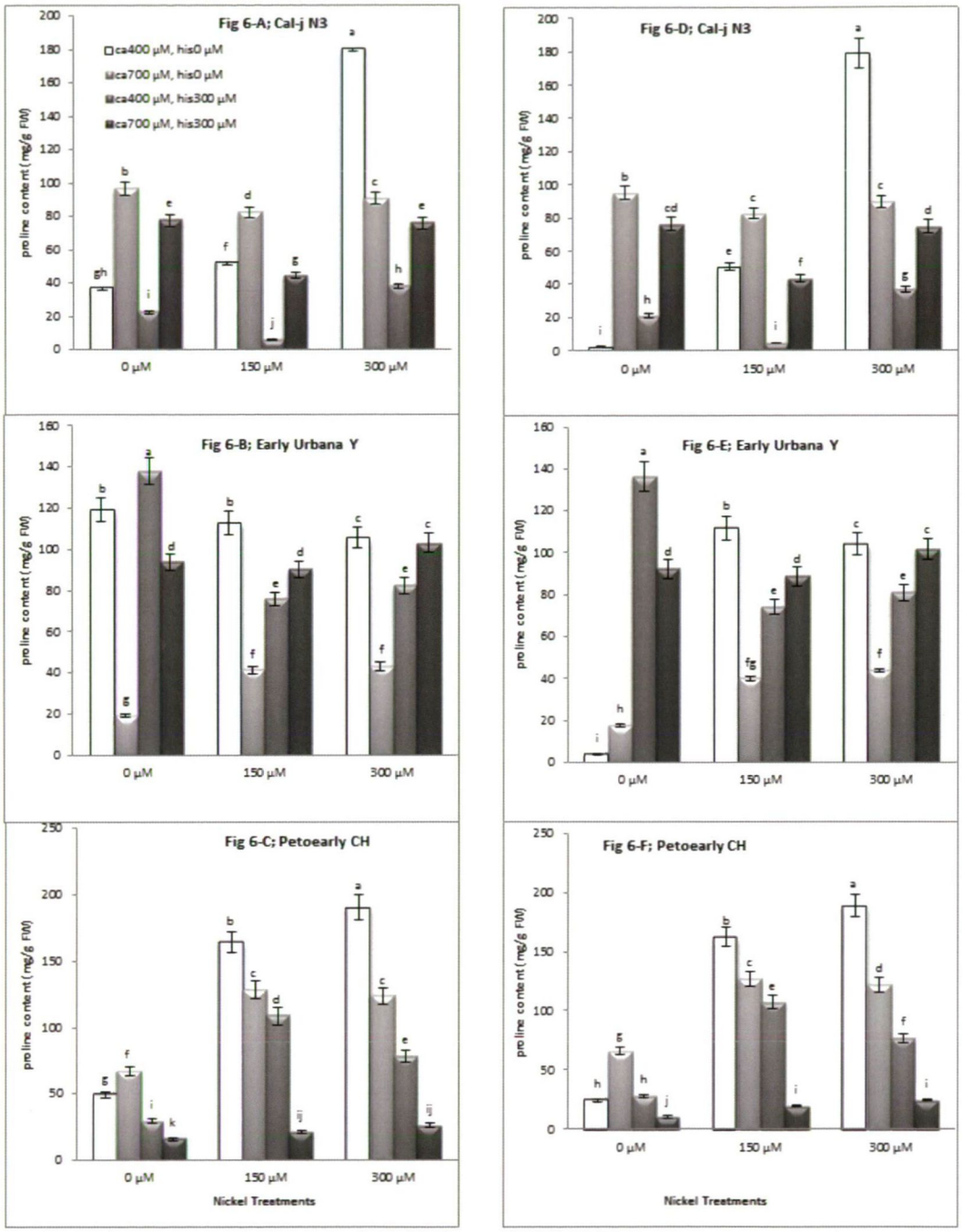

Figure 6. The mean of shoot and root proline (A-F) determined and three-way ANOVA with multiple but equal number of observations per test tube for the effects of individual treatments and their interactive effects on proline content changes in the tomato cultivars treated with a nutrient solution containing different concentrations of nickel, calcium and histidine ($P<0.05$). Vertical bars indicate the mean of four replications±SE (n=4). Different letters indicate significantly different values among the experimental treatments.

cultivars. Independent application of Ca^{2+} and His decreased the sugar content in the shoot of *Cal-J N3* cultivar, which was similar to the control. His alone also increased the sugar concentration in root of two cultivars (*Petoearly CH* and *Cal-J N3*) under 150 µM Ni^{2+} treatment.

Figure 8 shows the effect of the treatments on potassium concentration of the shoot and root tissues in the tomato cultivars resulted from ICP determination. When the concentration of the external Ca^{2+} and His was low beside the 300 µM Ni^{2+} level (Ni^{2+} treatments without Ca^{2+} and His), an increase in

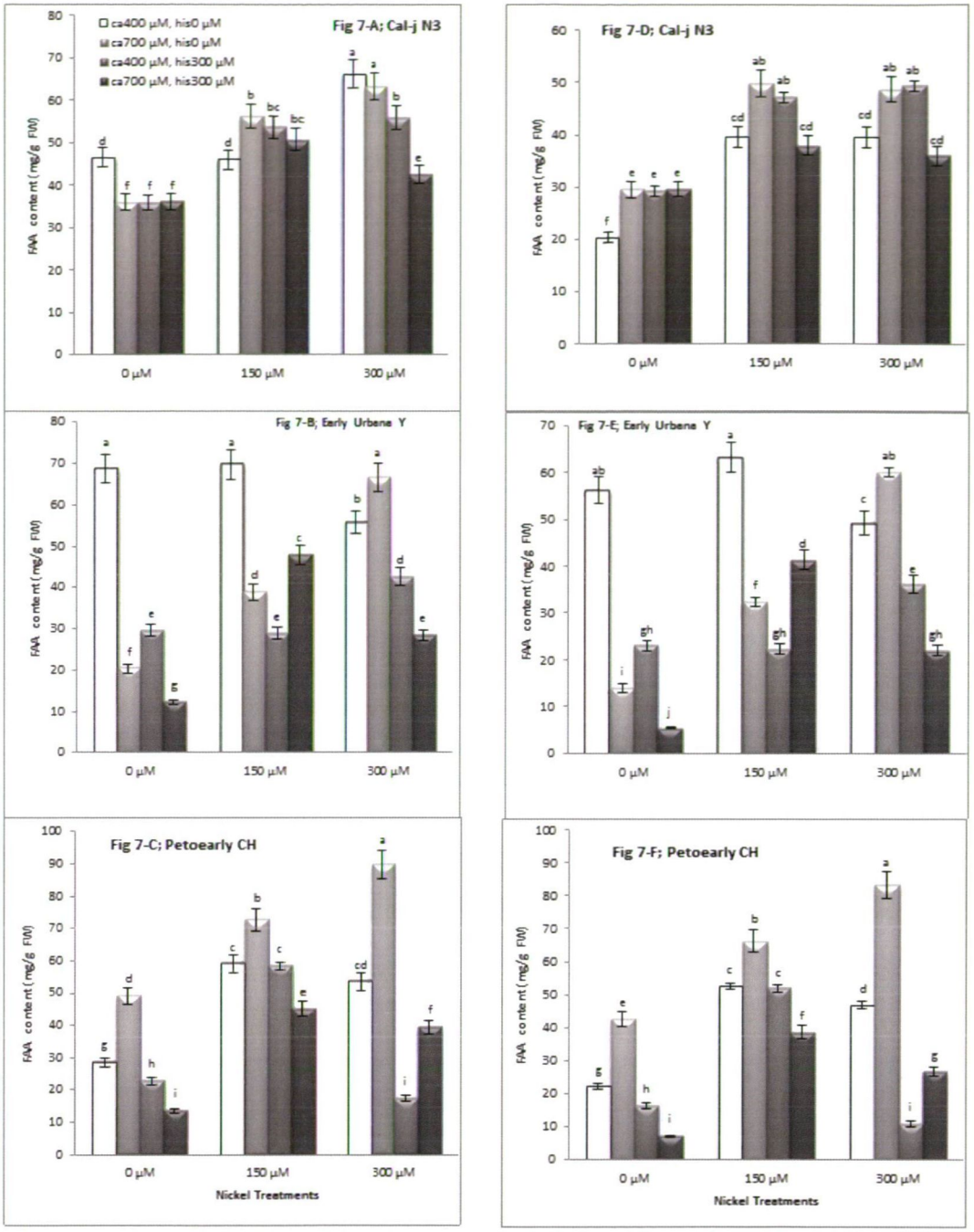

Figure 7. The mean of shoot and root FAA (A-F) determined and three-way ANOVA with multiple but equal number of observations per test tube for the effects of individual treatments and their interactive effects on FAA content changes in the tomato cultivar treated with a nutrient solution containing different concentrations of nickel, calcium and histidine ($P<0.05$). Vertical bars indicate the mean of four replications ± SE (n=4). Different letters indicate significantly different values among the experimental treatments.

Ca^{2+} and His (from 0 to 300 µM) significantly increased the K^+ uptake in shoot and root plants. In the *Cal-J N3* cultivar 150 µM Ni^{2+} combined with Ca^{2+} and His decreased the K^+ content in shoot compared to Ni^{2+}-free Ca^{2+} and His treatment (Fig. 8A). However, in the *Cal-J N3* cultivar, Ca^{2+} and His increased the K^+ concentration in shoot and root differently in stress and control conditions (Fig. 8A, 8D). In other cultivars we also observed similar results in K^+ accumulation in the *Cal-J N3* cultivar plants. Our data showed that, Ca^{2+} and His decreased K^+ accumulation in both root and shoot of

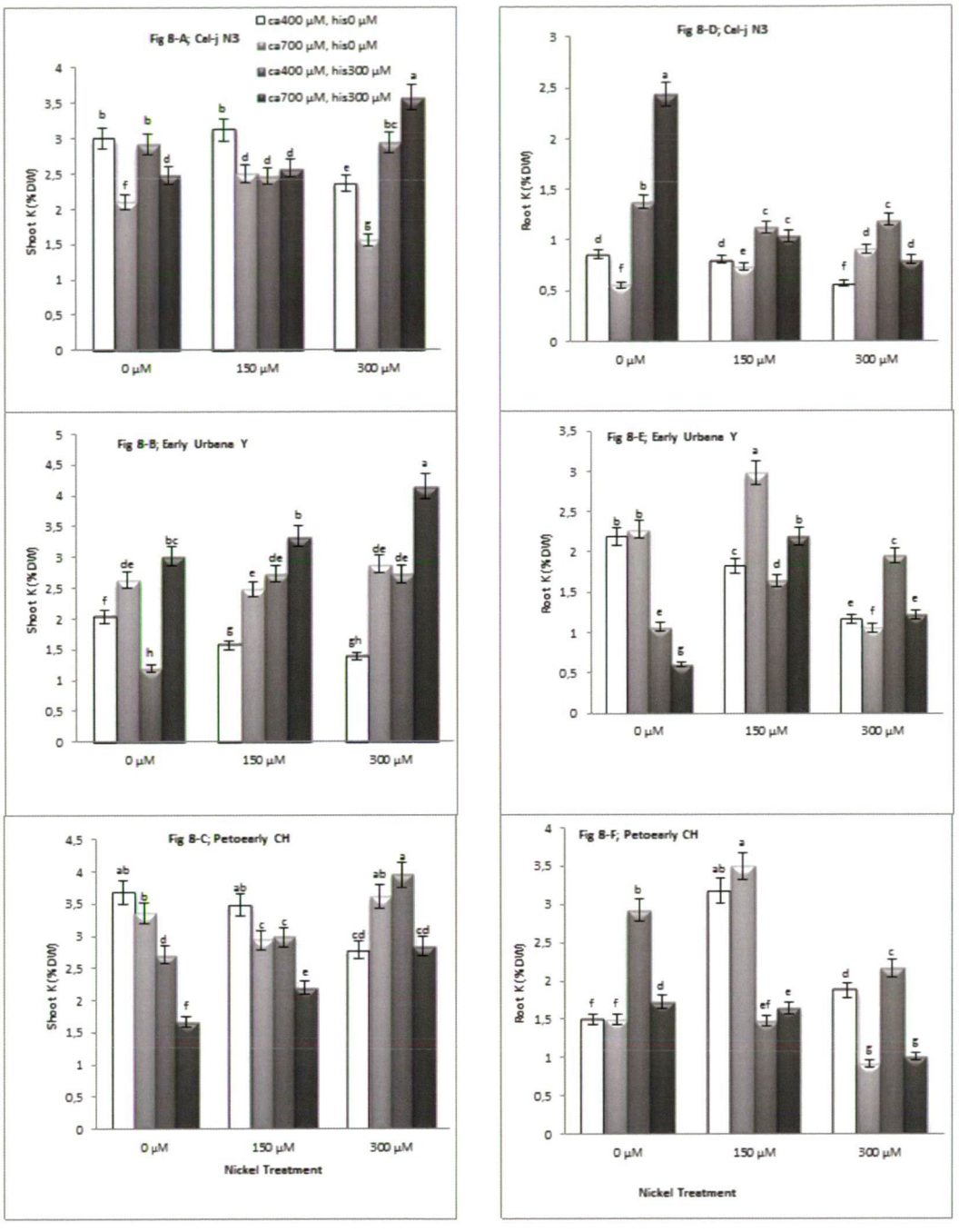

Figure 8. The mean of shoot and root K accumulation (A-F) determined and three-way ANOVA with multiple but equal number of observations per test tube for the effects of individual treatments and their interactive effects on K content changes in the tomato cultivars treated with a nutrient solution containing different concentrations of Nickel, calcium and histidine ($P<0.05$). Vertical bars indicate the mean of four replications ± SE (n=4). Different letters indicate significantly different values among the experimental treatments.

Petoearly CH cultivar under 150 µM Ni^{2+} (Fig. 8C, 8F). But K^+ accumulation and nutrition under 300 µM Ni^{2+} treatment (also containing Ca^{2+} and His) increased compared to the same Ni^{2+} treatment without Ca^{2+} and His.

Discussion

Ni is among those metals that the most cause for immediate concern in environment (Zafar et al. 2007). It is also phytotoxic causing growth inhibition, disturbances in nutrient

uptake and other metabolic and physiological processes of plants (Sanita di Toppi and Gabbrielli 1999, Molas 2002). In this study, we have shown that Ca^{2+} and His are highly effective in protecting tomato plants from growth inhibition caused by the high concentrations of Ni^{2+} under hydroponic culture experiments. Heavy metal tolerance in plants often include binding of metals by chelators such as His or Ca in cell wall, phytosiderophores and phytochelatins, volatilization and enhanced export from the cell (Cataldo et al. 1988). The ligands (such as cell wall and His), bind considerable amounts of Ni^{2+} in rhizosphere, root tissue and cell wall in pericycle layer cells under both resting and growing conditions (Cataldo et al. 1988). The described interactions could play a significant role in metal availability by absorbing and immobilizing toxic ions from soil solution (Wu et al. 2006).

Although the Ca^{2+} and Ni^{2+} accumulation in the root are usually inversely proportional, root ion accumulation more often accounted for a higher share of variability in root elongation than Ni^{2+} accumulation in root tissue at high concentration of Ca^{2+} than control conditions (Wu and Hendershot 2010). Therefore, in the evaluation of root elongation, certain predictors, such as Ni^{2+} and Ca^{2+} must have accounted, when environmental conditions (low Ca^{2+} concentrations) significantly affect the amount of the accumulated Ca^{2+}. The root Ca^{2+} and Ni^{2+} concentration can be determined from total Ca^{2+} and total Ni^{2+} solution. Root elongation revealed a strong positive correlation with total Ca^{2+} content in the roots (Wu and Hendershot 2010). Our data also showed that Ca^{2+} and Ni^{2+} together increased the root length in all tomato cultivars more significantly than the Ni^{2+} treatments without Ca^{2+} (Fig. 1 A-F). The treatments containing Ca^{2+} (300 µM), similar to root elongation, had positive effect on shoot length.

Excess concentration of Ni^{2+} in the growth medium of plants competes with other essential metals, such as potassium and iron, causing their deficiency and oxidative stress. These resulted in the decrease of the chlorophyll biosynthesis and the damage of the photosynthetic system (Buchanan et al. 2002). The visible effects of these changes, observed in our study, were chlorosis of leaves and a reduction in the biomass (FW) of shoot and root tissues. Ca^{2+} addition improved the effect of Ni^{2+} on the cultivars of tomato, especially on *Cal-J N3* cultivar. When tomato cultivars have grown in hydroponic media containing Ni^{2+}, the plants under stress showed the effects of Ni^{2+} toxication that increased in severity. At high Ni^{2+} concentration (300 µM), the leaves appear yellow and have necrotic edges. The amount of chlorophyll a and a+b is an indication of plant stress and they increase in line with the level of stress. During oxidative stress resulted after Ni^{2+} toxication, the decrease of chlorophyll b occurs first, due to its higher redox potential compared to chlorophyll a (Stearns et al. 2007). Our data showed that chlorophyll (a+b) pigment content significantly increased under Ca^{2+} treatment in unstressed conditions (Fig. 4 A-C). On the other hand, this pigment increasing shows that leaf growth and expanding can depend on Ca ion. In this condition, the accumulation of malonaldehyde (MDA) from the cell membrane decreased the oxidative stress. In our research, Ca^{2+} and His could not decrease MDA content in leaves of *Cal-J N3* cultivar under Ni^{2+} stress, but the effects of Ca^{2+} and His were observed on MDA, which caused decreasing in the other two cultivars, especially on the leaves of *Petoearly CH* (data not shown).

Metabolic stress caused by Ni^{2+} may result in decreasing plant growth (Epron et al. 1999; Dodd and Donavan 1999). Cellular events, such as ion compartmentation and osmotic adjustment in tolerant plants may allow continuous growth in the presence of toxic ions (Volkmar et al. 1998). Proline accumulation may be a general response to toxic ion stress (Fig. 6 A-F). Many investigators found the accumulation of amino acids, especially proline in plants exposed to stress, such as salinity, heavy metals, etc. Proline accumulation may contribute to osmotic adjustment at the cellular level (Perez Alfocea et al. 1993). Proline may act as an enzyme protectant, stabilizing the structure of macromolecules and organelles. Proline also acts as a major reservoir of energy and nitrogen upon exposure to Na ions. Energy for growth and survival may help in tolerance of salt stress in barley (Chandrasekhar and Sandhyarani 1996).

In our research, Ni stress increased the proline content in the tomato plants in all cultivars. Proline content was also high in the presence of Ni^{2+} without Ca^{2+} and His in all tomato cultivars compared to the control. Addition of $CaCl_2$ together Ni^{2+} caused increased proline oxidase activity in the plants under stress (Chandrasekhar and Sandhyarani 1996). Under some combined Ni^{2+} and Ca^{2+} treatments, the proline concentration was lower in the tomato cultivars than that of the control (Fig. 6 A-F).

Free amino acids (FAA), such as glycine-betaine act as an osmotic substrate. In different plants, an increase in glycine-betaine under stress can be observed (Sudhakar et al. 1993). Subcellular compartmentation of glycine-betaine biosynthesis in rice is important for increased toxic ion Na tolerance (Sakamoto et al. 1998). To draw conclusions from proline and FAA determination, we can say that both proline and FAA production were promoted by Ni stress in the tomato cultivars. Adding Ca^{2+} (300 µM) to hydroponic system leads to a decrease in the concentration of these two osmoprotectants. The proline oxidase activity is promoted, while the activity of γ–glutamyl kinase is decreased by Ca and proline synthesis (Girija et al. 2002). Because Ni is chelated by histidine, it does not take effect on proline biosynthesis pathway.

Treatments with low concentration of heavy metals, such as Cu, Ni and Cd exhibit an increase in the amounts of total carbohydrates in the root of the plants, and its reverse is true at treatments with high concentrations (Deef 2007). Heavy metal stress affects the enzyme activity by reducing the antioxidant glutathione pool and affecting the iron me-

diated defence processes (Pinto et al. 2003). Heavy metal, such as Ni toxication greatly impaired not only the decrease of soluble sugars, but also their translocation from the root to the shoot (Kuriakose and Prasad 2008). Hopkins (1995) reported that the moderate levels of heavy metals generally play an important role in plant growth and productivity. They act as activators or co-factors in all vital processes, but relatively elevated level of heavy metals induced harmful effects on all physiological processes of plants (Bonnet et al. 2000). Our experimental data showed that 150 μM Ni^{2+} treatment increased sugar accumulation in shoot of *Cal-J N3* and *Early Urbana Y* cultivars in comparison to the control. At the same time, the carbohydrate content decreased in root of *Early Urbana Y* and *Petoearly CH* cultivars under 150 and 300 μM Ni^{2+} stress. It seems that sugar translocation occurred from the root to the shoot as the sugar content in the roots of the tomato plants was declined (Bonnet et al. 2000).

The accumulation of Cd and Cu in bark decreased with increasing addition of Ca^{2+}. Ca^{2+} has earlier been found to reduce the absorption, uptake, translocation and/or accumulation of different plants (Kawasaki and Moritsugu 1987). Thus, it has been demonstrated that putative tonoplast Ca^{2+}/H^+ antiporters encoded by *calcium exchanger 1* (CAX1) and *calcium exchanger 2* (CAX2) from *Arabidopsis* are involved in the transport of heavy metals from the cytoplasm to the vacuole (Manohar et al. 2011). Another non-selective transmembrane transporter of Ca^{2+}, the low affinity cation transporter (LCT1) is expressed in wheat, also appears to mediate Cd^{2+} transport into the cell (Clemens 2006). Moreover, interactions between Ca^{2+} and other elements, such as Mn, Cd, Zn, Ni and Fe, have been reported in lettuce (Zorrig et al. 2010).

Thus, if the Ca^{2+} pool in the soil and nutrient media is decreased, the availability of heavy metals is increased. This may result in a deficiency of Ca^{2+} in plants caused by the competition for uptake, translocation and binding with heavy metals by interaction effect with ligands, which may negatively affect plant growth and nutrition (Österas and Greger 2006). Instead, the bioavailability of Ca^{2+} is increased in the soil and nutrient media it may decrease the uptake and accumulation of toxic metals in plants, thereby, ameliorating the toxicity of heavy metals in growth parameters similar to our research.

Our results suggest that Ca^{2+} and His interaction improved the growth of the tomato cultivars and K^+ nutrition conclusively, and decrease the Ni^{2+} toxication in tomato cultivars, especially in *Cal-J N3* cultivar through reducing the detrimental effects of heavy metal via His and Ca^{2+} effects in the tomato plants. Our results also put forward for the first time that, plant growth promoting interaction effect between Ca^{2+} and His could alleviate the heavy metal, such as Ni stress induced in plants. Further investigations aimed at understanding the basic mechanism underlying Ca^{2+} (as a plant multifunctional nutrient) effects on plant growth and nutrition under heavy metal stress, and field trials are warranted at contaminated soils with Ni ions for study the growth changes and plant tolerance in these sites.

References

Alam S, Kamei S, Kawai S (2001) Metal micronutrients in xylem sap of iron-deficient barley as affected by plant-borne, microbial and synthetic metal chelators. Soil Sci Plant Nutr 47:149-156.

Arduini L, Godbold DL, Onnis A, Stefani A (1998) Heavy metals influence mineral nutrition of tree seedlings. Chemosphere 36(4-5):739-744.

Ashraf M, Akhtar N (2004) Influence of salt stress on growth, ion accumulation and seed oil content in sweet fennel. Biol Plant 48(3):461-464.

Bates LS, Waldren RP, Teare ID (1973) Rapid determination of free proline for water-stress studies. Plant Soil 39:205-207.

Bonnet M, Camares O, Veisseire P (2000) Effect of zinc and influence of *Acremonium lolli* on growth parameters, chlorophyll A fluorescence and antioxidant enzyme activity of ryegrass. Exp Bot 51:945-953.

Buchanan BB, Gruissem W, Jones R (2002) Biochemistry and molecular biology of plants. American Society of Plant Physiologists. Rockville, MD, p. 1367.

Cataldo DA, McFadden KM, Garland TR, Wildung RE (1988) Organic constituents and complexation of nickel(II), iron(III), cadmium(II), and plutonium(IV) in soybean xylem exudates. Plant Physiol 86(3):734-739.

Chandrasekhar KR, Sandhyarani S (1996) Salinity induced chemical changes in *Crotalaria striata* DC. Indian J Plant Physiol 1:44-48.

Charest C, Phan CT (1990) Cold acclimation of wheat (*Triticum aestivum*): properties of enzymes involved in proline metabolism. Physiol Plantarum 80:159-168.

Clemens S (2006) Toxic metal accumulation, responses to exposure and mechanisms of tolerance in plants. Biochimie 88(11):1707-1719.

Clemens S (2001) Molecular mechanisms of plant metal tolerance and homeostasis. Planta 212(4):475-486.

Curie C, Panaviene Z, Loulergue C, Dellaporta SL, Briat J-F, Walker EL (2001) Maize *yellow stripe1* encodes a membrane protein directly involved in Fe(III) uptake. Nature 409:346-349.

Deef HE-S (2007) Cupper treatments and their effects on growth, carbohydrates, minerals and essential oils contents of *Rosmarinus officinalis* L. World J Agriccult Sci 3(3):322-328.

Delhaize E, Ryan PR (1995) Aluminium toxicity and tolerance in plants. Plant Physiol 107:315-321.

Demarty M, Morvan C, Thellier M (1984) Calcium and the cell wall. Plant Cell Environ 7:441-448.

Dodd GL, Donavan LA (1999) Water potential and ionic effects on germination and seedling growth of two cold desert shrubs. Am J Bot 86:1146-1153.

Epron D, Toussaint M-L, Badot P-M (1999) Effects of sodium chloride salinity on root growth and respiration in oak seedlings. Ann For Sci 56:41-47.

Girija C, Smith BN, Swamy PM (2002) Interactive effects of sodium chloride and calcium chloride on the accumulation of proline and glycinebetaine in peanut (*Arachis hypogaea* L.). Environ Exp Bot 47:1-10.

Greenway H, Munns R (1980) Mechanisms of salt tolerance in Nonhalophytes. Annu Rev Plant Physiol 31:149-190.

Ha S-B, Smith AP, Howden R, Dietrich WM, Bugg S, O'Connell MJ, Goldsbrough PB, Cobbett CS (1999) Phytochelatin synthase genes from *Arabidopsis* and the yeast *Schizosaccharomyces pombe*. Plant Cell 11:1153-1163.

Hanson JB (1984) The functions of calcium in plant nutrition. In Tinker PB, Läuchli A, eds., Advances in plant nutrition. Praeger, New York, pp. 149-208.

Hepler PK, Wayne RO (1985) Calcium and plant development. Annu Rev Plant Physiol 36:397-439.

Hoagland DR, Arnon DI (1950) The water-culture method for growing plants without soil. Circular California Agricultural Experiment Sta-

tion 347(2):1-32.
Hopkins WG (1995) Plant and inorganic nutrients. Introduction to plant physiology. Second edition, John Wiley & Sons Inc, New York, part 2:51-76.
Hwang M-N, Ederer GM (1975) Rapid hippurate hydrolysis method for presumptive identification of Group B Streptococci. J Clin Microbiol 1:114-115.
Joho M, Ishikawa Y, Kunikane M, Inouhe M, Tohoyama H, Murayama T (1992) The subcellular distribution of nickel in Ni-sensitive and Ni-resistant strains of *Saccharomyces cerevisiae*. Microbios 71:149-159.
Kawasaki T, Moritsugu M (1987) Effect of calcium on the absorption and translocation of heavy metals in excised barley roots: Multi-compartment transport box experiment. Plant Soil 100:21-34.
Kinraide TB (1998) Three mechanisms for the calcium alleviation of mineral toxicities. Plant Physiol 118:513-520.
Kramer U, Cotter-Howells JD, Charnock JM, Baker AJM, Smith JAC (1996) Free histidine as a metal chelator in plants that accumulate nickel. Nature 379:635-638.
Kuriakose SV, Prasad MNV (2008) Cadmium stress affects seed germination and seedling growth in *Sorghum bicolor* (L.) Moench by changing the activities of hydrolyzing enzymes. Plant Growth Regul 54:143-156.
Küpper H, Lombi E, Zhao F-J, Wieshammer G, McGrath SP (2001) Cellular compartmentation of nickel in the hyperaccumulators *Alyssum lesbiacum, Alyssum bertolonii* and *Thlaspi goesingense*. J Exp Bot 52:2291-2300.
Lichtenthaler HK (1987) Chlorophylls and carotenoids - pigments of photosynthetic biomembranes. Methods Enzymol 148:350-382.
Lu L, Tian S, Zhang M, Zhang J, Yang X, Jiang H (2010) The role of Ca pathway in Cd uptake and translocation by the hyperaccumulator *Sedum alfredii*. J Hazard Mater 183:22-28.
Manohar M, Shigaki T, Hirschi KD (2011) Plant cation/H^+ exchangers (CAXs): biological functions and genetic manipulations. Plant Biol 13:561-569.
Marschner H (1995) Mineral nutrition of higher plants. Second edition, Academic Press, London.
McLaughlin SB, Wimmer R (1999) Tansley review no. 104 calcium physiology and terrestrial ecosystem processes. New Phytol 142:373-417.
Molas J (2002) Changes of chloroplast ultrastructure and total chlorophyll concentration in cabbage leaves caused by excess of organic Ni(II) complexes. Environ Exp Bot 47:115-126.
Nelson MT (1986) Interactions of divalent cations with single calcium channels from rat brain synaptosomes. J Gen Physiol 87:201-222.
Österas AH, Greger M (2006) Interactions between calcium and copper or cadmium in Norway spruce. Biol Plantarum 50:647-652.
Perez Alfocea F, Estan MT, Caro M, Bolarín MC (1993) Response of tomato cultivars to salinity. Plant Soil 150:203-211.
Pinto E, Sigaud-kutner TCS, Leitao MAS, Okamoto OK, Morse D, Colepicolo P (2003) Heavy metal-induced oxidative stress in algae. J Phycol 39:1008-1018.
Rivetta A, Negrini N, Cocucci M (1997) Involvement of Ca^{2+}-calmodulin in Cd^{2+} toxicity during the early phases of radish (*Raphanus sativus* L.) seed germination. Plant Cell Environ 20:600-608.
Sagner S, Kneer R, Wanner G, Cosson JP, Deus-Neumann B, Zenk MH (1998) Hyperaccumulation, complexation and distribution of nickel in *Sebertia acuminata*. Phytochemistry 47:339-347.
Sakamoto A, Murata A, Murata N (1998) Metabolic engineering of rice leading to biosynthesis of glycinebetaine and tolerance to salt and cold. Plant Mol Biol 38:1011-1019.
Saleh AAH, El-Meleigy SA, Ebad FA, Helmy MA, Jentschke G, Godbold DL (1999) Base cations ameliorate Zn toxicity but not Cu toxicity in sugar beet (*Beta vulgaris*). J Plant Nutr Soil Sc 162:275-279.
Sanita di Toppi L, Gabbrielli R (1999) Response to cadmium in higher plants. Environ Exp Bot 41:105-130.
Scheller HV, Huang B, Hatch E, Goldsbrough PB (1987) Phytochelatin synthesis and glutathione levels in response to heavy metals in tomato cells. Plant Physiol 85(4):1031-1035.
Schützendübel A, Polle A (2002) Plant responses to abiotic stresses: heavy metal-induced oxidative stress and protection by mycorrhization. J Exp Bot 53:1351-1365.
Seregin IV, Kozhevnikova AD (2006) Physiological role of nickel and its toxic effects on higher plants. Russ J Plant Physl+ 53(2):257-277.
Somogyi M (1952) Notes on sugar determination. J Biol Chem 195:19-23.
SPSS Inc. Released 2009. PASW Statistics for Windows, Version 18.0. Chicago: SPSS Inc.
Stearns JC, Shah S, Glick BR (2007) Increasing plant tolerance to metals in the environment. In Willey N, ed., Phytoremediation: Methods and Reviews, Humana Press, USA, pp. 15-26.
Sudhakar C, Reddy PS, Veeranjaneyulu K (1993) Effect of salt stress on the enzymes of proline synthesis and oxidation of greengram (*Phaseolus aureus* roxb.) seedlings. J Plant Physiol 141:621-623.
Volkmar KM, Hu Y, Steppuhn H (1998) Physiological responses of plants to salinity: A review. Can J Plant Sci 78:19-27.
Wagner GJ (1993) Accumulation of cadmium in crop plants and its consequences to human health. Adv Agron 51:173-212.
Wu CH, Wood TK, Mulchandani A, Chen W (2006) Engineering plant-microbe symbiosis for rhizoremediation of heavy metals. Appl Environ Microb 72:1129-1134.
Wu Y, Hendershot WH (2010) The effect of calcium and pH on nickel accumulation in and rhizotoxicity to pea (*Pisum sativum* L.) root-empirical relationships and modeling. Environ Pollut 158:1850-1856.
Wu Y, Hu Y, Xu G (2009) Interactive effects of potassium and sodium on root growth and expression of K/Na transporter genes in rice. Plant Growth Regul 57(3):271-280.
Yan F, Schubert S, Mengel K (1992) Effect of low root medium pH on net proton release, root respiration, and root growth of corn (*Zea mays* L.) and broad bean (*Vicia faba* L.). Plant Physiol 99:415-421.
Zafar MN, Nadeem R, Hanif MA (2007) Biosorption of nickel from protonated rice bran. J Hazard Mater 143:478-485.
Zorrig W, Rouached A, Shahzad Z, Abdelly C, Davidian JC, Berthomieu P (2010) Identification of three relationships linking cadmium accumulation to cadmium tolerance and zinc and citrate accumulation in lettuce. J Plant Physiol 167:1239-1247.
Turkan I, Bor M, Zdemir F, Koca H (2005) Differential responses of lipid peroxidation and antioxidants in the leaves of drought-tolerant *P. acutifolius* and drought-sensitive *P. vulgaris* subjected to polyethylene glycol mediated water stress. Plant Sci 168:223–231.

Volume 57(2):145-148, 2013
Acta Biologica Szegediensis
http://www.sci.u-szeged.hu/ABS

ARTICLE

Sensorial analysis of a functional beverage based on vegetables juice

Alina G. Profir*, Camelia Vizireanu

Food Science, Food Engineering and Applied Biotechnology Department, Faculty of Food Science and Engineering, "Dunărea de Jos" University of Galați, Galați, Romania

ABSTRACT Functional food products have become an important segment of food industry. They have been defined as products that provide physiological benefits or reduce the risk of chronic disease beyond primary nutritional functions. The continuous growth of functional food market is a consequence of the increasing interests for products that offering health benefits. The elaborations of new functional products lead to an increasing competition so that the consumer acceptance of the new products is important. The sensorial analysis can provide essential information to obtain a good understanding of consumer food choice. Due to the bioactive compounds contained, vegetables juice can be a convenient medium for the development of a functional beverage. The present study is focused on the consumer acceptance of a fermented juice made from beetroot, carrot and celery. This juice has been inoculated with three probiotic strains: *Lactobacillus acidophilus, Lactobacillus casei* and *Saccharomyces boulardii*. After lactic fermentation, the functional beverage has been evaluated by trained panelists. All the data has been analyzed using *Senpaq* statistical software. **Acta Biol Szeged 57(2):145-148 (2013)**

KEY WORDS

sensorial analysis
vegetables
fermentation

The notion of functional food occurred from identification and understanding of potential mechanisms of biologically active compounds in food, which can reduce the risk of disease (Binns and Lee 2010). The definition of functional food proposed by EC Concerted Action on Functional Food Science in Europe (FUFOSE) is: "a food that beneficially affects one or more target functions in the body beyond adequate nutritional effects in a way that is relevant to either an improved state of health and well-being and/or reduction of risk of disease".

Consumer interest for potential health benefits of a proper alimentation has led to a growing importance of the relationship between diet, specific food ingredients and health (Bornkessel et al. 2014). The alimentation has a major influence on the human well-being, but today's consumers may not have the time to consume their optimal diet. Functional foods can provide a high concentration of ingredients in a proper form.

The principal reason of consumers for purchasing functional foods is the growing desire to use foods in prevention of chronic illnesses. Consumers consider that base product is the most important attribute in selecting of a probiotic functional food and prevention claim is the most valuable (Annunziata and Vecchio 2013). The functional products represent a sustainable trend in food industry. Functional food market is growing worldwide and that increase the competition in this field (Bigliardi and Galati 2013). The success of functional foods is correlated with consumer acceptance of the products as part of the daily diet (Annunziata and Vecchio 2011).

Fermented dairy products are generally good food matrices for development of functional foods, but the consumption of these products is limited due to growing vegetarianism and the large number of individuals who are lactose intolerant or on cholesterol-restricted diets (Martins et al. 2013). A clear orientation toward innovation in adopting a new model followed by a complete strategy of following relevant knowledge and resources through more extensive structures may lead the course for innovative new functional food products in future (Khan et al. 2013). Developing new beverage based on vegetables, which can meets consumer demands and increase vegetable consumption are of major importance. New product development requires detailed knowledge of both the products and the customer choice (Prado et al. 2008). The responses of consumers to the sensory properties of beverage, like flavor, mouthfeel, aftertaste and odor, are determinant factor in determining the acceptance of innovative new products. Thus our study is focused to development of a new functional beverage using sensory analysis as a design tool.

Materials and Methods

Materials

Vegetables juice used for this study was obtained from beetroot, carrot and celery (in ratio 11:5:4). The vegetables were

Accepted April 4 2014
*Corresponding author. E-mail: alina.leescu@ugal.ro

Table 1. Experimental design.

Sample	Proportion yeast / bacteria	Amount of inoculum (Log CFU/mL)	Amount of *L. acidophilus* inoculum (Log CFU/mL)	Amount of *L. casei* inoculum (Log CFU/mL)	Amount of *S. boulardii* inoculum (Log CFU/mL)
1	0.6	7	0	4.38	2.62
2	0.6	7	4.38	0	2.62
3	0.2	5	2.08	2.08	0.84
4	0.343	7	2.61	2.61	1.78
5	0.6	4.1716	1.30	1.30	1.5716
6	0.2	7	2.92	2.92	1.16
7	0.0343	5	2.42	2.42	0.16
8	1.1657	4.1716	0.96	0.96	2.2516
9	0.6	4.1716	2.61	0	1.5616
10	0.6	4.1716	0	2.61	1.5616

Table 2. Results of experimental design for all samples after fermentation.

Sample	Proportion yeast /bacteria	Amount of bacteria inoculum (Log CFU/mL)	Amount of yeast inoculum (Log CFU/mL)
1	0.94	9.48	8.95
2	0.85	9.30	7.90
3	0.99	8.30	8.23
4	0.89	8.95	7.98
5	1.09	7.70	8.38
6	0.96	8.90	8.54
7	0.86	8.40	7.20
8	1.01	7.57	7.64
9	1.14	7.00	8.00
10	1.03	8.48	8.77

purchased from a local market. After the preliminary operations like washing, peeling and slicing, the vegetables were juiced with a centrifugal juicer provided by Philips.

Freeze dried *Lactobacillus acidophilus* LA-5 and *Lactobacillus casei* 431 were obtained from CHR Hansen SRL (Brașov, Romania) and directly used as starter culture. *Saccharomyces boulardii* was obtained from Biocodex Laboratories (Montrouge, France). Samples were inoculated by adding bacteria and yeast in different proportion and incubated at 37°C. The fermentations were carried until the pH value of 4.6 was reached (after ca. 6-8 h) and stopped by quick cooling. All samples were stored under refrigerated conditions for 7 days.

Sensorial analysis

Sensory profiles of 10 samples were evaluated in laboratory, by the trained panel of five assessors using the preferential method that is an affective method (Lea et al. 1998). Fermented juice was served in 100 mL portions in white polystyrene cups, labeled randomly with selected codes. These portions were served at room temperature (ca. 20°C) to better differentiate odors and flavors and facilitate the characterization and comparison of each sample. The samples were evaluated on the perceived intensity of 7 attributes (odor, acidity, flavor, mouthfeel, aftertaste, color, general aspect). Subjects evaluated samples on 0-5 line scales anchored at 0 'not at all' at the left end and 5 'very' at the right end.

Statistical analysis

The Unscrambler X software v. 10.1 (CAMO Software, Norway) was used for the experimental design (Table 1). Intensity ratings were collected and Principal Component Analysis was performed using SENPAQ 4.7 (QiStatistics, UK, 2008). PCA is a multivariate statistical method applicable, where there are common descriptors, and enables the visualization of the data in a two- or three-dimensional space, enabling the identification of which samples were the most different and which sensory descriptors were predominantly responsible for those product differences (Mavrommatis et al. 2011).

Results and Discussion

After fermentation of vegetables juice the total CFU for bacteria and yeast was counted (Table 2). A good viability of samples inoculated with *L. casei* was found compared with that inoculated with *L. acidophilus*. All the samples were accepted by the panelists. An important factor that influences negatively the attributes of samples was the acidity caused

Table 3. Average intensity scores of all attributes generated by the sensory panel of all samples. Averages in the same row followed by the same letter are not significantly different at a level of 5% significance.

	Sample 1	Sample 2	Sample 3	Sample 4	Sample 5	Sample 6	Sample 7	Sample 8	Sample 9	Sample 10
General aspect	3.4^{a}	3.8^{a}	3.6^{a}	4.0^{a}	4.2^{a}	4.0^{a}	3.4^{a}	3.8^{a}	3.2^{a}	3.4^{a}
Color	4.0^{a}	4.2^{a}	4.2^{a}	3.6^{a}	4.6^{a}	4.4^{a}	4.0^{a}	3.8^{a}	3.6^{a}	3.4^{a}
Odor	2.4^{b}	3.0^{ab}	2.4^{b}	3.4^{ab}	4.0^{a}	3.8^{a}	4.2^{a}	3.4^{ab}	3.8^{a}	3.6^{ab}
Acidity	2.4^{ab}	1.8^{b}	2.6^{ab}	3.2^{ab}	3.4^{a}	3.0^{ab}	2.8^{ab}	3.2^{ab}	2.2^{ab}	3.6^{a}
Flavor	2.2^{c}	3.0^{abc}	2.4^{bc}	3.4^{abc}	3.4^{abc}	3.6^{abc}	4.0^{a}	3.6^{abc}	2.6^{abc}	3.8^{ab}
Mouthfeel	2.8^{a}	2.6^{a}	2.4^{a}	3.8^{a}	3.4^{a}	3.0^{a}	2.8^{a}	3.2^{a}	2.6^{a}	3.8^{a}
Aftertaste	2.4^{b}	3.0^{ab}	2.6^{ab}	4.2^{a}	3.6^{ab}	3.2^{ab}	2.8^{ab}	3.8^{ab}	2.8^{ab}	3.2^{ab}

by lactic fermentation of vegetables juice. These results are similar with observation of Öztürk et al. (2013).

All the samples were evaluated by trained panelists and average ratings for all samples and attributes are represented in Table 3. The samples inoculated with *L. acidophilus* obtained a better score at attributes odor and color compared with samples inoculated with *L. casei.* Samples with *L. casei* were perceived more acid and the mouthfeel was better that the samples inoculated with *L. acidophilus.* The color scores were highest as compared to mouthfeel, odor, acidity, aftertaste and general aspect of the samples. These observations are similar to that of Daneshi et al. (2013).

As we can see in Figure 1, a good correlation between mouthfeel and acidity of samples was observed. The correspondence found between attributes mouthfeel and aftertaste was equal with that between flavor and odor (0.77). A negative correspondence between color and all other attributes excepting general aspect of samples was observed.

The best average score was obtained by samples inoculated with 1.3 log CFU/mL *L. acidophilus*, 1.3 log CFU/mL *L. casei* and 1.5716 log CFU/mL *S. boulardii* (Sample 5). Samples inoculated with *L. acidophilus* and *L. casei* had obtained a better average intensity scores towards samples inoculated with one of the strains. The best scores for attributes general aspect and color were obtained by sample 5 (Fig. 2). The best mouthfeel and aftertaste were given by sample 4. Sample 10 had the best score for attribute aroma. Reddy et al. (2013) were obtained in beetroot fermented juice higher scores for attributes flavor and color than the scores obtained in our study. The color of the samples achieved a lower score (3.4-4.6) compared to the scores of fermented multi-vegetables juice (4.5-4.83) obtained by Radyko et al. (2006) after 7 days of storage.

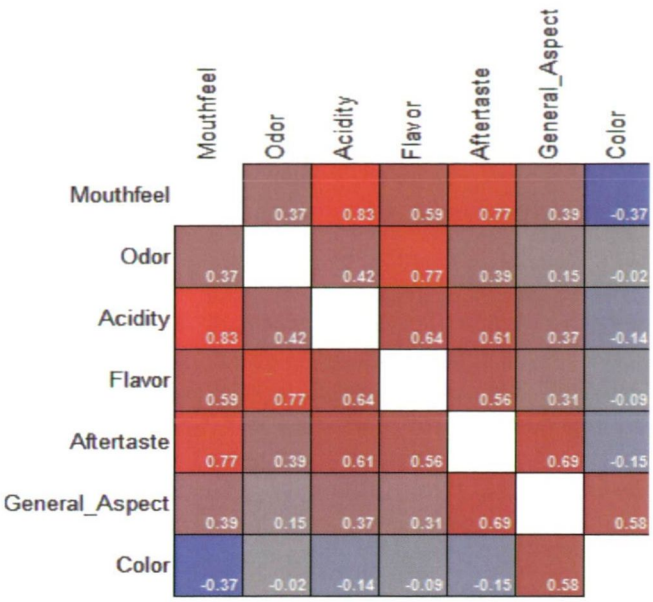

Figure 1. Correspondence between all attributes of samples.

These data were then subjected to principal component analysis (PCA) and the first two principal components explained 75.4% of the variance as shown in Figure 3. These results show that the use of variables is adequate for sensorial evaluation of fermented juices. Principal component PC1 had high loadings on all attributes scores, except color. PC2 had positive loading for color attribute. The bi-plot scores for all samples on the two components were also projected. The samples in the right quadrants were the most liked and were rated as being acceptable for consumers. The positive part of

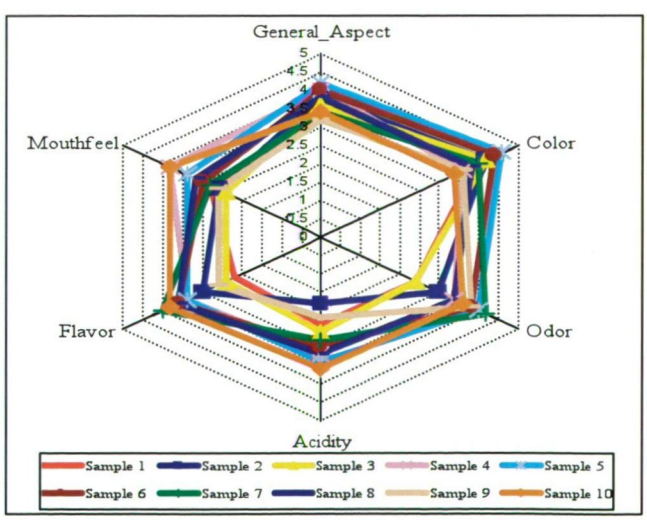

Figure 2. Star diagram for all attributes and samples.

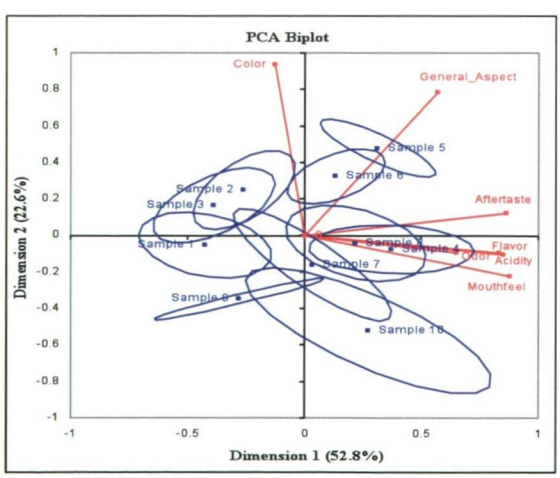

Figure 3. PCA-Bi-plot showing sample mean scores in relation to the attribute loadings on the first two principal components. Ellipses indicate sample confidence intervals.

PC1 and the negative part of PC2 reflected the acid variable. This observation is correlated with the results obtained by Karovičová and Kohajdová (2002).

Conclusions

Sensory analysis is an important instrument for development of new functional products. It can provide a clear understanding of product characteristics, increases researcher confidence in product quality and it identifies the sensory attributes according to consumer preference. Our study demonstrates that affective (subjective) test can give significant information for development of new products. Application of principal component analysis can selected the most important variables an increase the accuracy of sensorial evaluation. Acceptability of products had a major relevance on the functional products market, where the competition is in a continuous growing.

Acknowledgment

We gratefully acknowledge the help of Prof. Gabriela Iordăchescu and her team of panelists from Sensory Analysis Laboratory, Faculty of Food Science and Engineering.

References

Annunziata A, Vecchio R (2013) Consumer perception of functional foods: A conjoint analysis with probiotics. Food Qual Prefer 28:348-355.

Annunziata A, Vecchio R (2011) Functional foods development in the European market: A consumer perspective. J Funct Foods 3:223-228.

Bigliardi B, Galati F (2013) Innovation trends in the food industry: The case of functional foods. Trends Food Sci Tech 31:118-129.

Binns C, Lee MK (2010) The use of probiotics to prevent diarrhea in young children attending child care centers: a review. J Exp Clin Med 2(6):269-273.

Bornkessel S, Bröring S, Omta (Onno) SWF, van Trijp H (2014) What determines ingredient awareness of consumers? A study on ten functional food ingredients. Food Qual Pref 32:330-339.

Daneshi M, Ehsani MR, Razavi SH, Labbafi M (2013) Effect of refrigerated storage on the probiotic survival and sensory properties of milk/carrot juice mix drink. Elect J Biotech 16:5.

Karovičová J, Kohajdová Z (2002) The use of PCA, FA, CA for the evaluation of vegetable juices processed by lactic acid fermentation. Czech J Food Sci 20:135-143.

Khan RS, Grigor J, Winger R, Win A (2013) Functional food product development - Opportunities and challenges for food manufacturers. Trends Food Sci Tech 30:27-37.

Lea P, Næs T, Rødbotten M (1998) Analysis of Variance for Sensory Data. John Wiley & Sons, West Sussex, England.

Martins EMF, Ramos AM, Vanzela ESL, Stringheta PC, Pinto CLO, Martins JM (2013) Products of vegetable origin: A new alternative for the consumption of probiotic bacteria. Food Res Int 51:764-770.

Mavrommatis Y, Moynihan PJ, Gosney MA, Methven L (2011) Hospital catering systems and their impact on the sensorial profile of foods provided to older patients in the UK. Appetite 57:14-20.

Öztürk Í, Karaman S, Törnük F, Sağdiç O (2013) Physicochemical and rheological characteristics of alcohol-free probiotic boza produced using *Lactobacillus casei* Shirota: estimation of the apparent viscosity of boza using nonlinear modeling techniques. Turk J Agric For 37:475-487.

Prado FC, Parada JL, Pandey A, Soccol CR (2008) Trends in non-dairy probiotic beverages. Food Res Int 41:111-123.

Reddy M, Beatrice DA, Bhavani V (2013) Sensory and microbial quality of newly developed fermented beetroot beverage. World J Pharm Pharmaceut Sci 3(1):361-367.

Warmińska-Radyko I, Łaniewska-Trokenheim Ł, Gerlich J (2006) Fermented multi-vegetable juices supplemented with propionibacterium cell biomass. Polish J Food Nutr Sci 15(4):433-436.

Volume 57(2):149-151, 2013
Acta Biologica Szegediensis
http://www.sci.u-szeged.hu/ABS

ARTICLE

Antibacterial action of copper ions on food-contaminating bacteria

Ulrike Zanzen[1,2]*, Gudrun Lisa Bovenkamp[3], Katla Sai Krishna[3], Josef Hormes[3,4], Alexander Prange[1,2,3]

[1]Microbiology and Food Hygiene, Niederrhein University of Applied Sciences, Mönchengladbach, Germany, [2]Institute of Microbiology and Virology, University of Witten/Herdecke, Witten, Germany, [3]Center for Advanced Microstructures and Devices, LSU, Baton Rouge, LA, USA, [4]Canadian Light Source, University of Sasketchewan, Saskatoon, SK, Canada

ABSTRACT Silver and copper ions are widely used as antibacterial agents but the basic molecular mechanism of this effect is still poorly understood. The analysis of our investigation gives clear indications that Ag^+ do react with the bacterial cells and do not stay as silver in the system. Significant lower silver cysteine content coupled with higher silver histidine content in Gram-positive cells indicate that the peptidoglycan multi-layer could be buffering the biocidal effect of silver for the Gram-positives at least in part. Interaction with DNA or proteins can occur through Ag-N bonding. The formation of silver cysteine can be confirmed for both bacterial cell types which thus supports the hypothesis that enzyme catalyzed reactions and the electron transport chain within the cell is disrupted. The antibacterial property of copper is attributed mainly to adhesion with bacteria because of their opposite electrical charges, resulting in a reduction reaction at the bacterial cell wall. Nanoparticles with a larger surface-to-volume ratio might provide more efficient means for antibacterial activity. First results suggest that copper ions do not react compared to silver ions.
Acta Biol Szeged 57(2):149-151 (2013)

KEY WORDS

silver ions
copper ions
XANES
antibacterial effects
amino acids

The antimicrobial properties of silver and copper ions were known since ancient times, but although silver ions (e.g. silver nitrate) and silver nanoparticles are already widely used for various antibacterial purposes, the exact antibacterial mechanism has not yet been elucidated. An *in situ* tool for speciation analysis on an atomic/ molecular level such as X-ray absorption near edge structure (XANES) spectroscopy is the method of choice. XANES allows not only the determination of the valence of an excited atom but also gives information about type of neighboring atoms. In a previous study (Bovenkamp et al. 2013) the antibacterial effect of silver on three types of bacteria, *Staphylococcus aureus*, *Escherichia coli*, and *Listeria monocytogenes* was investigated. Ag L_{III}-edge XANES spectra of the different bacteria confirm that a reaction occurs after the application of silver ions in solution (e.g. from silver nitrate). Silver bonding to Ag-S in cysteine and Ag-N or Ag-O bonding in histidine, alanine, and DL-aspartic acids was detected using synthesized silver-amino acids as reference compounds for linear combination fitting (LCF) analysis. The aim of the present study is to analyze the molecular reactions of selected food-relevant bacteria on copper ions. The antibacterial properties of copper are attributed mainly to adhesion on bacteria because of their opposite electrical charges, resulting in a reduction reaction at the bacterial cell wall.

Accepted April 5, 2014
*Corresponding author. E-mail: Ulrike.Zanzen@hs-niederrhein.de

Materials and Methods

Materials

Bacterial strains: *Staphylococcus aureus* DSMZ 2569, *Escherichia coli* DSMZ 1103, and *Listeria monocytogenes* DSMZ 20600.

Medium: Yeast-Peptone-Dextrose broth (Difco Becton Dickinson, Franklin Lakes, NJ, USA).

Reference compounds/ chemicals: copper-I-acetate, copper-II-acetate, and copper nitrate were purchased from Sigma-Aldrich (St. Louis, MO, USA).

Cultivation of the bacteria and sample preparation

S. aureus DSMZ 2569, *E. coli* DSMZ 1103, and *L. monocytogenes* DSMZ 20600 were grown in a shaker (100 rpm) for 24 to 48 h at 30°C in YPD. Bacteria were washed with sterile deionized water and centrifuged twice. The bacteria were diluted to 10^6 CFU/mL with sterile deionized water (to avoid chemical reactions of silver or copper ions with medium contents). Then 50 µL of a 0.1 M stock solution (e.g. copper acetate) was added to 1 mL cell culture (about to 10^6 CFU/mL). The samples were incubated at 20°C for 10 min

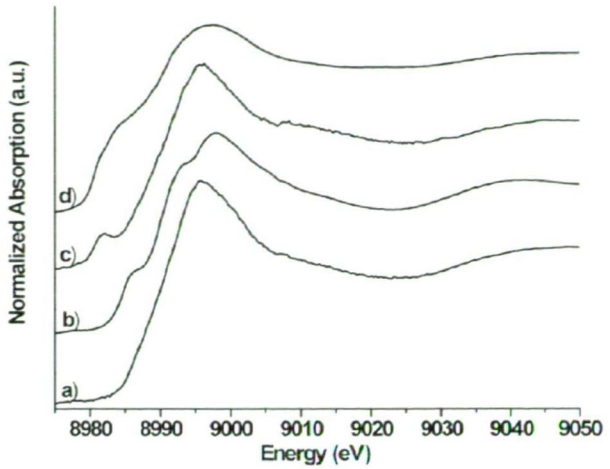

Figure 1. Copper *K*-edge XANES spectra of copper reference compounds a) copper-II-acetate solution, b) copper-II-acetate, c) copper-I-acetate solution, d) copper-I-acetate.

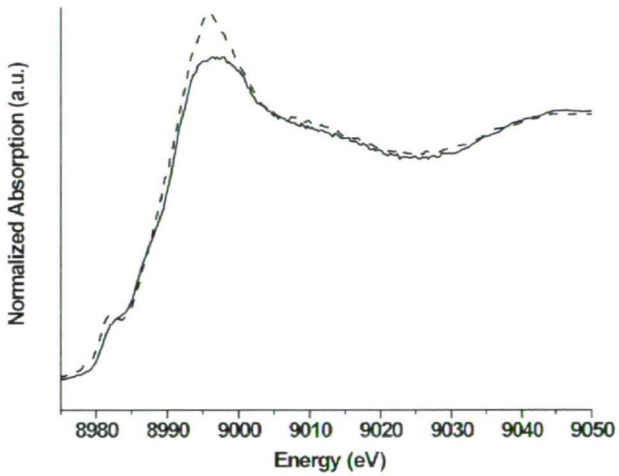

Figure 2. Copper *K*-edge XANES spectra of Cu^{+}-acetate solution (•••) and *L. monocytogenes* cells treated with Cu^{+}-acetate (—).

in darkness and then washed again with 0.5 mL deionized water to remove unreacted silver or copper compounds. About 20 µL cell material was put on filter paper and attached to Kapton tape. These samples were dried in darkness for 1 to 2 h. A control set was prepared as described above without adding copper-containing solutions. Samples for XANES analysis were prepared and handled according to Prange et al. (2002).

Experimental XANES spectroscopy

Cu *K*-edge XANES spectra were recorded at the Double Crystal Monochromator (DCM) beamline of the Center for Advanced Microstructures and Devices (CAMD), Louisiana State University, Baton Rouge, LA, USA (Hormes et al. 2006) and at the beamline of the Angströmquelle Karlsruhe (ANKA). The monochromators were equipped with Ge(220) and Ge(422) crystals, respectively. Measurements of the bacterial samples were performed in fluorescence mode to record the fluorescence photons and an ionization chamber for the incident photons with ambient pressure at the Cu *K*-edge inside the ionization chambers and sample chambers. Measurements of reference compounds were performed in transmission mode. For energy calibration of the copper spectra, the spectrum of elemental copper was used as a standard. Data were normalized and analyzed with the ATHENA program of the IFFEFIT package (Ravel and Newville 2006). The error of the percentage contributions for the compounds in the linear combination fitting (LCF) results can be estimated to ± 10%.

Results and Discussion

Cu *K*-edge XANES spectra of bacteria without the application of copper ions reveal that there is a small amount of copper (10-100 ppm) present in all bacteria samples (data not shown). This is not suprising since copper is an essential nutrient for all life. After the application of Cu-I-acetate solution or Cu-II-acetate solution (reference spectra see Figure 1) the Cu *K*-XANES spectra of the bacterial samples (data not shown) do not always show clear differences to the initial solution which was the case after the application of silver ions (Bovenkamp et al. 2013). For example the Cu *K*-XANES spectra of *L. monocytogenes* treated with Cu-I-acetate in comparison with the spectra of pure Cu^{+}-acetate solution show some differences (Pre-edge and White Line) which confirm that a reaction occurs (Fig. 2). However, the spectra are quite similar in the energy positions of peaks and shape resonances. The reason for the high similarity of the most spectra of bacteria to the solutions can be a reaction of copper with water molecules (complex formation).The $Cu_c(OH)_y$ complex might passivate the reactivity of copper. The high reactivity of Cu with water (also depending on the pH) is well known (Kruck and Sarkar 1973) and studied with XANES (Mesu et al. 2006). This also complicates the synthesis of copper amino acids as reference compounds. The application of copper ions using copper nitrate solution on the other hand resulted in much more pronounced differences of bacterial cell spectra and spectra of initial solution (will be published later). The mechanism of action of the copper ions is not yet fully understood. Detailed research and comparative study of strain-specific variability is required to determine the bactericidial efficiency.

Acknowledgements

The authors would like to thank CAMDs staff (Baton Rouge) and ANKAs staff (Karlsruhe) for their support during measurements at the beamlines.

References

Bovenkamp GL, Zanzen U, Katla SK, Hormes J, Prange A (2013) The interaction of silver ions with *Staphylococcus aureus*, *Listeria monocytogenes*, and *Escherichia coli* – an X-ray absorption near-edge structure (XANES) spectroscopy study. Appl Environ Microbiol 79(20):6385-90.

Hormes J, Scott JD, Suller VP (2006) Facility update: The Center for Advanced Microstructures and Devices: A Status Report. Synchr Rad News 19:27-30.

Kruck TPA, Sarkar B (1973) Structure of the Species in the Copper (II)–L-Histidine System. Can J Chem 51(21):3563-3571.

Mesu JG, Visser T, Soulimani F, van Faassen EE, de Peinder P, Beale AM, and Weckhuysen BM (2006) New insights into the coordination chemistry and molecular structure of copper(II) histidine complexes in aqueous solutions. Inorg Chem 45(5):1960-1971.

Prange A, Chauvistré R, Modrow H, Hormes J, Trüper HG, Dahl C (2002) Quantitative speciation of sulfur in bacterial sulfur globules: X-ray absorption spectroscopy reveals at least three different species of sulfur. Microbiol 148:267–276.

Ravel B, Newville M (2005) *ATHENA, ARTEMIS, HEPHAESTUS*: data analysis for X-ray absorption spectroscopy using IFEFFIT. J Synch Rad 12:537–541.

Volume 57(2):153-160, 2013
Acta Biologica Szegediensis
http://www.sci.u-szeged.hu/ABS

ARTICLE

Changes and relationship of somatosensory cortical electrical activity and hind paw defensive reflex in rats under various anesthetics

Katalin Mikite, Nóra Merész, András Papp*

Faculty of Medicine, Department of Public Health, University of Szeged Szeged, Hungary

ABSTRACT The effect of four common anesthetics on the spontaneous and evoked activity of the somatosensory cortex and on hind paw withdrawal reflex was studied in rats in acute preparation. The aim was to determine to what extent the choice of anesthetic and the depth of anesthesia may interfere with the effects of agents tested in such a system. Electrical activity was recorded on the dura surface after opening the skull, from the primary projection area of the whiskers which were stimulated electrically. Defensive reflex was elicited by manually pinching the toes of the left hind paw. Anesthesia was initiated with chloral hydrate or ketamine-xylazine, and continued with urethane or thiopental and then urethane. In the spontaneous cortical activity, delta band power was in strong correlation with the depth of anesthesia. Anesthesia also had a clear effect on the amplitude, but not on the latency, of the somatosensory evoked potential. Under effect of chloral hydrate the shape of the evoked potential was different from that seen under ketamine-xylazine or urethane. The results showed that properly chosen electrophysiological parameters can reliably indicate the depth of anesthesia, and that choice of anesthetic and level of anesthesia may effectively interfere with the effects of tested substances

Acta Biol Szeged 57(2):153-160 (2013)

KEY WORDS

evoked potential
electrocorticogram
defensive reflex
correlation
anesthesia
rat

In spite of all development of *in vitro* and *in silico* methods in the last decades, *in vivo* animal experimentation remains a fundamental tool of pure and applied biomedical research. In performing animal experiments with invasive measures, however, appropriate anesthesia is necessary for both ethical and practical reasons. Anesthesia in animal experiments is regulated at national and international level, e.g. in Article 14 of Directive 2010/63/EU (European Union 2010).

The way of action of all anesthetics includes interference with the functioning of the central nervous system – but that means that the „control" state of the animals in a particular experiment, before giving any test substance, is to some extent non-natural. This is inevitable and has to be taken in consideration when evaluating and interpreting the results, but in order to be able to do that, the own effects of the anesthetics need to be described. In this work, four parenteral anesthetics, used commonly in work with animals – urethane, chloral hydrate, ketamine-xylazine mixture and thiopental – were investigated.

Urethane is (or, mainly, used to be) a preferred anesthetic in animal experimentation because of its long-lasting effect without major depression of vital functions (Maggi and Meli 1986). Some reports identified the increase of inhibition via $GABA_A$ and glycine receptors, and decrease of glutamatergic excitation, as its chief mechanism of action (Hara and Harris 2002) while Maggi and Meli (1986) and Sceniak and macIver (2005) found only minor effect on GABAergic inhibition. Its effect is long-lasting (24 hours or longer) making it suitable primarily for terminal anesthesia. Urethane is being phased out from laboratory use mainly because of its human toxicity (IARC 1974; Koblin 2002).

Chloral hydrate, also known as trichloro acetaldehyde, was used also as a human anesthetic but is regarded today as obsolete because of its toxicity and its narrow therapeutic range (Pershad et al. 1999); the narrow range is a problem also in animals (Murray et al. 2000). It is, in fact, a prodrug, metabolized to trichloro ethanol which acts as a $GABA_A$ agonist (Lu and Greco 2006). Narcosis induced by chloral hydrate lasts up to 2 hours, an advantageous length, but the substance causes atonic ileus if injected intraperitoneally in concentration over 5% (Davis et al. 1985).

Ketamine is frequently used in human medicine (in contrast to the above two agents) first of all in children and in deteriorated patients. It is also common in veterinary practice and in animal experimentation. Ketamine is primarily a non-competitive antagonist of NMDA receptors, acting on a binding site within the open pore of the receptor-channel complex (Bergman 1999). At the dose causing complete anesthesia, it also acts as central muscarinergic as well as alpha- and beta-adrenergic agonist. An alternative hypothesis says that ket-

Accepted Febr 26, 2014
*Corresponding author. E-mail: papp.andras@med.u-szeged.hu

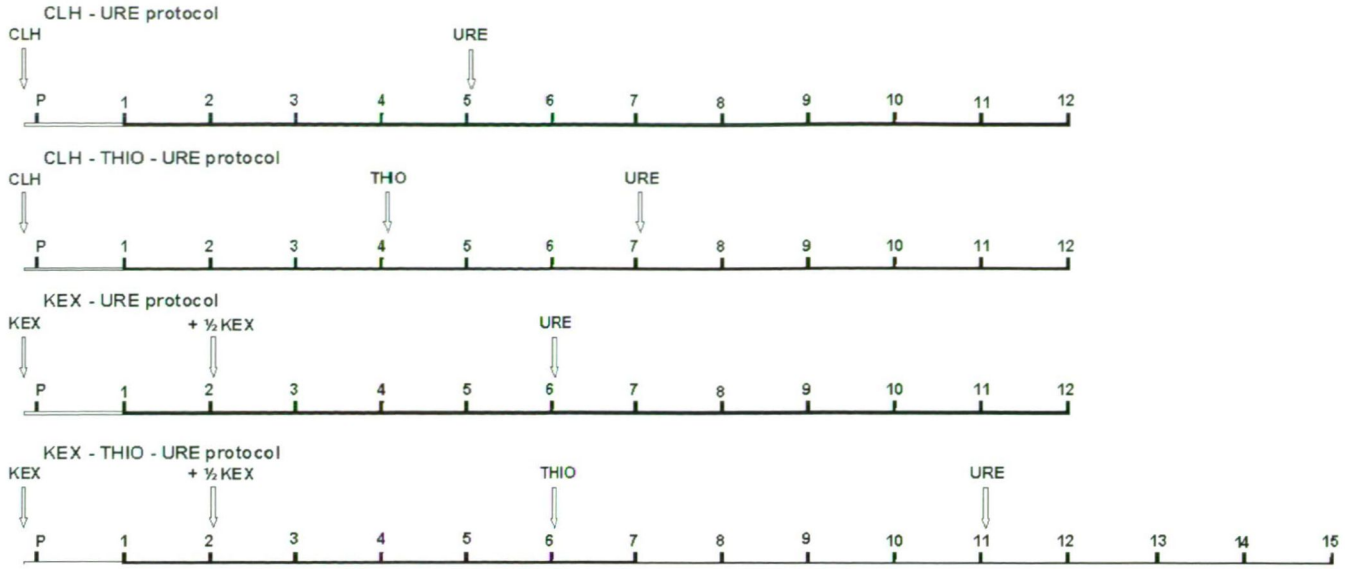

Figure 1. Timelines of the four protocols (*CLH – URE, CLH – THIO – URE, KEX – URE, KEX – THIO – URE)* used in the experiments. The time passed between injecting the first anesthetic (*CLH* or *KEX*) and preparing the scull for recording (P) was ca. 10 min; between P and the first recording session (1), 30 min were left; and between two subsequent recordings, 20 min.

amine blocks the hyperpolarization-activated neuronal cation channels, making cortical neurons tend to sleep-like rhythmic activity (Carr et al. 2007). For use in lab animals, ketamine is often combined with xylazine, an adrenergic agonist.

Pentobarbital was once a frequently used short-acting barbiturate for lab animals. Now, however, it is a restricted drug according to Schedule III of the UN Convention of Psychotropic Substances (United Nations 1971). Thiopental is a viable alternative with similar pharmacological properties (and its main metabolite is pentobarbital itself: Raj et al. 2011). Being a barbiturate, it acts on a distinct site of the $GABA_A$ receptor complex to enhance the efficacy of GABAergic inhibition (Twyman et al. 1989). Beyond short action, it is also important to remember that lower doses of thiopental induce narcosis without analgesia.

In the experiments presented here, two or three of the above mentioned anesthetics were given to rats one after another (see Fig. 1), and the changes in spontaneous and stimulus-evoked cortical electrical activity, and in peripheral defensive reflex (hind paw withdrawal on toe pinching, as a measure of the anesthetic action) were investigated in parallel.

Materials and Methods

Adult male Wistar rats (280-350 g body weight) were used, obtained from the breeding centre of the university. The animals were housed in an air conditioned animal room, maintained at 22°C, with 12-hour light/dark cycle (light on at 06:00) and free access to tap water and standard rodent chow.

The effect of the anesthetics was tested using the doses given in Table 1; the corresponding protocols are presented in Figure 1. The doses were based on the literature sources given in Table 1 and on previous own experience; and the time span of observing the effect of one anesthetic (*i.e.* number of recording sessions, see below) on the typical length of action of each drug seen previously in comparable experiments. The maximal length of one experiment (15 x 20 min, that is, 5 hours) was in line with the experience (Pecze et al. 2005) that after anesthesia of such length the rats' general state starts to deteriorate. In each protocol, 8 rats were finally evaluated.

The rats were prepared for electrophysiological recording under anesthesia by the first agent (*CLH* or *KEX*). The animal's head was fixed in a holding frame, and the left hemisphere was exposed by opening the bony skull. Lidocaine (10% spray; EGIS, Hungary) was applied on the wounds, and the exposed dura was protected by a thin layer of petroleum jelly. The rat was put aside for a 30 minutes recovery, covered in a warm cloth, and was then transferred to the recording setup. Normal body temperature was maintained here by

Table 1. Doses of the anesthetics applied.

Anesthetic	Dose applied in this work (mg/kg b.w., ip.)	Reference for dose
Urethane (*URE*)	1000	Mook (2006)
Chloral hydrate (*CLH*)	400	Field et al. (1993)
Ketamine+xylazine (*KEX*)	100+8	Farkas et al (1999)
Thiopental (*THIO*)	30	Wixson (1994)

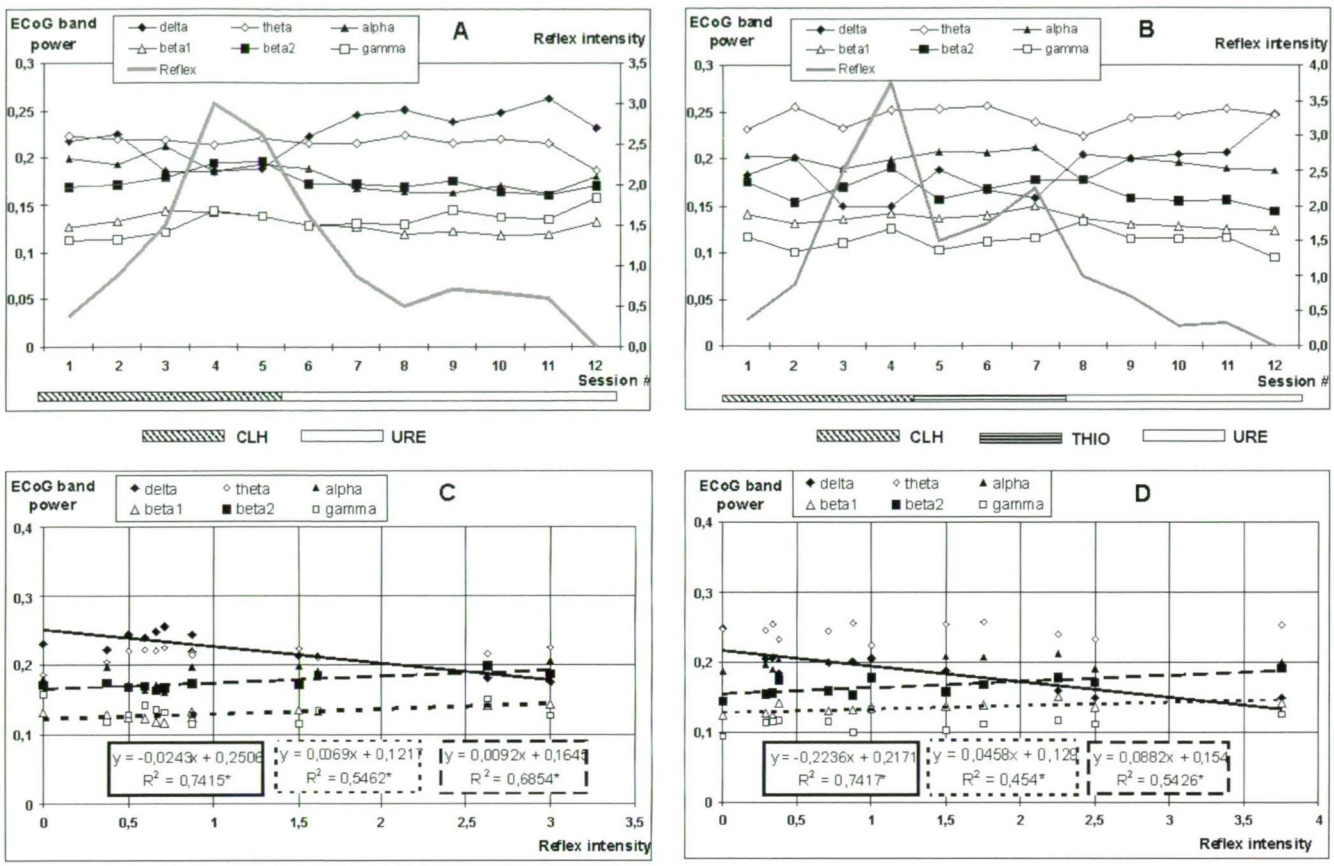

Figure 2. Top: time course of ECoG band power (left ordinate) and hind foot withdrawal reflex intensity (right ordinate) in rats treated using the *CLH – URE* (A) and *CLH – THIO – URE* (B) protocols (for the protocols, see Fig. 1). Recording sessions followed in 20 min intervals. The presented values are means, error ranges are omitted for clarity. Bottom: the corresponding correlation diagrams of reflex intensity and ECoG band powers (*CLH – URE* protocol, C; *CLH – THIO – URE* protocol, D). For substantial correlations, the trend line and its equation is given. Corresponding trend lines and equation boxes have the same line style (delta, solid; beta1, dotted; beta2, dashed), significant correlation (F>0.05 from Fisher's test included in "linear fit") is marked with * in the equation box and the data point symbols are enlarged.

the support plate thermostated to 36.5°C. A ball-tipped (tip diameter ca. 0.6 mm) silver wire electrode was placed on the primary somatosensory (SS) projection area of the whiskers ("barrel field": Waite 2004); there, punctum maximum of the evoked potentials (EPs) was found by moving the electrode as necessary. The indifferent electrode was a stainless steel clip placed on the cut skin surface. In a recording session, first the spontaneous activity (electrocorticogram, ECoG) was taken for 6 minutes. Then, sensory cortical EPs were recorded by stimulating the contralateral whisker pad with square electric pulses (3-4 V; 0.05 ms; 1 Hz), given in one train of 50 stimuli through a pair of hook-shaped steel electrodes inserted ca. in the middle of the uppermost row of whiskers. This recording session was repeated every 20 minutes. All cortical activity was amplified (10^4 x, low- and high-pass filters set to 1.6 and 1000 Hz), digitized (at 4096 Hz) and stored on PC.

From the ECoG records, the relative spectral power of the frequency bands (delta, 0.5-4 Hz; theta, 4-7 Hz; alpha, 8-13 Hz; beta1, 13-20 Hz; beta2, 20-30 Hz; gamma, 30-50 Hz: Kandel and Schwartz 1985) was determined automatically by the software used by means of FFT analysis. The recorded EPs were averaged. On the averaged curve, the latency and amplitude data of specific points were measured manually. Latency was measured between stimulus artifact (point"0") and the points numbered 1 to 6, and amplitude between opposed peaks of the main waves (see Fig. 4). The complete electrophysiological recording and analysis was done by means of the Neurosys 1.11 software (Experimetria, Budapest, Hungary).

The depth of anesthesia was determined on a semiquantitative scale based on the defensive reflex response elicited by a strong pinch to the toes of the hind paw (as described in Zandieh et al. 2003). The pinch was applied once before and after each recording session (this was infrequent enough to avoid habituation) and the grade observed, or the mean of the two grades if it was different before and after, was assigned to the session in question. No or minimal response was grade 0; weak response (one faint movement), grade 1; moderate re-

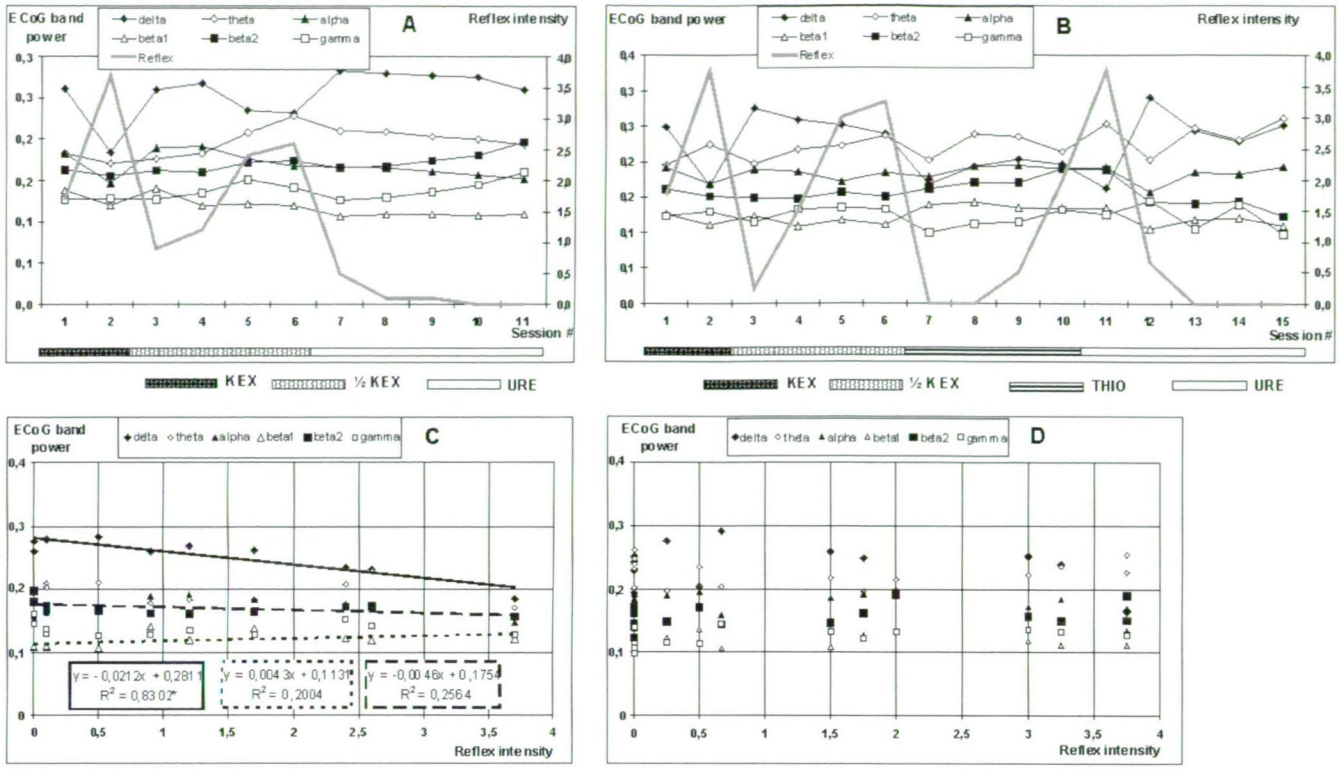

Figure 3. Top: time course of ECoG band power and hind paw withdrawal reflex intensity in rats treated using the *KEX – URE* (A) and *KEX – THIO – URE* (B) protocols. Bottom: the corresponding correlation diagrams of reflex intensity and ECoG band powers (*KEX – URE* protocol, *C; KEX – THIO – URE* protocol, D). The same display as in Figure 2.

sponse (one explicit movement), 2; vivid response (one strong movement or repeated weaker ones), 3; and strong response (repeated powerful movements), 4. On reaching grade 4, the next anesthetic in the protocol was administered forthwith.

For evaluation, all data – response grade (reflex intensity), ECoG band powers, EP latency and amplitude values – were averaged for whole groups (n=8) session by session; and were plotted against recording session number (*i.e.*, against time, see Fig. 1). Amplitude, and to a lesser extent, latency, of the EP was variable among the rats within a group, so that these values were first normalized to the mean of the values measured during the effect of the first anesthetic (that is, for the mean of sessions 1 to 5 in the *CLH – URE* protocol, of sessions 1 to 4 in the *CLH – THIO – URE* protocol, and of sessions 1 and 2 in both protocols starting with *KEX*). These plots then showed the time course of depth of anesthesia (response intensity) and the above mentioned electrophysiological parameters while the effect of the anesthetics was developing and fading out. Relationships suggested by the time courses were tested by means of correlation plots and R^2 values, calculated with the "linear fit" function of MS Excel. This function uses the least squares method to fit a straight line to the measurement data, and examines the strength of relationship with Fisher's F test. The value of R^2 (determina-

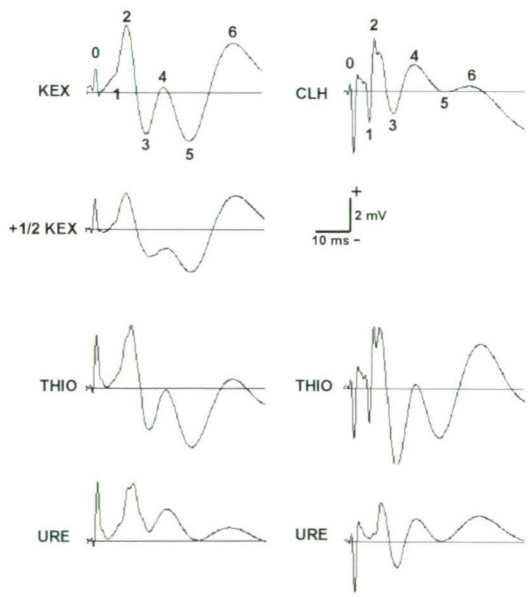

Figure 4. Typical examples of the somatosensory cortical evoked potential recorded according to the *KEX – THIO – URE* (left) and *CLH – THIO – URE* (right) protocols. Latency of the specific points (marked with numbering) was measured from the stimulus artifact (point 0); main wave peak-to-peak amplitudes were measured between points 2-3, and 5-6. Positive deflection is upwards.

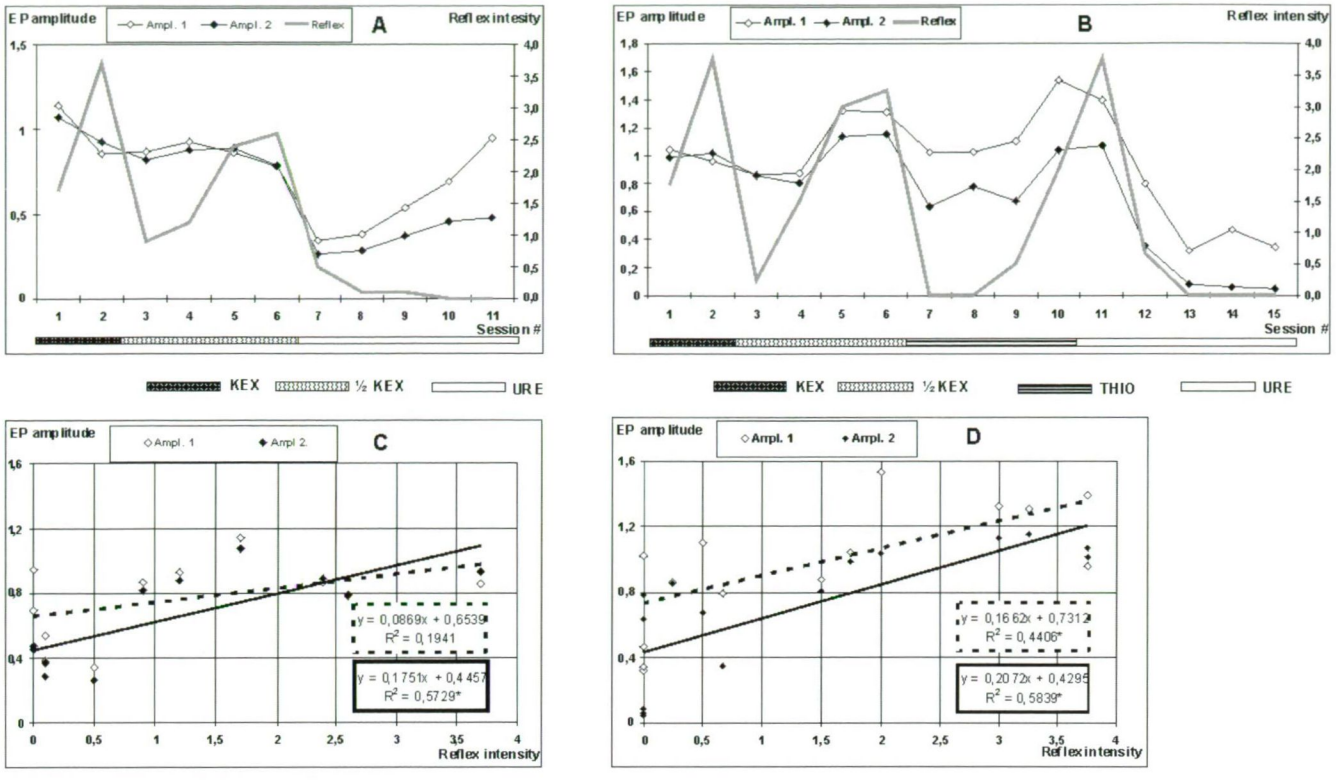

Figure 5. Top: time course of the EP main wave amplitudes (left ordinate) and hind paw withdrawal reflex intensity (right ordinate) in rats treated using the *KEX – URE* (A) and *KEX – THIO – URE* (B) protocols. Recording sessions followed in 20 min intervals. The presented values are means, error ranges are omitted for clarity. Bottom: the corresponding correlation diagrams of reflex intensity and EP amplitude (displayed as in Fig. 2: amplitude 1, light symbols and dotted line; amplitude 2, dark symbols and solid line), significant correlation (F>0.05 from Fisher's test included in "linear fit") is marked with * in the equation box.

tion coefficient) shows to what extent the variability of one (here: electrophysiological) parameter is explained by the other one (here: depth of anesthesia).

In the course of the whole study, the principles of the Ethical Committee for the Protection of Animals in Research of the University were strictly followed.

Results

Effects of the anesthetics on the electrcorticogram

CLH – URE, *CLH – THIO – URE* protocols: As seen in Fig. 2A, reflex intensity gradually increased – that is, the depth of anesthesia achieved by *CLH* gradually decreased – in the first ca. 1.5 hours of these experiments. In parallel with that, ECoG delta activity decreased while beta and gamma activity increased. On administering *URE*, deep anesthesia was reached again after ca. 40 minutes and remained stable, and the shift in the ECoG band powers was reversed. Reflex intensity was quite strongly and significantly correlated with ECoG delta, beta1 and beta2 activity (Fig. 2C). In the *CLH – THIO – URE* protocol (Fig. 2B, D) the same effects were observed but the short action of *THIO* was also obvious.

KEX – URE, *KEX – THIO – URE* protocols: The action of *KEX* was short, so that reflex intensity became high (ca. 3.5) already at the 2nd recording session and a booster dose of *KEX* (1/2 of the original dose) had to be injected. The effect of this booster is clearly reflected in Fig. 3A. ECoG delta activity showed strong, significant correlation to reflex intensity, but for beta1 and beta2, R^2 values were lower (in contrast to the protocols with *CLH:* Fig. 3C). In the *KEX – THIO – URE* protocol, the time course of reflex intensity was similar to that seen with *CLH – THIO – URE*, but ECoG changes were less clear (Fig. 3B). Correlations were poor for the whole course of this protocol (hence, no trend lines are given in Fig. 3D)

Changes in the cortical evoked potential

In the rats anesthetized using the *KEX – URE* and *KEX – THIO – URE* protocols, the general shape of the cortical EP (Fig. 4) was identical to that seen in earlier experiments (Pecze et al. 2005; Takács et al. 2009) performed under pure *URE* anesthesia. Latency and amplitude values, determined by means of the specific points defined in Methods and marked in Figure 4, showed that presence of various anesthetics and depth of anesthesia had much more weak and inconsistent

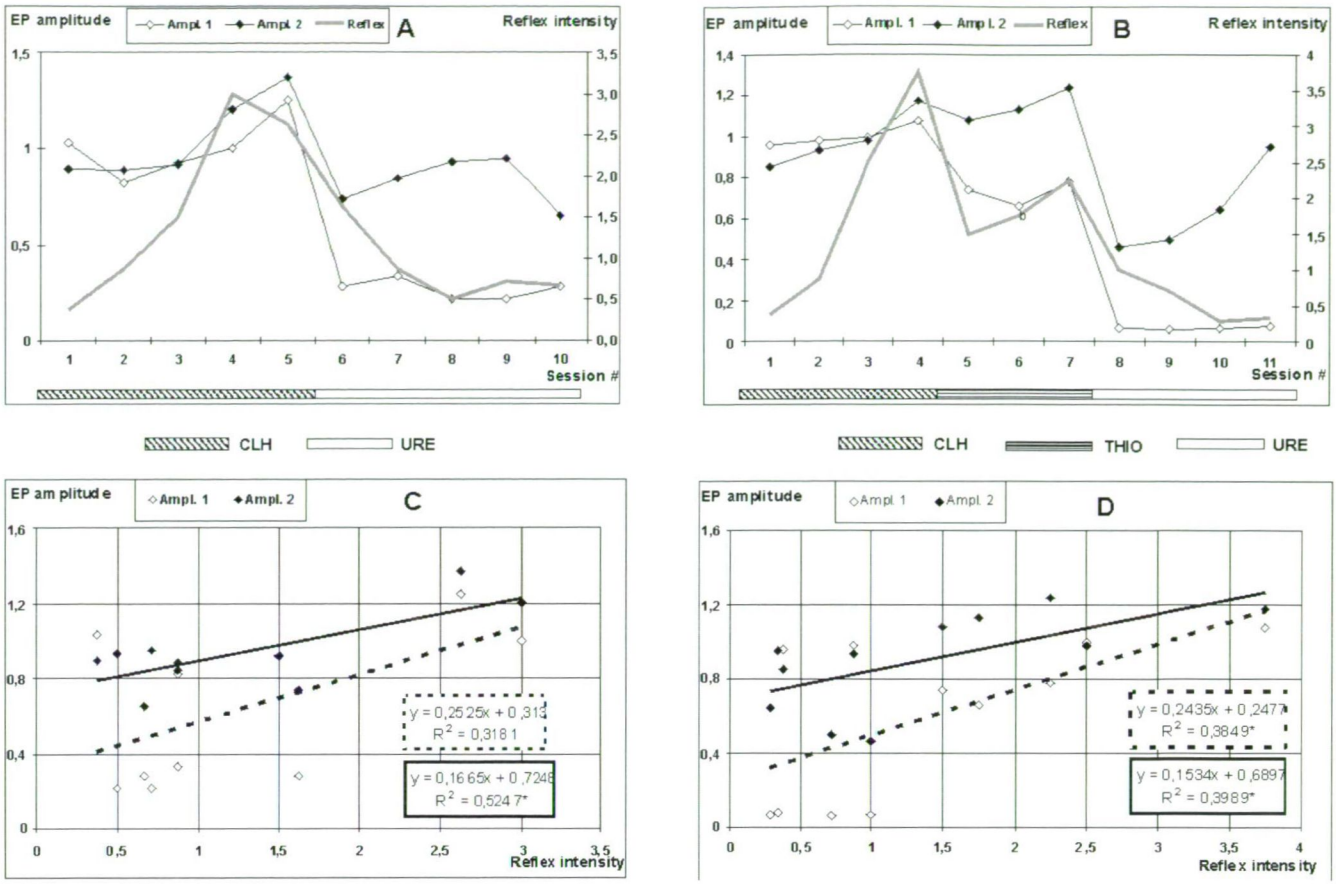

Figure 6. Top: time course of the EP main wave amplitudes (left ordinate) and hind paw withdrawal reflex intensity (right ordinate) in rats treated using the *CLH – URE* (A) and *CLH – THIO – URE* (B) protocols. Bottom: the corresponding correlation diagrams of reflex intensity and EP amplitude. The same display as in Fig. 5.

effect on the latencies of the EP than on its amplitude. The time course curves of Figure 5A and C also show that EP amplitude did not follow the changes of depth of anesthesia before and after the *KEX* repeat dose. Regarding the whole course of the protocols it can be stated all the same that the amplitude of the first wave (Y axis difference of points 2 and 3 in Figure 4) showed less strong correlation to reflex intensity (depth of anesthesia) than that of the later wave (difference of points 5 and 6).

When anesthesia was initiated using *CLH* (*CLH – URE* and *CLH – THIO – URE* protocols) the cortical EP had a different shape (Fig. 4); it was dominated by a very early sharp wave (sometimes present also under *KEX* or *URE* in rudimentary form) while the later parts were diminished. As the effect of *CLH* gradually subsided and that of *URE* set in, the shape of the EP was closer to that seen in the *KEX – URE* protocol but the unusually high and sharp early phase often remained. The parallelism between depth of anesthesia and EP amplitude was generally less strong than in case of *KEX* (Fig. 6).

Discussion

Spectral composition of the ECoG and amplitude of SS EP both showed a clear, monotonous, and mostly significant relationship to the intensity of the defensive reflex (withdrawal of hind paw on toe pinching). Such a relationship, and its potential use to monitor the depth of anesthesia, has repeatedly occurred in the literature. Field et al. (1993) tested *CLH* (300-450 mg/kg b.w.), *URE* (1.2-1.5 mg/kg b.w.) and pentobarbital (40 mg/kg b.w.) on rats, and found that the toe pinch response disappeared permanently under *URE*, but only for ca. 1 hour under *CLH*, and not at all under pentobarbital (experience from our lab also showed that *THIO* alone cannot produce surgical level anesthesia). The time course of the likelihood of response on toe pinch in rats treated with *URE* or *CLH* was similar to our curves of response intensity, indicating that both would be reliable measures of depth of anesthesia. In human volunteers receiving ketamine, subjective pain rating and amplitude of the cortical evoked response on a non-noxious galvanic stimulus changed in parallel (Kochs et al. 1996) and the authors mentioned the usability of evoked

response recording to assess the depth of anesthesia (our results, however, are at variance with this statement). According to other sources (Horn et al. 2009) only sophisticated joint analysis of EEG and auditory EPs of patients might provide a reliable indicator of level of anesthesia. The influence of anesthetic depth on the vibrissa–cortex transmission in rats, more exactly the shrinking receptive field of VPM thalamic neurons with deepening anesthesia (indicated by decreasing dominant ECoG frequency) is another clear illustration why and how the knowledge about the actual level of anesthesia in animal experimentation is a primary concern (Friedberg et al. 1999).

The artificial sleep in general anesthesia results from the imbalance between neuronal excitation and inhibition, induced by the drug applied. Most anesthetics are GABAergic agonists (*URE*: Hara and Harris 2002; *CLH*: Lu and Greco 2006). Suppression of glutamatergic excitation is also of importance, present in the action of *CLH* and *URE* (Kreuter et al. 2004) and being crucial in the action of *KEX* (Bergman 1999). Neurons of the thalamic reticular nucleus inhibit, by a GABAergic mechanism, thalamic pacemaker neurons, the slowed rhythm of which brakes specific afferentation to designated cortical areas via the relay nuclei. Sufficiently strong inhibition of the relay neurons can unmask the thalamic and cortical delta-oscillators, resulting in slow EEG typical for deep sleep (Otto 2008). The above mentioned GABA agonist effect of the anesthetics obviously enhances this intrinsic GABAergic inhibition while their glutamatergic antagonist effect reduces the activity of the ascending reticular activating system which acts not only directly on the cortex but also suppresses the inhibitory effect coming from the thalamic reticular nucleus (Otto 2008).

The qualitative difference between the shape of the SS EP recorded under *CLH* vs. under *URE* or *KEX* cannot be explained by the mentioned shift of excitation-inhibition balance. The very first deflections in the whole SS EP are, in all likelihood, of subcortical origin, arising from thalamic activation (Stienen et al. 2005) or from direct effect of the electric stimulus on the whisker pad muscles (Freeman and Sohmer 1996). Under effect of *CLH*, centripetal spread of excitation at and above the level of thalamus seems to be more strongly blocked than in case of *URE* or *KEX*, so that this fast, sharp wave is more pronounced in the cortical lead-off than with the other anesthetics.

The changes in the numerical parameters of the investigated cortical electrophysiological phenomena, resulting from the choice of the anesthetic and the actual level of anesthesia, were apparently large enough to interfere with the effects of test substances in neurotoxicological or neuropharmacological investigations, underlining the importance of correct choice and dosage of the anesthetic. The result also support that properly chosen electrophysiological parameters could reliably indicate the depth of anesthesia.

References

Bergman SA (1999) Ketamine: Review of its pharmacology and its use in pediatric anesthesia. Anesth Prog 46:10-20.

Carr DB, Andrews GD, Glen WB, Lavin A (2007) α2-Noradrenergic receptors activation enhances excitability and synaptic integration in rat prefrontal cortex pyramidal neurons via inhibition of HCN currents. J Physiol 584: 437-450.

Davis HG, Cox NR, Lindsay JR (1985) Diagnostic exercise: distended abdomens in rats. Lab Anim Sci 35:392-393.

European Union (2010) Directive 2010/63/EU of the European Parliament and of the Council of 22 September 2010 on the protection of animals used for scientific purposes. Official Journal of the European Union L 276/33.

Farkas T, Kiss Zs, Toldi J, Wolff JR (1999) Activation of the primary motor cortex by somatosensory stimulation in adult rats is mediated by associational connections from the somatosensory cortex. Neuroscience 90:353-361.

Field KJ, White WJ, Lang CM (1993) Anesthetic effects of chloral hydrate, pentobarbitone and urethane in adult male rats. Lab Anim 27:258-269.

Freeman S, Sohmer H (1996) A comparison of forepaw and vibrissae somatosensory cortical evoked potentials in the rat. Electroenceph Clin Neurophysiol 10:362-369.

Friedberg MH, Lee SM, Ebner FF (1999) Modulation of receptive field properties of thalamic somatosensory neurons by the depth of anesthesia. J Neurophysiol 81:2243-2252.

Hara K, Harris RA (2002) The anesthetic mechanism of urethane: the effects on neurotransmitter-gated ion channels. Anesth Analg 94:313-318.

Horn B, Pilge S, Kochs EF, Stockmanns G, Hock A, Schneider G (2009) A Combination of electroencephalogram and auditory evoked potentials separates different levels of anesthesia in volunteers. Anesth Analg 108:1512-1521.

IARC (International Agency for Research on Cancer) (1974) Summaries & Evaluations: Urethane. http://www.inchem.org/documents/iarc/vol07/urethane.html

Kandel ER, Schwartz JH (1985) Principles of Neural Science. Elsevier, New York; 643-644.

Koblin DD (2002) Urethane: help or hindrance? Anesth Analg 94:241-242.

Kochs E, Scharein E, Möllenberg O, Bromm B, Schulte am Esch J (1996) Aalgesic efficacy of low-dose ketamine. Somatosensory evoked responses in relation to subjective pain ratings. Anesthesiology 85:304-311.

Kreuter JD, Mattson BJ, Wang B, You ZB, Hope BT (2004) Cocaine induced FOS expression in rat striatum is blocked by chloral hydrate or urethane. Neuroscience 127:233-242.

Lu J, Greco MA (2006) Sleep circuitry and the hypnotic mechanism of $GABA_A$ drugs. J Clin Sleep Med15:S19-26.

Maggi CA, Meli A (1986) Suitability of urethane anesthesia for physiopharmacological investigations in various systems. Part 1: General considerations. Experientia 42:109-114.

Mook D (2006) Anesthetic Management of Rodents and Rabbits. http://www.dar.emory.edu/vet_drug_anesthetic.htm#inj

Murray KA, Pekow C, Borkowski GL (2000) Laboratory Animals: Rodent Anesthesia & Analgesia. Laboratory Animal Medicine and Science – Series II. University of Washington, Seattle.

Otto KA (2008) EEG power spectrum analysis for monitoring depth of anaesthesia during experimental surgery. Lab Animals 42:45-61.

Pecze L, Papp A, Nagymajtényi L, Dési I (2005) Effect of acute administration of certain heavy metals and their combinations on the spontaneous and evoked cortical activity in rats. Environ Toxicol Pharmacol 19:775-784.

Pershad J, Palmisano P, Nichols M (1999) Chloral hydrate: the good and the bad. Pediatr Emerg Care 15:432-435.

Raj D, Gulati S, Lodha R (2011) Status epilepticus. Indian J Pediatr 78, 219-226.

Sceniak MP, MacIver BM (2005) Urethane anesthesia: a novel and specific mechanism of action. Anesthesiology 103:A141.

Stienen PJ, de Groot HNM, Venker-van Haagen AJ, van den Broma WE, Hellebrekers LJ (2005) Differences between somatosensory-evoked potentials recorded from the ventral posterolateral thalamic nucleus, primary somatosensory cortex and vertex in the rat. Brain Res Bull 67:269-280.

Takács Sz, Bankó S, Papp A (2009) Altered stimulus frequency and intensity dependence of the somatosensory evoked potential in rats after acute application of two mitochondrial toxins. Acta Biol Szeged 53:99-103.

Twyman RE, Rogers CJ, Macdonald RL (1989) Differential regulation of gamma-aminobutyric acid receptor channels by diazepam and phenobarbital. Ann Neurol 25:213-220.

United Nations (1971) http://www.unodc.org/pdf/convention_1971_en.pdf

Waite PM (2004) Trigeminal sensory system. In Paxinos G, ed., The Rat Nervous System. Academic Press, New York, 817-851.

Wixson SK (1994) Rabbits and Rodents: Anesthesia and Analgesia. In Smith AC, Swindle MM, eds., Research Animal Anesthesia, Analgesia and Surgery. Scientist Center for Animal Welfare, Greenbelt, MD

Zandieh S, Hopf R, Redl H, Schlag MG (2003) The effect of ketamine/xylazine anesthesia on sensory and motor evoked potentials in the rat. Spinal Cord 41:16-22.

Volume 57(2):161-166, 2013
Acta Biologica Szegediensis
http://www.sci.u-szeged.hu/ABS

ARTICLE

Xylotomic similarities and natural habitat of the fossil remains of Bükkábrány

Eszter Antalfi, Sándor Fehér

University of West Hungary, Sopron, Hungary

ABSTRACT The unique remains of a 7.2-million-year-old forest consisting of Bald cypress and Coast redwood were found in the area of Bükkábrány in County Borsod-Abaúj-Zemplén of Hungary. The trees of the fossil remains comprising 16 stems, which were discovered in a lignite mine, were standing in their original locality, and preserved their original cellular structure. No petrification occurred, which is general characteristics of wood remains preserved for millions of years. What makes the findings unique is that they make it possible to carry out the traditional histological examination of the intact wood structure. The results of light and electron microscopic investigations definitely proved that in addition to Bald cypress, the wood species of the ancient forest remains also included Coast redwood. Today, the natural habitat of Coast redwood is definitely in North-America, but millions of years ago, they were also present in Europe including the Carpathian basin. The xylotomic analysis has unambiguously revealed that two of the investigated five trunks are Bald cypress (*Taxodium distichum)* or the already extinct *Taxodioxylon germanicum*, while the other three trunks are Coast redwood (*Sequoia sempervirens*) or a member of the already extinct family, the *Sequoioxylon sp.*

Acta Biol Szeged 57(2):161-166 (2013)

KEY WORDS

Bükkábrány
fossil remains
wood identification
Bald cypress
Coast redwood

In the summer of 2007, miners in the Bükkábrány Lignite Mine of Mátra Erőmű Zrt. discovered the remains of an ancient forest consisting of 16 stems from the late Miocene Period (Fig. 1). The ground level of the original "forest" was covered by a layer of wet sand or mud of a height of 6 metres. A sudden geological event such as a mudslide may have been the cause of the demise, thus hermetically sealing and conserving the lower 6-metre-high section of the stems. Since no air contacted the trunks, which were surrounded by a continuously wet medium, constant humidity and the conserving effect prevented petrification of the stems, which therefore remained intact. The ancient stems were later transported to Ottó Herman Museum (Miskolc, Hungary). The fossil remains were conserved during the past few years, and six of the intact stems were displayed in the Nature Reserve of Ipolytarnóc Fossils (Ipolytarnóc, Hungary) and another two trunks were exhibited in Ottó Hermann Museum following a special conservation treatment.

During the last centuries, different species of driftwood were often discovered, however never in their own original locality or natural habitat, but within uncertain geographical circumstances. Fossil remains were found in several locations throughout Europe (Pinna and Meischner 2000) including Hungary. The most famous fossil remains ever found in Hungary is the petrified tree discovered in Ipolytarnóc, which as examination proved is such a pine species that bears no similarities to any species either living or fossilised that is having gone extinct or conserved (Tuzson 1901). Its anatomical structure resembles to species belonging to genus *Pinus* that is why Tuzson called it *Pinus tarnocziensis*. Later, Greguss (1967) labelled the petrified remains as *Pinoxylon tarnocziensis*. However, the trunks found in the marshland of Bükkábrány, which were standing in their own locality preserving their original structure, are peculiar and offer researchers a unique chance for scientific examination and interpretation.

Figure 1. Location Bükkábrány Lignite Mine (Bükkábrány, Hungary).

Accepted March 1, 2014
*Corresponding author. E-mail: eszter.antalfi@skk.nyme.hu

Figure 2. Fossil remains in the lignite mine (Bükkábrány).

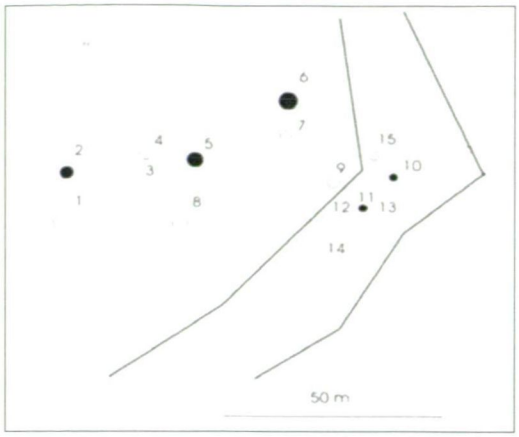

Figure 3. Location of the examined stems (Kázmér 2011).

Plant remains were already investigated after the excavation of the lignite mine in Bükkábrány in 1980. Based on the leaf fossils both coniferous and hardwood species were identified such as, *Glyptostrob us*, *Ginkgo*, as well as *Alnus* and *Byttneriophyllum* (László 1992). Investigating fruit and seed remains additional species were found such as *Glyptostrobus*, *Potamogeton*, *Ceratophyllum*, as well as *Acer*, *Alnus*, *Pterocarya* and *Spirematospermum* (László 1992). Similar fossil remains were found, however, earlier elsewhere. In the lignite mine in Gyöngyösvisonta located only 50 km from Bükkábrány a *Sequoioxylon gypsaceum* (Pálfalvy and Rákosi 1979) was found that was suggested to a Coast redwood (*Sequoia sempervirens*) of our days by Greguss.

Following the discovery of the trunks, the great majority of scientists stated that based on the visual examination of the form and characteristics of the bark, the remains were part of an ancient forest consisting of Bald cypresses (*Taxodium distichum*) (Kázmér 2007). By today it has been proved that the above theory is only partly true as the discovered forest consisted of different species. Specific morphology of the discovered trunks, characteristics of the bark, as well as earlier literature like researches of Kordos and Begun (2002) clarified, however, that the fossil remains belongs to the *Cupressaceae* family. Trunks discovered in the mine are strongly sprawling and ostentatiously ribbed (Fig. 2). The bark is deeply cracked with long vertical strips. It is rich in cork and easily peeling. The shape and size of the fossil tree trunks discovered in Bükkábrány as well as the results of the investigation of other European fossils (Kräusel 1949; Greguss 1955, 1967, 1972; Van der Burgh 1973; Dolezych and Van der Burgh 2004) angled the members of the *Cupressaceae* family such as the *Taxodium*, the *Sequoia*, the *Metasequoia*, and the *Glyptostrobus* genus. Results of the phylogenetic analysis require more or less also the study of the above genus, although the four recent genera do not compose a monophyletic clade, because the *Sequoia* and the *Metasequoia* and possibly the *Sequoiadendron* genus are more closely connected (belong to one clade). Contrarily, the *Gliptostrobus* composes another clade with the *Cryptomeria* and the *Taxodium* rather belongs to this clade (Li 1998; Kusumi et al. 2000). Analysis of the earlier European fossils proves that the *Taxodium*, *Glyptostrobus*, *Sequoia* and *Metasequoia* should not be excluded from the investigation. Phylogenetic researches may also require the investigation of the *Cryptomeria* genus but based on the morphology of the Bükkábrány fossils and the results of previous fossil analysis this genus can be excluded.

Several researchers have been engaged in wood identification, and named different species including Coast redwood (*Sequoia sempervirens*) and Bald cypress (*Taxodium distichum*) among the wood species (Molnár et al. 2007, 2008). Antalfi and Fehér (2012) said that in addition to Coast redwood and Bald cypress the discovered species might also include *Taxodioxylon germanicum* and *Sequoioxylon* sp., since from the perspective of xylotomy there was a minimal difference only between existing species and those which had already became extinct; and Hably (2008) also presumed to identify *Taxodioxylon germanicum*, a species that had already became extinct. Further studies suggested that in addition to *Taxodioxylon germanicum*, *Glyptostroboxylon sp.* might also be found among the fossil remains (Erdei et al. 2009). Furthermore, based on the examination of leaf and cone remains, *Glyptostroboxylon europaeus* was also identified. The examination of the five ancient trunks displayed in Ipolytarnóc, which was carried out by Gryc and Sakala (2010), produced similar results, and identified *Glyptostroboxylon rudulfii* and *Taxodioxylon germanicum* among the remains.

Materials and Methods

The investigations were focused on the species identification of the trunks, for which samples were collected from five different stems. Figure 3 indicates the location of the

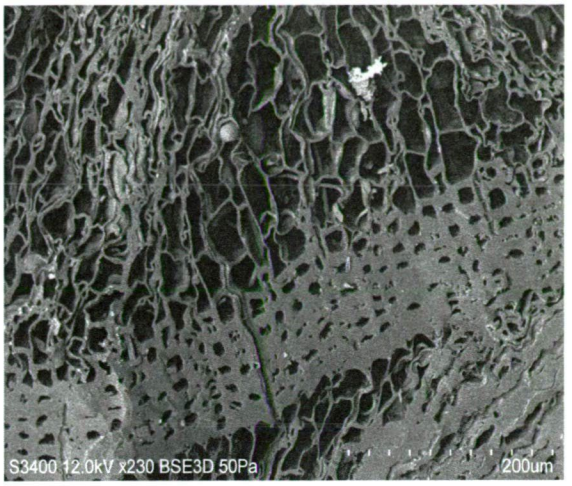

Figure 4. Cross section of sample 10 (*Sequoioxylon sp.*).

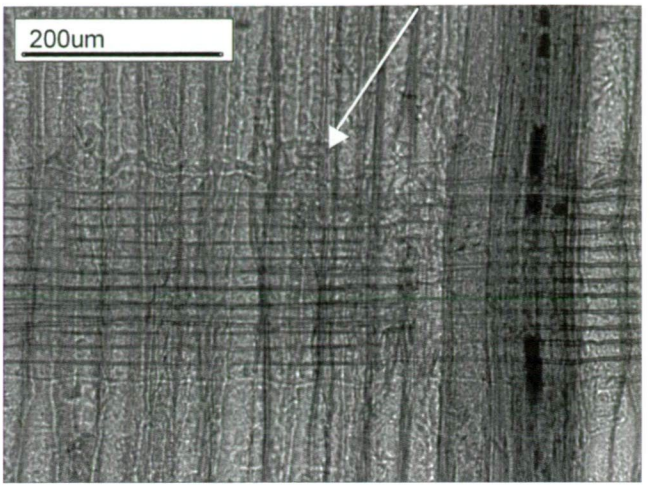

Figure 5. Rays are heterogeneous (*Sequoioxylon sp.*).

stems in the marsh forest of the Bükkábrány mine based on Kázmér (2011).

The samples were taken from the upper part of trunk No 10 and 11 so as not to damage the stems, while we received smaller specimens from trunk No 2, 5 and 6 to use during the examination.

Following the appropriate preparation of the samples, the sections were prepared by using a Leitz Wetzlar sledge microtome. For examinations required for wood species identification, a Nikon SMZ-2T zoom stereo microscope and a Hitachi S-3400N scanning electron microscope were applied. Since the wood is an orthogonal anisotropic material, analysis of all of the three anatomical directions (radial, tangential and longitudinal) is necessary to determine the wood species. The buried ancient woods have lost some of their cellulose content (Molnár et al. 2008) that is responsible for the cell wall strength. Therefore, before the light microscope analysis, samples had to be embedded into paraffin to be able to produce appropriate sections. For a good quality section, the right anatomical direction must be taken carefully. The thickness of the sections was between 15 and 20 µm. For SEM investigations, however, a different method was applied for sample preparation. The proper quality of the surfaces was achieved by charring at elevated temperature.

Results

The longitudinal tracheids on the cross sections of trunks No 2, 6 and 10 show a regular pattern, and therefore, evidently refer to pine species (Fig. 4). The borderline between the early and late wood is relatively abrupt. No real resin canal may be found in the samples. There are a great number of axial parenchymae dispersed especially in the early wood. In the tangential direction, rays are a single cell wide only, with their height ranging from 1-30 cell lines. The end wall of

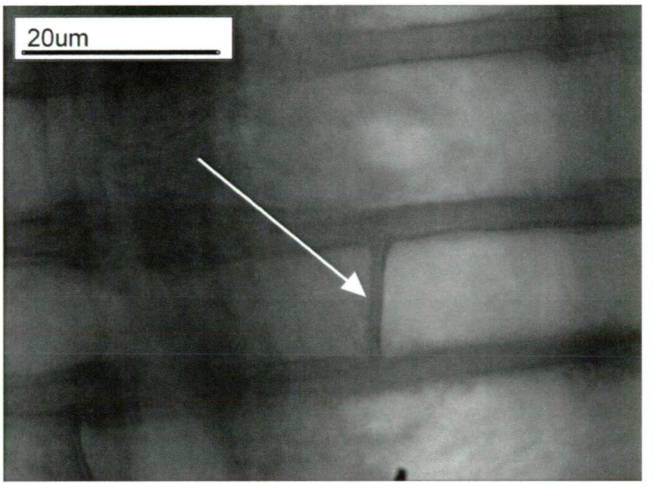

Figure 6. End wall of ray parenchyma is smooth; sample 2 (*Sequoioxylon sp.*).

axial parenchymae is smooth. In the parenchyma cells, dark-coloured substances may be observed. In the cross sections, bordered pits of longitudinal tracheids are arranged in 1-3 rows. The rays are heterogeneous, as there are ray parenchymae in the middle, and ray tracheids in the end of the ray (Fig. 5). The walls of ray tracheids are smooth or have toothlike ingrowths, but no other cell wall alteration may be observed. The tangential walls of ray parenchymae are smooth (Fig. 6), or occasionally nodular. In the crossfield, 1-3 taxodioide pits or cupressoides may be seen. The occurrence of taxodioide pits is more prevalent. The above anatomical characteristics refer to Coast redwood (*Sequoia sempervirens*), which belongs to the *Sequoia* genus, or to *Sequoioxylon sp*, one of the species of the genus, which already became extinct.

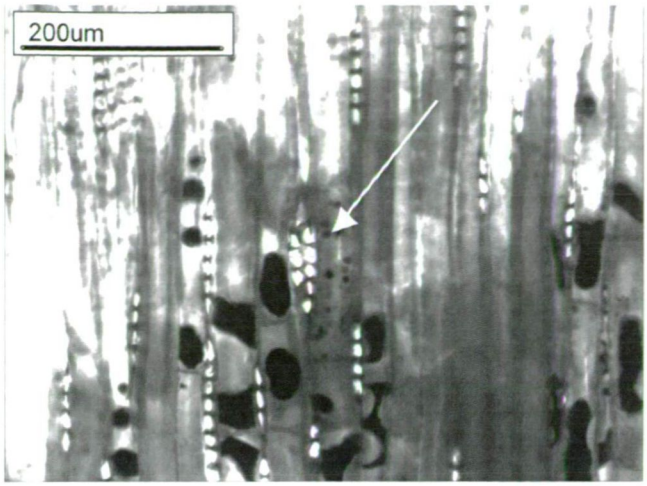

Figure 7. The rays are sometimes two seriate; sample 11 (*Taxodioxylon germanicum*).

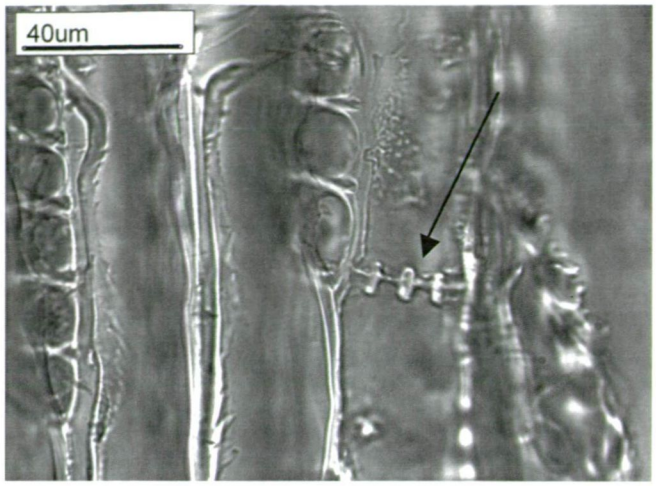

Figure 8. The end walls of axial parenchymae are nodular (*Taxodioxylon germanicum*).

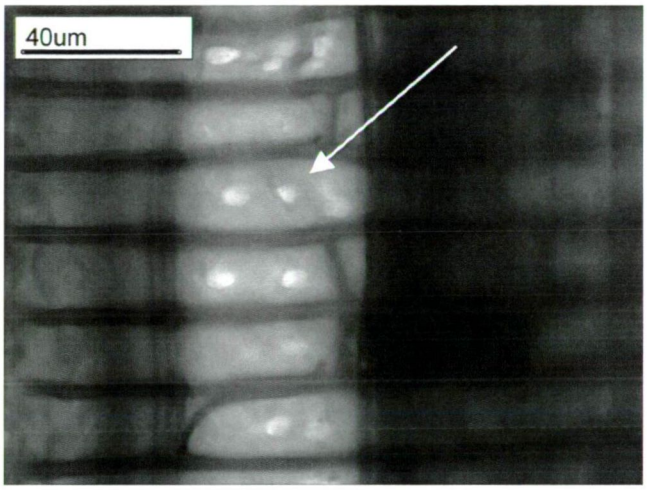

Figure 9. Crossfield pits are taxodioid; sample 5 (*Taxodioxylon germanicum*).

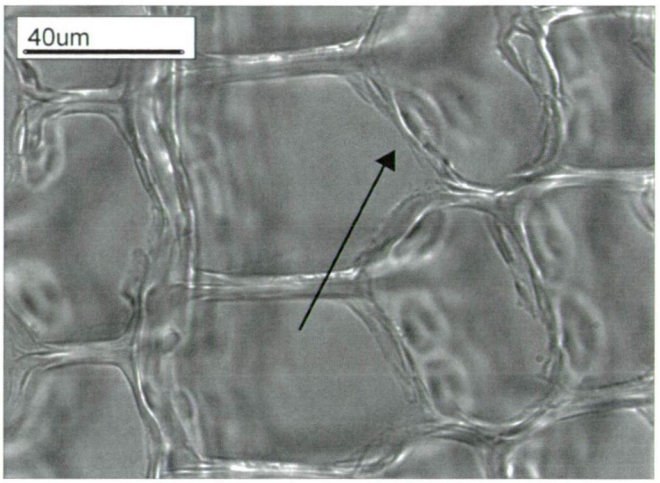

Figure 10. Tracheids are five or six-sided (*Metasequoia glyptostroboides*).

Based on their microscopic characteristics, trunks No 5 and 11 belong to a different species. The longitudinal tracheids on the cross sections show a regular pattern. The borderline between the early and late wood is abrupt. The autumn wood is very narrow. There are a relatively great number of axial parenchymae, which are either dispersed or arranged in lines in the tangential direction. In the tangential section it can be observed that the rays are mostly one or two-cell-wide (Fig. 7). As far as their length is concerned, they can be as high as 35 cell-lines. The end walls of axial parenchymae are not smooth but nodular (Fig. 8). In the axial parenchyma cells, dark-coloured substances may often be observed. In the tangential direction, the rays are homogeneous as they are composed of one cell-type only (ray parenchymae). On the cell walls of longitudinal tracheids the alteration is caused by pits only. The bordered pits are arranged in 1, 2 or 3 rows. The end walls of ray cells (tangential walls) are smooth. In the crossfield, cupressoide and taxodioide pits (Fig. 9) may be observed. Their numbers vary from 1 to 4 depending on whether being examined in the early or late wood. Based on the above, the examined two trunks belong to the *Taxodium* genus, being either *Taxodioxylon germanicum*, a species which already became extinct, or Bald cypress (*Taxodium distichum*), one of its existing relative.

In addition to the similarities, slight differences may also be observed in the xylotomic analysis of the wood species detailed in several studies, which might as well challenge the results of such examinations. The species of the *Taxodiaceae*

family have been examined by several xylotomists including Greguss (1972), Hollendonner (1913), Hoadley (2000) and Wheeler (1986), among others. The anatomic descriptions are correct, though minor differences may also be seen, that is why I applied existing control species. Based on the examination of the control species, I examined which genus of ancient pine trees or species they belong to. In the case of the control species, samples were collected by using a so-called Pressler drill from three species including Bald cypress (*Taxodium distichum)*, Coast redwood (*Sequoia sempervirens*) and Dawn redwood (*Metasequoia glyptostroboides*) as the latter species is also a member of the *Taxodiaceae* family.

From an anatomic perspective, Dawn redwood bears the most similarities to Coast redwood, therefore in our research we also compared these two species. The xylotomic data of Dawn redwood are different from both those of the ancient trunks and Coast redwood, which differences were also supported by the microscopic examinations. In the cross sections it can be seen that tracheids in Coast redwood are arranged in a regular pattern, while Dawn redwood has five or six-sided cells (Fig. 10). Another significant difference may be observed in the tangential section: in the case of Coast redwood rays are heterogeneous that is they consist of ray tracheids in addition to ray parenchymae, while in the case of Dawn redwood rays are composed of parenchyma cells only. Based on the research carried out so far, we have not managed to undoubtedly prove the presence of Dawn redwood, or one of its relative, *Glyptostroboxylon sp*, which already became extinct.

Discussion

From a histological perspective, Coast redwood is identical to Bald cypress, but there is a difference in the red colour of the heartwood cell walls, which is yellowish or golden in the case of Bald cypress. Another difference may be observed in the tannic acid content of the cell walls: the heartwood of *Taxodium* turned green only following a prolonged exposure to ferrous chloride, while that of *Sequoia* instantly went black. The reason behind this change in colour is that the reddish-brownish substances of tray cells contain tannic acid, and some yellowish-brownish substances in the tracheids are also composed of water soluble materials with tannic acid content. As it can be seen, a clear distinction may be easily made between the two species with macroscopic examination, however, they are much more difficult to differentiate by applying the method of microscopic investigation.

The results of the examination carried out on the fossil remains proved that the trunks are members of the *Taxodiaceae* family exclusively. Consequently, these species bear striking similarities from a xylotomic perspective, and those related species which became already extinct bear striking similarities to their existing counterparts.

The results of the xylotomic examination evidently proved that two (no 5 and 11) of the three trunks are *T. germanicum*, which already became extinct, while trunk No 2, 6 and 10 are *Sequoioxylon sp*, one of the extinct members of genus *Sequoia*.

The discovery of the marshland forest in Bükkábrány, which had been buried some 7.2 millions of years ago, made a unique examination of fossil remains possible. Our aim was to carry out the comprehensive anatomical and physical examination of the trunks belonging to the ancient forest, which also included determining the characteristics of the identified wood species by way of microscopic and macroscopic examinations. So far, five trunks have been identified. The histological study of the samples evidently proved that the trees discovered in the area belonged to a pine wood. It was observed as early as at the beginning of the examinations that every trunk was member of the *Taxodiaceae* family, which was also supported by the morphology of the trunks and the characteristics of the bark including its width and structure. The results of the xylotomic examinations evidently proved that two of the five trunks examined so far are *T. germanicum*, already extinct, which bears striking similarities to Bald cypress (*T. distichum*), an existing species even today, and that the three other trees are *Sequoioxylon sp.*, which had already become extinct, a species closely related to Coast redwood (*S. sempervirens*). Based on the examinations carried out so far it has been proved that further investigation is required to determine whether the extinct species already identified in Bükkábrány and the strikingly similar existing wood species are the same or actually belong to different species.

Acknowledgement

This research was realized in the frames of TÁMOP 4.2.4. A/2-11-1-2012-0001 'National Excellence Program – Elaborating and operating an inland student and researcher personal support system convergence program'. The project was subsidized by the European Union and co-financed by the European Social Fund.

References

Antalfi E, Fehér S (2012) A bükkábrányi fosszilis fatörzsmaradványok fafaj meghatározása mikroszkópos módszerekkel. Faipar (Scientific Journal of Wood Industry) 60(1):5-9 [in Hungarian].

Dolezych M, Van der Burgh J (2004) Xylotomische Untersuchungen an inkohlten Hölzern aus dem Braunkohlentagebau Berzdorf (Oberlausitz/ Deutschland). Feddes Repert 115(5/6):397-437.

Erdei B, Dolezych M, Hably L (2009) The buried Miocene forest at Bükkábrány, Hungary. Palaeobot Palynol 155:69-79.

Greguss P (1955) Xylotomische Bestimmungen der heute lebenden Gymnospermen. Akadémiai Kiadó, Budapest, p. 308.

Greguss P (1967) Fossil gymnosperm wood in Hungary – from the Permian to the Pliocene, Akadémiai Kiadó, Budapest, p. 136.

Greguss P (1972) Xylotomie of the Living Conifers. Akadémiai Kiadó, Budapest, p. 329.

Hably L (2008) Magyar Florida, avagy Bükkábrány igazi arca, Természet Világa, 139(4):178-180 [in Hungarian].

Hoadley RB (2000) Understanding Wood. Wood identification. Newtown, pp. 47-73.

Hollendonner F (1913) A fenyőfélék fájának összehasonlító szövettana. Országos Erdészeti Egyesület, Budapest, p. 187 [in Hungarian].

Kázmér M (2007) Taxodium mocsárerdő a bükkábrányi felsőpannon rétegekben. Kirándulásvezető a Magyarhoni Földtani Társulat Őslénytan-Rétegtani Szakosztályának 2007. július 24-i terepbejárásához, p. 2 [in Hungarian].

Kázmér M (2011) Structure of the 7 Ma Bükkábrány fossil forest in Hungary. Jap J Hist Bot 19(1-2):47-54.

Kordos L, Begun DR (2002) Rudabánya: A late miocene subtropical swamp deposit with evidence of the origin of the African apes and humans. Evol Anthr 11:45-57.

Kusumi J, Tsumura Y, Yoshimaru H, Tachida H (2000) Phylogenetic relationships in Taxodiaceae and Cupressaceae sensu stricto based on matK gene, chlL gene, trnL-trnF IGS region, and trnL intron sequences. Am J Bot 87(10):1480-1488.

László J (1992) Ősnövénymaradványok a bükkábrányi lignitkülfejtésből.- A Magyar Állami Földtani Intézet Évi Jelentése az 1990. évről (Annual Report of the Geological Institute of Hungary), Budapest, pp. 321-337 [in Hungarian].

Li J (1999) Metasequoia: An overview of its phylogeny, reproductive biology, and ecotypic variation. Arnoldia 58/59:54-59.

Molnár S, Fehér S, Börcsök Z, Ábrahám J (2007) A bükkábrányi Taxodiaceae leletek anatómiai és kémiai vizsgálatának néhány eredménye, Nemzetközi Konferencia, Miskolc.

Molnár S, Albert L, Fehér S, Börcsök Z, Ábrahám J, Hofmann T, Antalfi E (2008) Anatomical and chemical characteristics of Miocene Taxodiaceae species from Bükkábrány (Hungary), Wood Matters – A celebration of the work of John Barnett, The Linnean Society of London, International Academy of Wood Science, International Association of Wood Anatomists, London.

Pálfalvy I, Rákosi L (1979) Die Pflanzenreste des Lignitflöz-führenden Komplexes von Visonta.- A Magyar Állami Földtani Intézet Évi Jelentése az 1977. évről (Annual Report of the Geological Institute of Hungary), Budapest, pp. 47-66.

Pinna G, Meischner D (2000) Europäische Fossillagerstätten. European Palaeontological Association, Springer Verlag, Berlin.

Tuzson J (1901) A tarnóczi kövült fa (Pinus tarnocziensis n. sp.). Természetrajzi füzetek 24:273-316 [in Hungarian].

Van der Burgh J (1973) Hölzer der niederrheinischen Braunkohlenformation. 2. Hölzer der Braunkohlengruben "Maria Theresia" zu Herzogenrath, "ZukunftWest" zu Eschweiler und "Victor" (Zülpich-Mitte) zu Zülpich. Nebst einer systematisch-anatomischen Bearbeitung der Gattung Pinus L. Rev Palaeobot Palynol 15:73-275.

Wheeler EA, Pearson RG, LaPasha CA, Hatley W, Zack T (1986) Computer-aided wood identification. Stat Bull 474, N.C. Ag. Res. Serv., Raleigh, N.C.

Instructions to Authors

Submission of manuscripts

Submission of a manuscript to Acta Biologica Szegediensis automatically involves the assurance that it has not been published and will not be published elsewhere in the same form. Manuscripts should be written in English. Since poorly-written material will not be considered for publication, authors are encouraged to have their manuscripts corrected for language and usage by a trusted expert.

There are no explicit length limitations: a normal research article will occupy 4-6 printed pages; reviews might be considerably longer. Authors should submit three sets of the complete manuscript and illustrations, together with a computer disk containing an electronic version of their manuscript. The elctronic file is considered the final material. Both Macintosh and PC versions will be accepted. The disk should be labeled with the date, the first author's name, the file name of the manuscript and the software, disk format and hardware used. Acta Biologica Szegediensis will not return copies of submitted manuscripts and figures. Requests to return original figures will be honored as a courtesy, but cannot be guaranteed. If instructions are not followed, authors will be asked to retype their manuscripts.

Manuscript format

Only good-quality laser printouts will be accepted. All pages should be printed with full double spacing, 2.5 cm margins, and a nonjustified right margin. A standard 12 point typeface (e.g. Times, Helvetica or Courier) should be used throughout the manuscript, with symbol font for Greek letters. Boldface, italics or underlined text should not be used anywhere in the manuscript. Footnotes are not permitted. Each page should be numbered at the bottom as follows:

Page 1. Title page: Complete title, first name, middle initial, last name of each author; where the work was done (authors' initials in parentheses if necessary); mailing address, phone, fax, and e-mail of the corresponding author; a running title of no more than 48 characters and spaces.

Page 2. Abstract: no more than 200 words, followed by 4-6 key words.

Beginning on page 3: Introduction, Materials and Methods, Results, Discussion, Acknowledgments, References, Figure Legends, Tables. Each section should be begun on a new page.

The manufacturer's name and location should be given in parentheses for reagents and instruments. Sources for all antibodies and nucleotide sequences should be indicated. Customary abbreviations in common use need not be defined in the text (e.g. DNA or ATP). Other abbreviations should be defined the first time that they are used. Quantitative results must be presented as graphs or tables and supported by appropriate experimental design and statistical tests. Only SI units may be used. For studies that involve animals or human subjects, the institutional, national or international guidelines that were followed should be indicated.

References

Only work that has been published or is in the press may be referred to. Personal communications should be acknowledged in the text and accompanied by written permission. In the text, references should be cited by name and year, e.g. Bloom (1983) or (Schwarz-Sommer et al. 1990) or (Maxam and Gilbert 1977). In the References, references should be listed alphabetically by first authors (including all co-authors) and chronologically for a given author (beginning with the most recent date of publication). Where the same author has more than one publication in a year, lower case letters should be used (e.g. 1999a, 1999b, etc.). Periods should not be used after authors' initials or abbreviated journal titles (e.g. Acta Biologica Szegediensis should be cited as Acta Biol Szeged). Inclusive page numbers should be used. Examples:

Bloom FE (1983) The endorphins: a growing family of pharmacologically pertinent peptides. Annu Rev Pharmacol Toxicol 23:151-170.

Coons AH (1978) Fluorescent antibody methods. In Danielli JF, ed., General Cytochemical Methods. Academic Press, New York, 399-422.

Maxam AM, Gilbert WA (1977) A new method for sequencing DNA. Proc Natl Acad Sci USA 74:560-564.

Monod J, Changeux J-P, Jacob F (1963) Allosteric proteins and cellular control systems. J Mol Biol 6:306-329.

Schwarz-Sommer Z, Huijser P, Nacken W, Saedler H, Sommer H (1990) Genetic control of flower development by homeotic genes in Antirrhinum majus. Science 250:931-936.

Illustrations

Three complete sets, including a high-quality "original" for publication, must be submitted with the manuscript. The back of each figure or composite plate should be labeled in soft lead pencil, indicating the orientation, the figure number, and the first author's name. The back of the best set should be marked "use for reproduction" or "original". Authors are encouraged to submit digital images of photographs, line drawings or graphs for printing. Most major image editing and drawing/illustrator computer software files (both Macintosh and PC) in TIFF or EPS formats are acceptable. It is particularly important that adequate resolution (at least 300 dpi, preferably 600 dpi) is used in making the original image.

Figure legends

Figures should be numbered consecutively with Arabic numerals. Material in the text should not be duplicated and methods should not be described. The size of scale bars should be indicated when appropriate. The first figure in the text should be referred to as Fig. 1, and so on.

Tables

Tables should be numbered consecutively with Arabic numerals. A brief title should be included above the table. Each table should be printed double spaced, without vertical or horizontal lines, and on a separate sheet. Material in text should not be duplicated and methods should not be described. The first table in the text should be referred to as Table 1, and so on.

Submission of manuscripts

Acta Biologica Szegediensis is a no-fee open access journal providing high-visibility of all scientific achievements published in the journal.
Manuscripts should be submitted to the Editor-in-Chief as an electronic attachment to **abs@bio.u-szeged.hu**. All submitted manuscripts should be complete in themselves and firmly supported by properly detailed experimental data.
Instructions to Authors is published in each issue and also available at **http://www2.sci.u-szeged.hu/ABS**.
Correspondence relating to the status of the manuscripts, proofs, publication, reprints and advertising should be sent also to **abs@bio.u-szeged.hu**.

Editor-in-Chief: Csaba Vágvölgyi
Department of Microbiology, Faculty of Science and Informatics
University of Szeged, Közép fasor 52., H-6726 Szeged, Hungary
Phone: 36 (62) 544-822, fax: 36 (62) 544-823
E-mail: csaba@bio.u-szeged.hu

Technical Editor: Tamás Mikola
Acta Biologica Szegediensis, Editorial Office
4 Somogyi u., H-6720 Szeged, Hungary
Phone: 36 (62) 544-569, fax: 36 (62) 544-569
E-mail: abs@bio.u-szeged.hu

Subscriptions

All subscriptions relate to the calendar year and must be pre-paid. The annual subscription rate is currently 100 USD and includes air mail delivery and handling.
Acta Biologica Szegediensis is indexed in BIOSIS Database, EMBASE, Excerpta Medica, Elsevier BIOBASE (Current Awareness in Biological Sciences) and Zoological Record.

The Table of Contents for the current issue and those for previous issues can be found at:
http://www2.sci.u-szeged.hu/ABS.